

# Synthesis of Small Molecules Targeting ADP-Ribosyltransferases and Total Synthesis of Resveratrol Based Natural Products

Anders Lindgren



**Doctoral Thesis, 2015**  
Department of Chemistry  
Umeå University

Responsible publisher under swedish law: the Dean of the Faculty of Science and Technology

This work is protected by the Swedish Copyright Legislation (Act 1960:729)

ISBN: 978-91-7601-329-8

Electronic version available at <http://umu.diva-portal.org/>

Printed by: VMC-KBC Umeå

Umeå, Sweden, 2015





# Table of Contents

<b>Abstract</b>	<b>iii</b>
Diphtheria Toxin-like ADP-Ribosyltransferases	iii
Total Synthesis of Resveratrol Based Natural Products	iii
<b>List of Abbreviations</b>	<b>iv</b>
<b>List of Publications</b>	<b>vi</b>
Author's Contributions	vii
Papers by the Author Not Included in the Thesis.	vii
<b>Populärvetenskaplig sammanfattning</b>	<b>ix</b>
Små molekyler för att identifiera proteiners funktion	ix
Totalsyntes av naturprodukter	ix
<b>Introduction</b>	<b>1</b>
A Brief History of Drug Discovery and Organic Synthesis	1
Drug Discovery: Diphtheria Toxin-like ADP-Ribosyltransferases	6
Organic Synthesis: Polyphenol Based Natural Products	9
<b>Chapter 1: Development of ARTD3 Inhibitors (Paper I + II)</b>	<b>13</b>
Initial Compounds	14
Other Substituents at the Meso Position	16
The Linker Region	18
Aromatic Substituents	23
Homobenzylic and $\alpha$ -Amino Acid Analogs	24
Further Characterization of Selected Compounds	27
Concluding Remarks	31
<b>Chapter 2: Development of ARTD7, ARTD8, and ARTD10 Inhibitors (Paper III + IV)</b>	<b>33</b>
Virtual Screening Procedure	34
Evaluation of Hits from the Virtual Screen	35
Further Evaluation of Selected Compounds	37
Synthesis of Analogs	40
Merged Compounds	44
Macrocycles	49
Concluding Remarks	52
<b>Chapter 3: Biotinylated ARTD7, ARTD8, and ARTD10 Inhibitors for AlphaScreen</b>	<b>53</b>
Synthesis of Biotinylated Ligands	55
Concluding Remarks	57
<b>Chapter 4: Total Synthesis of Polyphenol Based Natural Products (Paper V)</b>	<b>59</b>
Cyclopropylmethyl, an Unconventional Protecting Group	62
Alkene Isomerization, <i>E</i> to <i>Z</i>	69
Concluding Remarks	71

<b>Conclusions and Outlook</b>	<b>73</b>
Diphtheria Toxin-like ADP-Ribosyltransferases	73
Total Synthesis of Polyphenol Based Natural Products	73
<b>Appendix 1</b>	<b>75</b>
Experimental Procedures for the Compounds Presented in Scheme 9.	75
<b>Appendix 2</b>	<b>83</b>
Experimental Procedures for the Compounds Presented in Scheme 10.	83
<b>Appendix 3</b>	<b>87</b>
Experimental Procedures for Previously Unpublished Compounds Presented in Scheme 11, 12, and 13.	87
<b>Appendix 4</b>	<b>93</b>
Experimental Procedures for Previously Unpublished Compounds Presented in Chapter 4.	93
<b>Acknowledgements</b>	<b>97</b>
<b>References</b>	<b>99</b>

# Abstract

## Diphtheria Toxin-like ADP-Ribosyltransferases

The Human ADP-ribosyl transferases (ARTDs) are a group of poorly studied enzymes which are believed to be involved in *e.g.* DNA repair, protein degradation, transcription regulation and cell death. Medicinal chemistry programmes aimed at developing selective inhibitors of these ARTDs were initiated. A suitable starting compound for one of these enzymes, ARTD3, was found by screening a library of NAD-mimics using a thermal shift assay. A virtual screening protocol was instead developed in order to find novel inhibitors of ARTD7, 8, and 10. The hit compounds were then further developed into selective inhibitors of the corresponding ARTDs by systematically varying different structural features using a combination of synthetic organic chemistry, computational chemistry and structural biology. Compounds were initially characterized using differential scanning fluorimetry which was later replaced with an enzymatic assay to obtain IC<sub>50</sub> values. Biotinylated analogs were also synthesized in an attempt to develop an AlphaScreen assay. A selective ARTD3 inhibitor was ultimately identified and found to delay DNA repair in cells after  $\gamma$ -irradiation. These compounds are potentially valuable tools for elucidating the biological role of the poorly characterized ARTD-family of proteins.

## Total Synthesis of Resveratrol Based Natural Products

The polyphenolic natural product (-)-hopeaphenol was found to inhibit the type III secretion system present in certain gram-negative bacteria. (-)-Hopeaphenol is a tetramer of resveratrol and in order to investigate whether the entire structure was essential for inhibition two resveratrol dimers,  $\epsilon$ -viniferin and ampelopsin B, were synthesized using a flexible and divergent synthetic route. Highlights of the synthetic strategy include the use of cyclopropylmethyl protecting groups, allowing an acid mediated three-step-one-pot deprotection-epimerization-cyclization of an advanced intermediate to form ampelopsin B. All previously reported syntheses of these two natural products include a dimerization of resveratrol which severely limits the possibilities to synthesize structural analogs. This new strategy enables the synthesis of a wide variety of analogs to  $\epsilon$ -viniferin and ampelopsin B.

# List of Abbreviations

Å	Ångström
ARTD	Diphtheria toxin-like ADP-ribosyltransferase
Ac	Acetyl
ADP	Adenosine diphosphate
cPr	Cyclopropyl
cPrMe	Cyclopropylmethyl
DBU	1,8-Diazabicyclo[5.4.0]undec-7-ene
DCM	Dichloromethane
DIC	<i>N,N'</i> -diisopropylcarbodiimide
DMF	<i>N,N'</i> -dimethylformamide
DMSO	Dimethyl sulfoxide
DNA	Deoxyribonucleic acid
dppa	Diphenyl phosphoryl azide
dppf	1,1'-Bis(diphenylphosphino)ferrocene
eq	Equivalent
Et	Ethyl
EtOAc	Ethyl acetate
FDA	U.S. Food and Drug Administration
Fmoc	9-Fluorenylmethoxycarbonyl
HATU	<i>O</i> -(7-azabenzotriazol-1-yl)- <i>N,N,N',N'</i> -tetramethyluronium hexafluorophosphate
HOAt	1-Hydroxybenzotriazole
HPLC	High performance liquid chromatography
HTS	High throughput screening
IC <sub>50</sub>	Inhibitory concentration 50%
ITC	Isothermal titration calorimetry
LC-MS	Liquid chromatography - mass spectrometry
mART	Mono-ADP-ribosyltransferase
MD	Molecular dynamics
Me	Methyl
MeCN	Acetonitrile

MeOH	Methanol
NAD <sup>+</sup>	Nicotinamide adenine dinucleotide
NCE	New chemical entity
NMP	<i>N</i> -methyl-2-pyrrolidinone
NMR	Nuclear magnetic resonance
PARP	Poly(ADP-ribose) polymerase
PARG	Poly(ADP-ribose) glycohydrolase
PBS	Phosphate-buffered saline
PC	Principal component
PCA	Principal component analysis
Pd/C	Palladium on charcoal
PDB	Protein data bank
Ph	Phenyl
QSAR	Quantitative structure-activity relationship
RCM	Ring closing metathesis
RMSD	Root-mean-square deviation
rt	Room temperature
SAR	Structure-activity relationship
SMD	Statistical molecular design
TBAF	Tetrabutylammonium fluoride
TBTU	<i>N,N,N',N'</i> -tetramethyl- <i>O</i> -(1 <i>H</i> -benzotriazol-1-yl)uronium tetrafluoroborate
TCEP	Tris(2-carboxyethyl)phosphine
TEA	Triethylamine
TFA	Trifluoroacetic acid
THF	Tetrahydrofuran
T <sub>m</sub>	Midpoint of transition
T <sub>3</sub> SS	Type III secretion system
UHP	Urea hydrogen peroxide
UV	Ultra violet

# List of Publications

This thesis is based on the following papers, which are referred to in the text by the corresponding Roman numerals.

- I            **Lindgren A. E. G.**, Karlberg T., Ekblad T., Spjut S., Thorsell A-G., Andersson C. D., Nhan T. T., Hellsten V., Weigelt J., Linusson A., Schüler H., Elofsson M.  
*Chemical Probes to Study ADP-Ribosylation: Synthesis and Biochemical Evaluation of Inhibitors of the Human ADP-Ribosyltransferase ARTD3/PARP3.*  
Journal of Medicinal Chemistry, 2013, 56(23): 9556-9568.
- II            **Lindgren A. E. G.#**, Karlberg T.#, Thorsell A-G., Hesse M., Spjut S., Ekblad T., Andersson C. D., Pinto A. F., Weigelt J., Hottiger M. O., Linusson A., Elofsson M., Schüler H.  
*PARP Inhibitor with Selectivity Toward ADP-Ribosyltransferase ARTD3/PARP3.*  
ACS Chemical Biology, 2013, 8(8): 1698-1703.
- III            Andersson C. D., Karlberg T., Ekblad T., **Lindgren A. E. G.**, Thorsell A-G., Spjut S., Eciechowska U., Niemiec M. S., Wittung-Stafshede P., Weigelt J., Elofsson M., Schüler H., Linusson A.  
*Discovery of Ligands for ADP-Ribosyltransferases via Docking-Based Virtual Screening.*  
Journal of Medicinal Chemistry, 2012, 55(17): 7706-7718.
- IV            Ekblad T.#, **Lindgren A. E. G.#**, Andersson C. D., Caraballo R., Thorsell A-G., Karlberg T., Spjut S., Linusson A., Schüler H., Elofsson M.  
*Towards small molecule inhibitors of mono-ADP-ribosyltransferases.*  
European Journal of Medicinal Chemistry, 2015, 95: 546-551.
- V            **Lindgren A. E. G.**, Öberg C. T., Hillgren J. M., Elofsson M.  
*Total Synthesis of the Resveratrol Oligomers (±)-Ampelopsin B and (±)-ε-Viniferin.*  
Manuscript.

# These authors contributed equally to this work.

All papers have been reprinted with kind permission from the publishers.

## Author's Contributions

Paper I:	Planning, most of the synthesis, major writing.
Paper II:	Planning, all of the synthesis, minor writing.
Paper III:	All of the synthesis, minor writing.
Paper IV:	Planning, most of the synthesis, major writing.
Paper V:	Planning, all of the synthesis, major writing.

## Papers by the Author Not Included in the Thesis.

- \* Bengtsson C., **Lindgren A. E. G.**, Uvell H., Almqvist F.  
*Design, synthesis and evaluation of triazole functionalized Ring-fused 2-pyridones as antibacterial agents.*  
European Journal of Medicinal Chemistry, 2012, 54: 637-646.
- \* Andersson E. K, Bengtsson C., Evans M. L., Chorell E., Sellstedt M., **Lindgren A. E. G.**, Hufnagel D. A., Bhattacharya M., Tessier P. M., Wittung-Stafshede P., Almqvist F., Chapman M. R.  
*Modulation of Curli Assembly and Pellicle Biofilm Formation by Chemical and Protein Chaperones.*  
Chemistry and Biology, 2013, 20(10): 1245-1254.
- \* Marwaha S., Uvell H., Salin O., **Lindgren A. E. G.**, Silver J., Elofsson M., Gylfe Å.  
*N-acylated derivatives of sulfamethoxazole and sulfafurazole inhibit intracellular growth of Chlamydia trachomatis.*  
Antimicrobial Agents and Chemotherapy, 2014, 58(5), 2968-2971.
- \* **Lindgren A. E. G.**, Larsson A., Linusson A., Elofsson M.  
*Statistical molecular design: a tool to follow up hits from small-molecule screening.*  
Methods in Molecular Biology, 2014, 1056, 169-188.



# Populärvetenskaplig sammanfattning

## Små molekyler för att identifiera proteiners funktion

Vår arvs massa innehåller cirka 24000 gener som i sin tur innehåller information för hur de tusentals proteiner vi är uppbyggda av ska framställas. Många läkemedel fungerar genom att en molekyl interagerar med ett av dessa proteiner och hämmar dess funktion för att på så sätt framkalla en önskad effekt. Vi vet dock inte vilken funktion många av våra proteiner fyller vilket ofta gör utvecklingen av nya läkemedel svår eller omöjlig. Den första delen av denna avhandling beskriver en grupp proteiner kallade ARTDs och hur små molekyler kan framställas och systematiskt förbättras för att till slut helt kunna slå ut vissa av dessa ARTDs. Genom att sedan studera vilka effekter detta medför kan man ta reda på vilken funktion proteinet fyller. På längre sikt skulle denna kunskap sedan kunna användas för att utveckla nya läkemedel genom att till exempel slå ut de proteiner som orsakar en sjukdom.

## Totalsyntes av naturprodukter

Naturprodukter definieras inom kemin som naturligt förekommande molekyler som produceras av levande organismer. De kan hittas i allt från mikroorganismer och växter till djur och kan vara en del av deras ämnesomsättning, en restprodukt eller ha någon annan funktion, känd eller okänd. Människor, och i vissa fall även andra djur, har sedan urminnes tider ovetandes använt dessa molekyler för en mängd olika syften, som gifter, färgämnen eller läkemedel. Penicillin är en av de mest kända, men mer än hälften av de nya läkemedel som godkänts de senaste trettio åren bygger på naturprodukter eller har inspirerats av dessa. De fortsätter således att vara viktiga för utvecklingen av nya läkemedel trots att vi idag har möjligheten att utveckla sådana från grunden.

Att framställa naturprodukter på konstgjord väg kallas totalsyntes och är ofta en mycket svår och tidskrävande process. Vanligtvis rör det sig om mycket stora och komplexa molekyler och det finns sällan ett uppenbart sätt att genomföra totalsyntesen. För att bättre klara av detta måste nya metoder utvecklas. Den andra delen av denna avhandling beskriver nya metoder för att framställa komplexa molekyler kallade polyfenoler. Målet var att dessa metoder skulle vara så pass flexibla att de även kan användas för att framställa nya polyfenoler som aldrig tidigare existerat men som har förbättrade egenskaper.



# Introduction

## A Brief History of Drug Discovery and Organic Synthesis

Mankind has been using therapeutic plants and minerals to cure diseases for thousands of years. The Chinese “Emperor of the Five Grains” Shen Nong (ca. 2500 BC) allegedly compiled what can be considered the earliest known pharmacopeia which included over 300 medicines, among them *ch’ang shan* containing the antimalarial  $\beta$ -dichroine<sup>1</sup> (Figure 1), and *ma huang* from which ephedrine<sup>2</sup> was later isolated. *Ipecacuanha root*, containing emetine<sup>3</sup>, was used in Brazil to treat dysentery and diarrhea, and coca leaves, containing cocaine<sup>4</sup>, was used in the Andes to overcome fatigue, hunger and thirst. In ancient Greece *hyoscyamus*, containing hyoscyamine<sup>5</sup>, was used as an anaesthetic. During the European Middle Ages *aloe*, containing aloin A<sup>6</sup>, was used as a laxative and during the 17<sup>th</sup> century Thomas Sydenham started using iron<sup>7</sup> to treat iron-deficiency anaemia.<sup>8</sup>

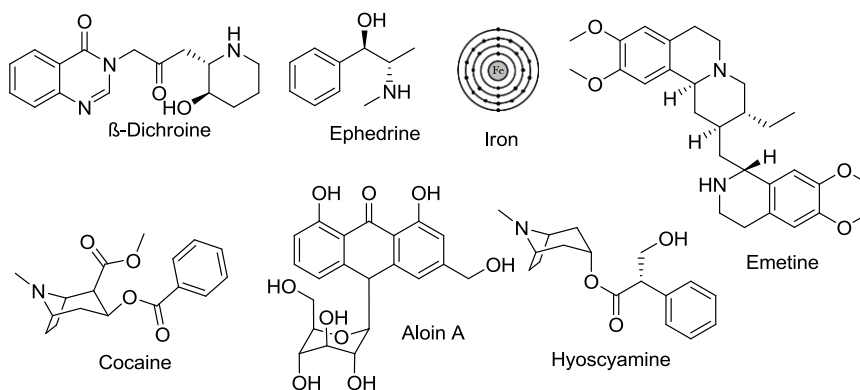


**Figure 1.** The active substances in some of mankind’s early used therapeutics.

These plants and minerals were of course used without knowledge of how, and why, they worked and of the active substances they contained. It was not until the 19th century that the techniques of chemical analysis and synthesis were sufficiently refined in order for organic chemistry to become important in the development of new therapeutics. This started with simple organic compounds such as the accidental synthesis of urea<sup>9</sup> (Figure 2) in 1828 by Friedrich Wöhler (he was trying to prepare ammonium cyanate), acetic acid<sup>10</sup> in 1849 by Adolph Kolbe and methane<sup>11</sup> in 1856 by Pierre Berthelot. William Perkins synthesis of the first synthetic dye, mauveine<sup>12,13</sup>, in 1856 can be considered the starting point for medicinal chemistry. He patented his discovery and started a dyeworks at Greenford. Over the coming decades

many more synthetic dyes were developed, *e.g.* indigo<sup>14</sup> in 1882 by Adolf von Baeyer. The dye industry realized that some of these had therapeutic side effects and by the end of the 19<sup>th</sup> century a pharmaceutical industry was beginning to form. In 1886 acetanilide<sup>15</sup> was introduced as an antipyretic (and later also analgesic) under the name Antifebrin (Figure 3) and in 1897 Felix Hoffman synthesized acetyl salicylic acid<sup>16</sup> which was marketed as Aspirin in 1899.<sup>17,18</sup>

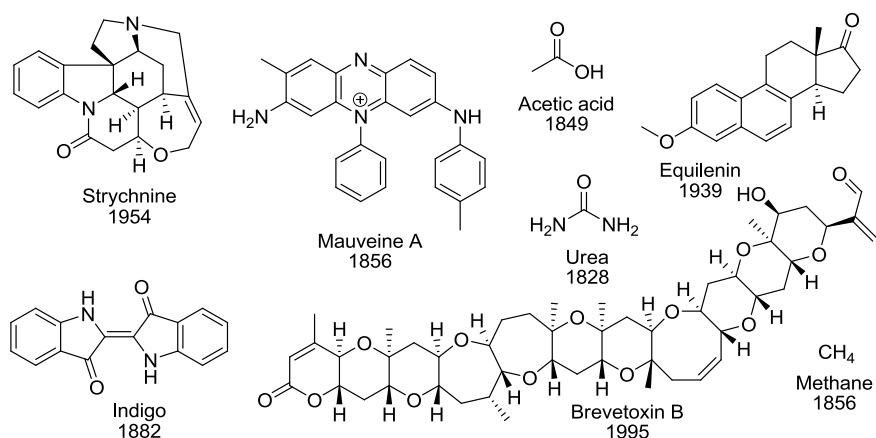


**Figure 2.** Accomplishments in organic synthesis from the 19<sup>th</sup> century until today.

The rapid progress in organic synthetic methodology continued and in 1939 the first steroid, equilenin<sup>19</sup>, was synthesized by Werner E. Bachmann. This was followed by strychnine<sup>20</sup> in 1954 by Robert B. Woodward and in 1995 Kyriacos C. Nicolaou completed the extremely complex brevetoxin B.<sup>21,22</sup> He has until recently been working on what could be considered the crowning achievement of organic synthesis, maitotoxin (Figure 4).<sup>23,24,25,26</sup>

These advances in organic chemistry allowed a more targeted approach for developing new therapeutics. Instead of merely extracting and purifying compounds from plants it became possible to synthesize them in factories and rationally design novel compounds with improved properties. The first of these novel therapeutics was arsphenamine<sup>27</sup>, which was synthesized by Paul Ehrlich in 1907 and introduced to the market in 1910 as Salvarsan. It remained the most effective drug for syphilis until the 1940s when penicillin<sup>28</sup> became available. The middle part of the 20<sup>th</sup> century is often considered the golden age of the pharmaceutical industry with important discoveries such as synthetic vitamins (vitamin D<sub>3</sub><sup>29</sup> in 1927 and vitamin C<sup>30</sup> in 1934), sulfonamides (sulfamidochrysoidin<sup>31</sup> in 1935), hormones (thyroxine<sup>32</sup> in 1955), psychotropics (iproniazid<sup>33</sup> in 1958) and antihistamines (piperoxan<sup>34,35</sup> in 1933). This was also the period when

pharmaceutical research shifted from natural product extraction via modified natural products and finally to novel synthetic compounds.<sup>17,18</sup>

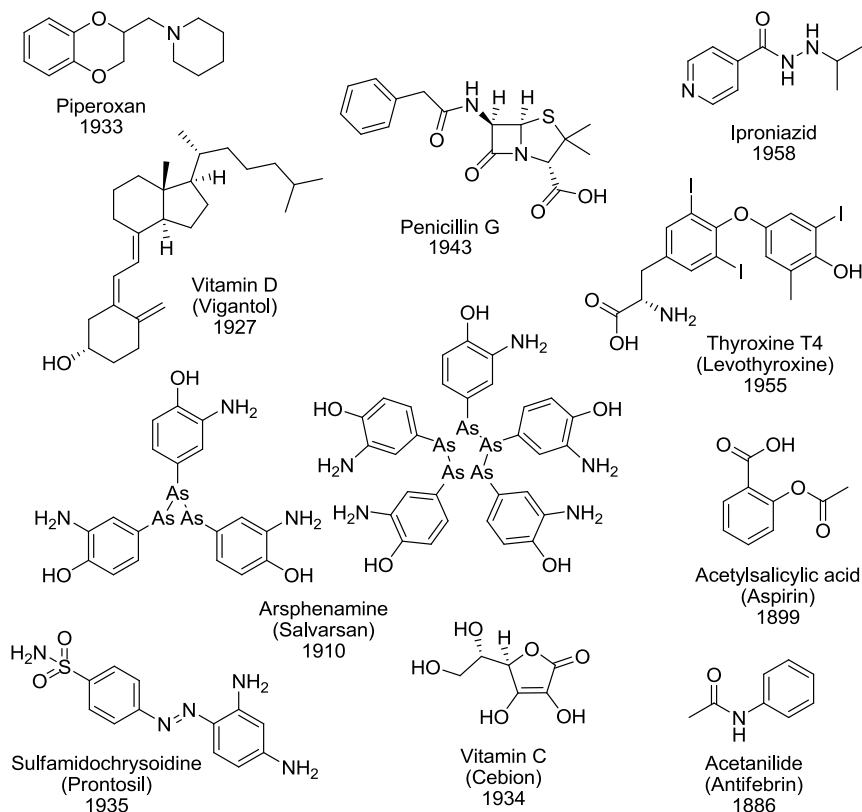


**Figure 3.** Chemical structures of some important pharmaceuticals and the year in which they were first introduced. Salvarsan is a mixture of trimer and pentamer.<sup>36</sup>

During the later part of the 20<sup>th</sup> century the development-cost and -time for new pharmaceuticals rapidly increased<sup>37</sup> and new methods were invented to meet the new challenges the field was facing. Quantitative structure-activity relationships (QSARs) were introduced by Corwin Hansch and Toshio Fujita in 1962 as a mathematical tool to relate the physicochemical properties of compounds to their biological activities.<sup>38,39</sup> In 1958 John Kendrew reported the first X-ray crystal structure of a protein; myoglobin (Figure 5).<sup>40</sup> This laid the groundwork for computational chemistry which began to emerge as a new discipline during the 1970s. The Journal of Computational Chemistry was first published in 1980<sup>41</sup> and computational methods such as using pharmacophores<sup>42,43</sup>, docking<sup>44</sup>, molecular dynamics (MD) simulations<sup>45</sup> and virtual screening (VS)<sup>46</sup> have since become

increasingly important in the development of new pharmaceuticals.<sup>47</sup> High Throughput Screening (HTS), which was introduced in the 1980s and became widely adopted in the 1990s, made it possible to quickly screen large compound libraries to find a suitable starting point for a medicinal chemistry program.<sup>48</sup>

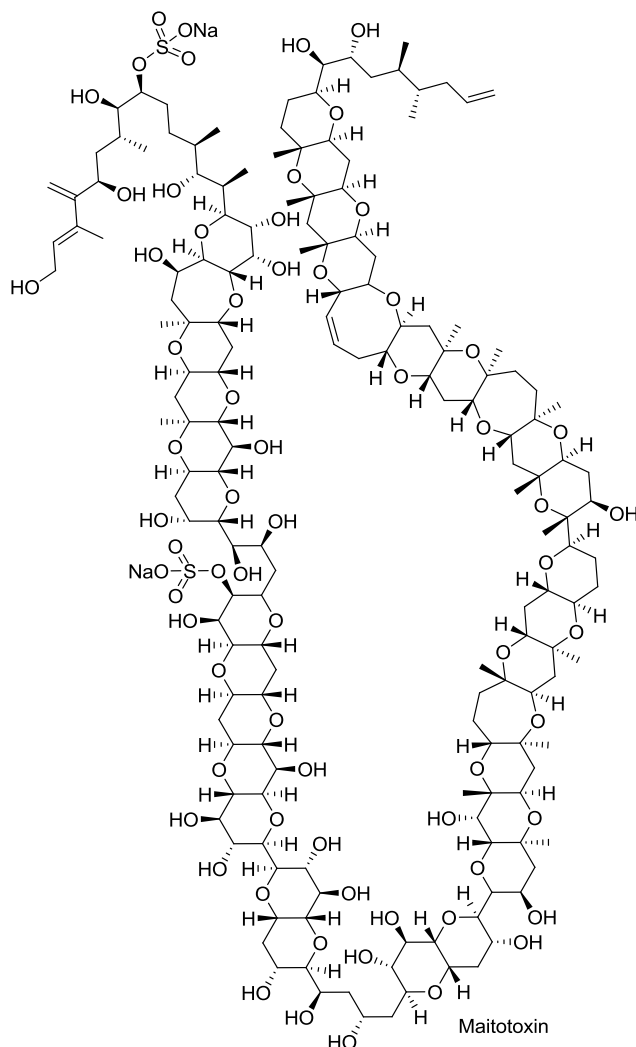


**Figure 4.** Maitotoxin, which is not yet synthesized, contains 32 rings and 98 stereocenters. It was first isolated from the striated surgeonfish whose Tahitian name is *maito* but is actually produced by *Gambierdiscus toxicus*.<sup>49,50,51</sup>

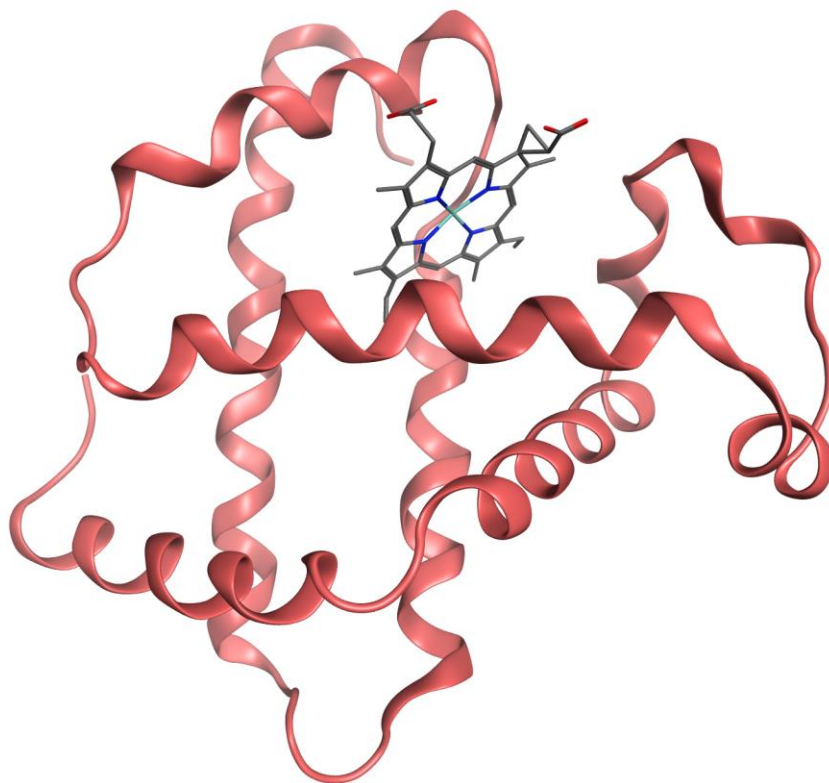


**Figure 5.** The earliest X-ray crystal structure of myoglobin available in the Protein Data Bank, PDB code: 1MBN.<sup>52</sup>

The development of new synthetic methodology has also continued with innovations such as solid phase synthesis<sup>53</sup> in 1963, combinatorial chemistry/parallel synthesis<sup>54</sup> in 1984 and microwave assisted synthesis<sup>55</sup> in the mid 1980s. The latest trend in organic synthesis is flow chemistry<sup>56</sup> which in many cases is a superior alternative to batch reactions.

## Drug Discovery: Diphtheria Toxin-like ADP-Ribosyltransferases

ADP-ribosylation is a post-translational modification involved in *e.g.* DNA repair, protein degradation, transcription regulation, chromatin remodeling, epigenetic events and cell death.<sup>57,58,59</sup> Even though it was discovered more than 50 years ago it is still a poorly understood mechanism and most of the enzymes that catalyze this process are also not fully characterized.<sup>60</sup> Intracellular ADP-ribosylation is catalyzed mainly by the diphtheria toxin-like ADP-ribosyltransferases (ARTDs) which is a group of 17 proteins<sup>61</sup> sharing a conserved catalytic domain (Figure 6).<sup>62</sup> These ARTDs use nicotinamide dinucleotide (NAD<sup>+</sup>) as a cosubstrate to transfer ADP-ribose moieties onto certain acceptor proteins.<sup>60</sup> The ARTDs can be further divided into two subgroups, mono-ADP-ribose transferases (mARTs) which transfer a single ADP-ribose unit onto their targets<sup>61,63,64</sup>, and poly(ADP-ribose) polymerases (PARPs) which transfer ADP-ribose units to construct linear or branched chains of ADP-ribose on their target proteins (Figure 6 and Figure 7).<sup>65</sup> These ADP-ribose chains are recognized by various reader domains and eventually broken down by poly(ADP-ribose) glycohydrolases (PARGs).<sup>66</sup> The entire group of proteins was previously known as PARPs. However, the ARTD nomenclature proposed by Hottiger *et al*<sup>61</sup> will be used throughout this thesis. For clarity the corresponding PARP nomenclature is provided in Figure 6.

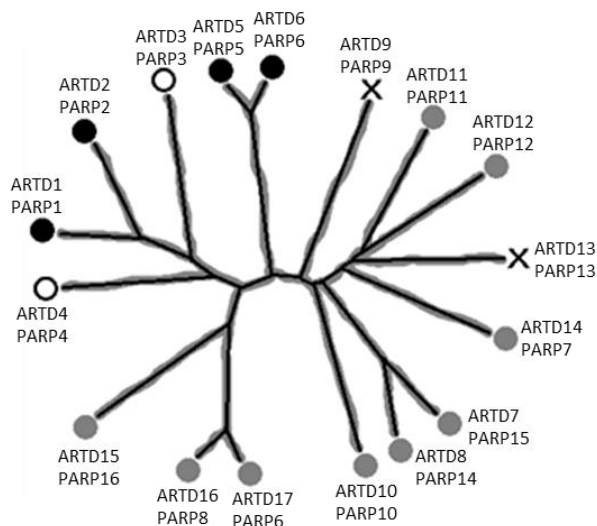


**Figure 6.** Phylogenetic tree of the human diphtheria toxin like ADP-ribosyltransferases (ARTDs). Black circles indicate poly(ADP-ribosylation), grey circles indicate mono(ADP-ribosylation), black rings indicate likely mono-ADP-ribosylation, and crosses indicate putative inactive enzymes.

ARTD1 is the most abundant and best characterized of the ARTD family members. It is a known regulator of DNA base excision repair and is thus an attractive target for cancer and ischemia drug development.<sup>67,68,69,70,71</sup> Inhibiting ARTD1 would enhance the effects of DNA damage during cytotoxic chemo- or radiotherapy treatments and it would also reduce the ARTD1 overactivation due to ischemia.<sup>72,73</sup> The U.S. Food and Drug Administration (FDA) recently approved<sup>74</sup> the first ARTD1 inhibitor, olaparib (Lynparza, Figure 8), for the treatment of advanced ovarian cancer and several other ARTD inhibitors are also in clinical trials.<sup>75</sup> Far less is known about the other ARTDs. However, ARTD3 is similar<sup>76</sup> to ARTD1 and is also involved in DNA repair<sup>77,78,79,80,81</sup>, ARTD7 and ARTD8 are overexpressed in diffuse large B-cell lymphoma.<sup>82</sup> ARTD8 is involved in Stat6-dependant transcription control<sup>83,84,85</sup> and cytokine-regulated control of cellular metabolism<sup>86</sup>, and ARTD10 takes part in the NF- $\kappa$ B signaling pathway.<sup>87</sup>

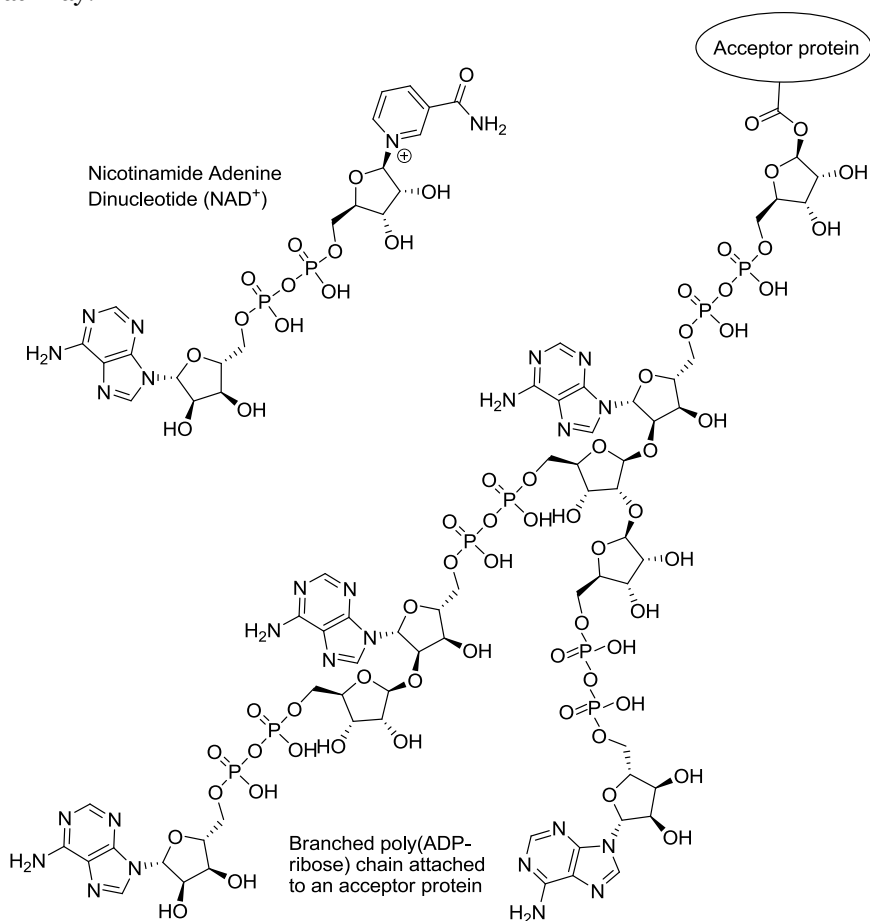


**Figure 7.** Poly(ADP-ribosylation) of an acceptor protein.

Most of the currently available ARTD inhibitors are nicotinamide mimics with poor selectivity between the different ARTDs.<sup>88,89</sup> This makes studying individual ARTDs *in vivo* difficult and selective inhibitors would thus be valuable tools to further our knowledge about these proteins, both in general and as potential therapeutic targets.

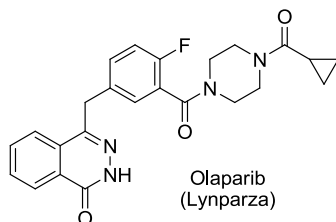


**Figure 8.** Olaparib, developed by KuDOS Pharmaceuticals which was later acquired by AstraZeneca, is an inhibitor of ARTD enzymes and sold under the name Lynparza.

The goal with this project has been to develop small organic molecules, chemical probes<sup>90</sup>, which can selectively inhibit certain ARTDs. A chemical probe can be defined as a compound that specifically binds to and modulates the activity of a particular cellular target. Such compounds would enable the scientific community to study ADP-ribosylation and its biochemical role by selectively inhibiting certain family members and investigate the resulting effects. We have been working mainly with ARTD1, ARTD3, ARTD7, ARTD8, and ARTD10 and by using a combination of synthetic organic chemistry, structural biology and structure based design several new selective inhibitors have been developed.

## Organic Synthesis: Polyphenol Based Natural Products

593 out of the 1130 new chemical entities (NCEs) approved by the FDA for treatment of human diseases between 1981 and 2010 are natural products (50), derivatives of natural product (247) or natural product mimics (296) (Figure 9).<sup>91</sup> Therefore, using natural products as a starting point for drug development is generally considered a promising strategy.<sup>92</sup>

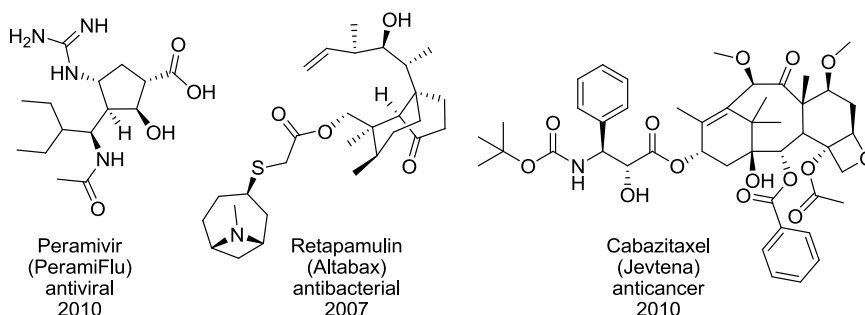


**Figure 9.** Structure, trade name, therapeutic area and introduction year for three natural product derived drugs.<sup>91</sup>

Polyphenols can be defined as “...*water-soluble plant phenolic compounds having molecular masses ranging from 500 to 3000-4000 Da and possessing 12-16 phenolic hydroxy groups on five to seven aromatic rings per 1000 Da of relative molecular mass. Furthermore the compounds should undergo the usual phenolic reactions and have the ability to precipitate some alkaloids, gelatin, and other proteins from solution*”.<sup>93,94</sup> They are a large group of plant-derived natural products often present in fruits, seeds, and vegetables and can be divided into three classes, proanthocyanidins, gallo-/ellagitannins and phlorotannins (Figure 10). Polyphenols were previously known as vegetable tannins due to their use in the preparation of animal skins to leather. It was not until the second half of the 20<sup>th</sup> century that research on polyphenols started to investigate their use beyond the tanning of leather. This has also led to wider definitions of polyphenols. The consumption of foodstuffs containing these compounds has often been considered beneficial to human health due to their ability to scavenge free radicals and thus reduce the likelihood of age-related diseases. This ability has over time become a defining property of polyphenols despite not being included in the definition above.<sup>93</sup>

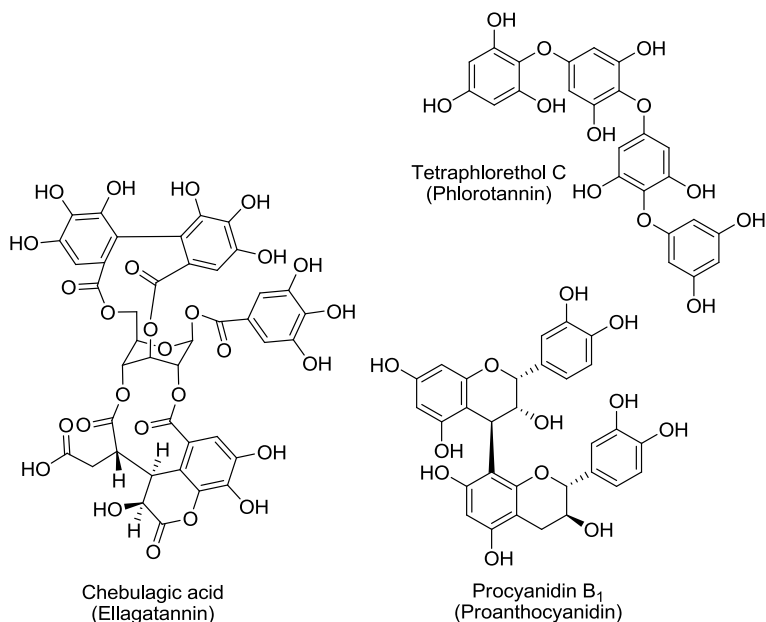


**Figure 10.** The structures of three polyphenols, one from each class.

(-)-Hopeaphenol<sup>95</sup>, which is a tetramer of resveratrol (Figure 11), was isolated from the stem bark of the south East Asian tree *Hopea hainanensis*. The Eskitis Institute at Griffith University in Brisbane, Australia, performed a screening campaign aimed at finding *Yersinia pseudotuberculosis* type III secretion system (T3SS) inhibitors. The screening was successful and (-)-hopeaphenol, among others, were identified as an inhibitor of the T3SS.<sup>96,97</sup> The T3SS is a conserved virulence system found in the gram-negative bacteria *Yersinia pseudotuberculosis* and *Pseudomonas aeruginosa*. It is essential for these pathogens to cause disease and is therefore an attractive target for the development of new antibacterial agents.<sup>98,99,100,101,102,103,104,105,106,107,108</sup>

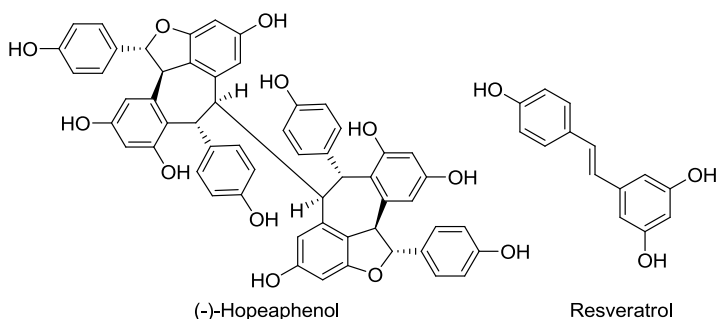


**Figure 11.** The structures of (-)-hopeaphenol which is a tetramer of resveratrol.

We wanted to investigate whether the entire tetrameric structure of (-)-hopeaphenol is crucial or if it could be reduced to a resveratrol dimer such as  $\epsilon$ -viniferin or its cyclized analog ampelopsin B (Figure 12). Biomimetic approaches for synthesizing ( $\pm$ )- $\epsilon$ -viniferin by an oxidative dimerization of resveratrol is already described and the following cyclization to form ( $\pm$ )-ampelopsin B is published as well.<sup>109,110,111</sup> However, we needed an adaptable and divergent synthetic route that allowed the synthesis of analogs with altered substitution patterns in order to further study the chemical and biological properties of resveratrol oligomers.

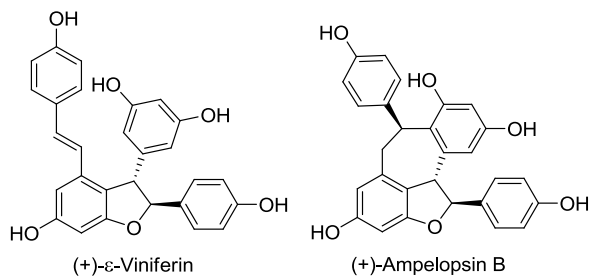


**Figure 12.** The structures of (+)- $\epsilon$ -viniferin and ampelopsin B.



# Chapter 1: Development of ARTD3 Inhibitors (Paper I + II)

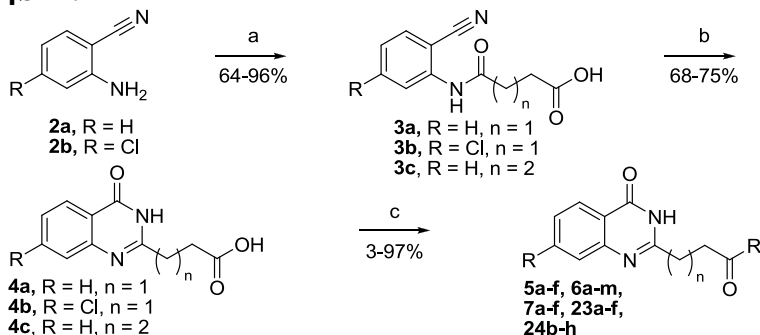
To investigate isoenzyme selectivity, a library consisting of 185 NAD<sup>+</sup> mimics was previously screened against 13 of the ARTD family members using a thermal shift assay.<sup>88</sup> This assay assumes that a protein-compound complex will have a higher melting point than the same protein without a bound ligand. In brief, protein and library compounds (in PBS buffer and with TCEP and SyproOrange) were mixed. Thermal stability was then measured by monitoring SyproOrange fluorescence while heating the samples. The difference in transition midpoints was then calculated for each sample and presented as  $\Delta T_m$ . In this screen, the racemic quinazolinone **1** (Table 1) was identified as a suitable starting point for a medicinal chemistry program aimed at finding ARTD3 selective chemical probes. The choice of this compound was rationalised by the high thermal shift, indicating tight binding, and seemingly good selectivity against ARTD3. In addition, the compound had advantageous properties such as low molecular weight and low lipophilicity. A straightforward synthetic route could also be visualized where a large degree of diversity could be introduced in the final amide coupling (Scheme 1).

**Table 1.** Thermal shift data for compound **1**<sup>a</sup>.

Entry	ID	Structure	ARTD3	ARTD1	ARTD2	ARTD5	ARTD8
			$\Delta T_m$ (°C)	$\Delta T_m$ (°C)	$\Delta T_m$ (°C)	$\Delta T_m$ (°C)	$\Delta T_m$ (°C)
1	<b>1</b>		8.46 ± 0.17	1.98 ± 0.06	1.35 ± 0.43	0.00 ± 0.04	-0.29 ± 0.51

<sup>a</sup>ARTD3 is more closely related to ARTD1 and ARTD2 than ARTD5 and ARTD8, see also the phylogenetic tree in Figure 6.

**Scheme 1.** Synthetic route to target compounds **5a-f**, **6a-m**, **7a-f**, **23a-f** and **24b-h**<sup>a</sup>.



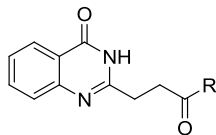
<sup>a</sup>Reagents and conditions: (a) succinic or glutaric anhydride, toluene, 90 °C, 3-18 h; (b) K<sub>2</sub>CO<sub>3</sub>, UHP, H<sub>2</sub>O:acetone 1:1, 82 °C, 18-40 h; (c) amine, amide coupling reagents, DMF, 20 °C, overnight.

## Initial Compounds

Since compound **1** was tested as a racemate the first priority was to assess the importance of the methyl group and stereochemistry at the *meso* position. The two enantiomers were synthesized separately according to Scheme 1. Simultaneously, the nitrogen in the pyridinyl ring was investigated since benzyl amines are readily available while pyridinyl analogs are scarce. Two indanyl analogs were also synthesized so that the effects of more rigid structures could be understood.

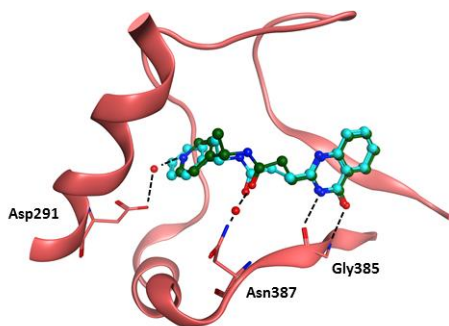
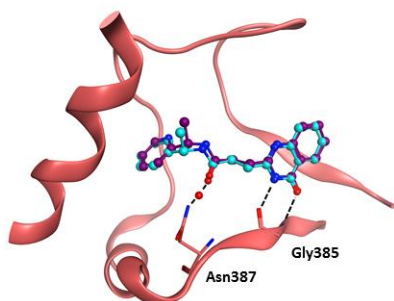
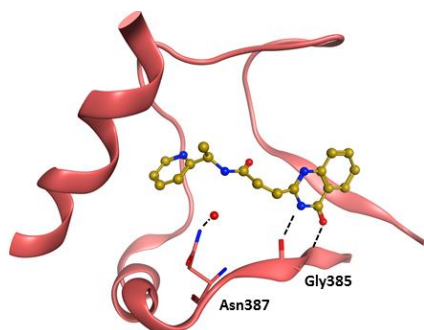
A general synthetic route to these compounds is shown in Scheme 1. Aminobenzonitrile **2a** reacted with succinic anhydride to give anilide **3a** which was cyclized to quinazolinone **4a** under alkaline conditions. The target compounds, **5a-f**, were then obtained using DIC/HOAt together with the required amines. (*R*)- and (*S*)-1-(pyridin-2-yl)ethanamine, used for **5c** and **d**, were not commercially available and had to be synthesized from the corresponding alcohols. DPPA was used to convert the hydroxygroups into azides which were then reduced using Staudinger conditions.<sup>112</sup>

**Table 2:** Thermal shift measurements for the initial compounds, **5a-i**, against five members of the ARTD family.



Entry	ID	R	ARTD3 $\Delta T_m$ (°C)	ARTD1 $\Delta T_m$ (°C)	ARTD2 $\Delta T_m$ (°C)	ARTD5 $\Delta T_m$ (°C)	ARTD8 $\Delta T_m$ (°C)
1	<b>5a</b>		5.97 $\pm 0.47$	3.05 $\pm 0.03$	1.95 $\pm 0.18$	0.35 $\pm 0.02$	-0.22 $\pm 0.12$
2	<b>5b</b>		8.45 $\pm 0.59$	1.80 $\pm 0.05$	1.16 $\pm 0.10$	0.13 $\pm 0.05$	-0.23 $\pm 0.08$
3	<b>5c</b>		4.79 $\pm 0.21$	2.35 $\pm 0.08$	1.26 $\pm 0.25$	0.12 $\pm 0.05$	-0.23 $\pm 0.06$
4	<b>5d</b>		9.71 $\pm 0.39$	1.96 $\pm 0.24$	0.74 $\pm 0.55$	0.13 $\pm 0.06$	0.31 $\pm 0.25$
5	<b>5e</b>		6.84 $\pm 0.14$	2.37 $\pm 0.01$	1.92 $\pm 0.27$	0.80 $\pm 0.07$	0.10 $\pm 0.28$
6	<b>5f</b>		6.72 $\pm 0.49$	2.38 $\pm 0.05$	1.39 $\pm 0.08$	0.84 $\pm 0.07$	0.18 $\pm 0.09$
7 <sup>a</sup>	<b>5g</b>		2.63 $\pm 0.30$	2.16 $\pm 0.03$	1.77 $\pm 0.22$	0.32 $\pm 0.06$	-0.28 $\pm 0.19$
8 <sup>a</sup>	<b>5h</b>		4.83 $\pm 0.26$	1.93 $\pm 0.02$	1.48 $\pm 0.15$	0.15 $\pm 0.08$	-0.25 $\pm 0.04$
9 <sup>a,b</sup>	<b>5i</b>		5.02 $\pm 0.52$	2.68 $\pm 0.01$	1.82 $\pm 0.59$	0.30 $\pm 0.05$	0.00 $\pm 0.12$

<sup>a</sup>Commercial compound included in the screened library. <sup>b</sup>Racemic mixture.

**a****b****c**

**Figure 13.** X-ray crystal structures of inhibitors in complex with ARTD3. Important interactions with Gly385, Asn387 and Asp291 are shown. (a) Due to a water-mediated hydrogen bond, the pyridine of **5i** (green, PDB ID 4L6Z) ring is anchored ca 1 Å outward compared to **5b** (teal, PDB ID 4GV4). Despite being a racemic mixture only the *S*-enantiomer of **5i** was observed in the X-ray crystal structure. (b) **5b** (teal) and **5d** (purple, PDB ID 4GV0) share a similar binding pose and the pyridinyl nitrogen does not find any additional interactions. (c) The amide group in **5c** (PDB ID 4GV2) is rotated away from Asn387 resulting in the loss of a hydrogen bond interaction.

Compounds **5a-i** were evaluated using the previously mentioned thermal shift assay and the results are presented in Table 2. In brief, the *S*-enantiomers **5b** and **d** exhibited higher thermal stabilization and better selectivity towards ARTD3 compared to the *R*-enantiomers **5a** and **c**. Also, the methyl group at the *meso* position seems critical as the indanes (**5e** and **f**) and unsubstituted analogs (**5g** and **h**) dropped in both affinity and selectivity. Curiously, removing the pyridinyl nitrogen (**5b**) did not impair the affinity or selectivity for ARTD3 while shifting it to *para* position (**5i**) seemed unfavorable. X-ray crystal structures of **5b-d** and **5i** in complex with ARTD3 were obtained in an attempt to explain these observations at a molecular level. The pyridinyl nitrogen in **5i** is involved in a water-mediated hydrogen bond to the side chain carbonyl group in Asp291, this anchors the pyridin ring ca. 1 Å outward from the binding pocket compared to **5b** resulting in reduced ARTD3 affinity (Figure 13a). As can be seen in Figure 13b compounds **5b** and **d** have similar binding poses and the protein conformation is highly conserved. The pyridinyl nitrogen does not find any additional interactions explaining these compounds similar affinity for ARTD3. Both compounds also take part in a water-mediated hydrogen bond between the amide and Asn387. Since the amide group in **5c** is rotated away from Asn387 this hydrogen bond is lost which can explain the lower affinity of this compound (Figure 13c). When these crystals were grown in presence of racemic **1** only **5d** was observed in the X-ray crystal structure, consistent with the inability of **5c** to thermally stabilize ARTD3.

## Other Substituents at the Meso Position

Based on the  $\Delta T_m$  values and the fact that no additional interactions to ARTD3 were found for the pyridinyl compounds (**5c** and **d**) it was concluded that this nitrogen is nonessential and that the ensuing work therefore should focus on ordinary or substituted phenyl rings, instead of heterocycles, in this position. The observed bifurcated interaction between the amide part of the quinazolinone and Gly385 is a well known feature of nicotinamide mimetic ARTD inhibitors.<sup>88,113</sup> It anchors these inhibitors inside the active site and this part of the compound should therefore be left unaltered.

Using this information, another series of compounds (Table 3) was designed in order to further investigate the importance of the stereochemistry and functionalization at the *meso* position. Compounds **6a-d** investigated if the methyl group could be replaced with a larger substituent. Compound **6e** was used to further study the effects of rigidifying **5g** and **6f-j** probed if the stereocenter could be removed and the effects of homobenzylic amides. Three compounds (**6k-m**) where a chlorine is added to C7 on the quinazolinone were also synthesized to see if small lipophilic

substituents were accepted in this part of the binding pocket. These compounds were synthesized according to the above procedure (Scheme 1) with the exception that HATU replaced DIC/HOAt in some cases due to difficulties with purification. The low yields in some of the final amide couplings are also attributed to these problems since quantitative conversion was generally observed and no side products derivable from **4b** were identified.

Most of these compounds displayed poor to modest affinity towards ARTD3 compared to **5b** and **d**. The binding pose of **6a** is very similar to that of **5b** despite the considerably lower  $\Delta T_m$  (Figure 14). The reason for this behaviour is unclear. Compound **6j** is the exception which despite slightly worse selectivity was comparable to the top-ranked compounds in terms of affinity. The thermal shifts also indicated that the chlorine substituent at C7 was disadvantageous as these three compounds, **6k-m**, showed poor ARTD3 affinity and two of them were selective towards ARTD1 or ARTD2.

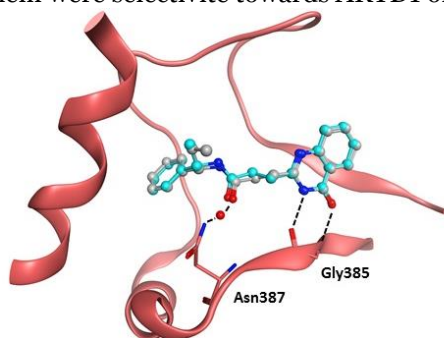


**Figure 14.** The X-ray crystal structure of compounds **5b** (teal) and **6a** (grey, PDB ID 4L70) in ARTD3. They have similar binding poses despite their different ability to stabilize ARTD3

**Table 3:** Thermal shift measurements for compounds **6a-r** against five members of the ARTD family.

Entry	ID	R	R'	ARTD3 $\Delta T_m$ (°C)	ARTD1 $\Delta T_m$ (°C)	ARTD2 $\Delta T_m$ (°C)	ARTD5 $\Delta T_m$ (°C)	ARTD8 $\Delta T_m$ (°C)
1	<b>6a</b>	H		2.80 $\pm 0.15$	1.49 $\pm 0.02$	0.94 $\pm 0.14$	0.33 $\pm 0.06$	0.31 $\pm 0.08$
2 <sup>b</sup>	<b>6b</b>	H		5.96 $\pm 0.36$	0.9 $\pm 0.03$	0.74 $\pm 0.16$	0.44 $\pm 0.04$	0.16 $\pm 0.10$

3	<b>6c</b>	H		0.20 ± 0.04	0.2 ± 0.06	0.30 ± 0.27	0.22 ± 0.02	0.45 ± 0.54
4	<b>6d</b>	H		3.57 ± 0.31	2.83 ± 0.07	1.64 ± 0.12	0.82 ± 0.13	0.38 ± 0.42
5	<b>6e</b>	H		4.73 ± 0.14	1.15 ± 0.16	-0.17 ± 0.18	0.14 ± 0.11	-0.07 ± 0.01
6	<b>6f</b>	H		5.39 ± 0.40	1.85 ± 0.12	1.64 ± 0.14	0.48 ± 0.03	0.26 ± 0.13
7	<b>6g</b>	H		3.29 ± 0.42	4.00 ± 0.16	0.53 ± 0.39	0.97 ± 0.05	-0.11 ± 0.21
8	<b>6h</b>	H		6.31 ± 0.64	2.79 ± 0.11	1.30 ± 0.35	0.70 ± 0.06	-0.27 ± 0.04
9	<b>6i</b>	H		6.23 ± 0.27	2.83 ± 0.05	1.57 ± 0.19	0.49 ± 0.02	0.20 ± 0.39
10	<b>6j</b>	H		9.82 ± 0.39	3.59 ± 0.02	1.37 ± 0.17	0.60 ± 0.05	0.08 ± 0.16
11	<b>6k</b>	Cl		0.16 ± 0.05	0.92 ± 0.23	1.28 ± 0.21	0.43 ± 0.04	0.05 ± 0.34
12	<b>6l</b>	Cl		0.35 ± 0.10	0.11 ± 0.06	0.83 ± 0.18	0.20 ± 0.17	0.82 ± 0.05
13	<b>6m</b>	Cl		0.50 ± 0.06	0.76 ± 0.08	0.98 ± 0.03	0.36 ± 0.04	-0.25 ± 0.13
14	<b>6n</b>	H		2.28 ± 0.47	2.44 ± 0.06	1.11 ± 0.21	1.83 ± 0.03	0.24 ± 0.05
15	<b>6o</b>	H		2.96 ± 0.34	1.45 ± 0.06	1.14 ± 0.21	0.54 ± 0.10	0.23 ± 0.29
16 <sup>a</sup>	<b>6p</b>	H		0.45 ± 0.07	2.17 ± 0.10	0.77 ± 0.22	0.52 ± 0.01	-0.28 ± 0.88
17	<b>6q</b>	H		4.20 ± 0.12	3.11 ± 0.07	1.37 ± 0.24	0.69 ± 0.13	0.69 ± 0.18
18	<b>6r</b>	H		0.78 ± 0.23	3.39 ± 0.04	1.35 ± 0.19	0.96 ± 0.02	0.31 ± 0.62

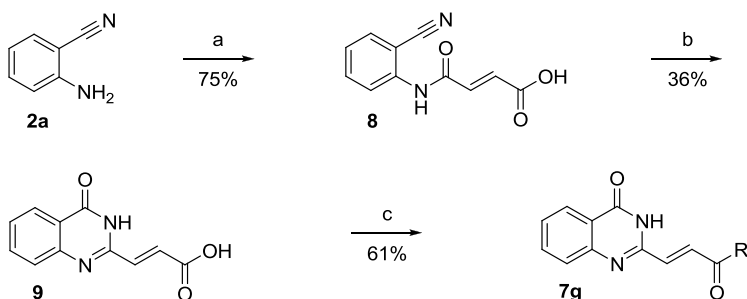
<sup>a</sup>Racemic mixture.

## The Linker Region

The ethylene linker connecting the quinazolinone to the amide part of the compounds was also investigated. It appeared that by elongating the linker from ethylene to propylene it should be possible to find interactions similar to those of **6j**. This synthesis proceeded smoothly according to Scheme 1 by

replacing succinic anhydride with glutaric anhydride and then cyclize the product under alkaline conditions to reach **4c**. We expected that forcing the ligands into a different binding pose by replacing the ethylene linker with an ethynylene equivalent should impair the affinity. In order to verify this, intermediate **9** was prepared analogously (Scheme 2) by replacing succinic anhydride with fumaryl chloride. Target compounds **7a-g** (Table 4) were then obtained using the previously described HATU mediated amide coupling protocol. The low yields in some of these reactions are again attributed to difficulties with purification as quantitative conversion was generally observed.

**Scheme 2.** Synthetic route to target compound **7g**<sup>a</sup>.



<sup>a</sup>Reagents and conditions: (a) fumaryl chloride, chloroform, 20 °C, 30 min; (b) K<sub>2</sub>CO<sub>3</sub>, UHP, H<sub>2</sub>O:acetone 1:1, 82 °C, 3 d; (c) (S)-1-phenylethylamine, HATU, TEA, DMF, 20 °C, 18 h.

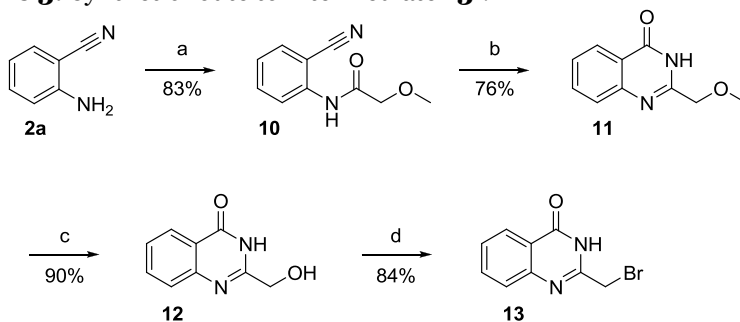
We also wanted to investigate the effects of a shorter linker (**7h** and **i**, Table 4) and of additional possibilities for hydrogen bonds by replacing the amide group with a urea moiety (**7j** and **k**). The same synthetic route was used for these four compounds up to intermediate **13** (Scheme 3), after which the synthesis diverged. Intermediate **13** was prepared starting from 2-aminobenzonitrile (**2a**) which was acylated to form anilide **10** using methoxyacetyl chloride. This compound was subsequently cyclized to quinazolinone **11** under alkaline conditions after which the methoxy ether was cleaved in 47% HBr to form alcohol **12**. The alcohol was further transformed to bromide **13** under Appel conditions<sup>114</sup> using CBr<sub>4</sub> and PPh<sub>3</sub>.<sup>115</sup>

**Table 4:** Thermal shift measurements for compounds **7a-k** against five members of the ARTD family.

Entry	ID	X	R	ARTD3 $\Delta T_m(^{\circ}\text{C})$	ARTD1 $\Delta T_m(^{\circ}\text{C})$	ARTD2 $\Delta T_m(^{\circ}\text{C})$	ARTD5 $\Delta T_m(^{\circ}\text{C})$	ARTD8 $\Delta T_m(^{\circ}\text{C})$
1	<b>7a</b>	CH <sub>2</sub> CH <sub>2</sub> CH <sub>2</sub>		4.27 $\pm 0.15$	1.56 $\pm 0.04$	0.21 $\pm 0.25$	1.37 $\pm 0.02$	-0.05 $\pm 0.19$
2	<b>7b</b>	CH <sub>2</sub> CH <sub>2</sub> CH <sub>2</sub>		4.58 $\pm 0.25$	1.51 $\pm 0.06$	0.37 $\pm 0.32$	0.52 $\pm 0.10$	-0.21 $\pm 0.14$
3	<b>7c</b>	CH <sub>2</sub> CH <sub>2</sub> CH <sub>2</sub>		3.46 $\pm 0.06$	1.52 $\pm 0.14$	2.29 $\pm 0.16$	1.20 $\pm 0.03$	0.13 $\pm 0.24$
4	<b>7d</b>	CH <sub>2</sub> CH <sub>2</sub> CH <sub>2</sub>		4.69 $\pm 0.18$	1.88 $\pm 0.24$	1.27 $\pm 0.33$	0.59 $\pm 0.05$	-0.18 $\pm 0.17$
5	<b>7e</b>	CH <sub>2</sub> CH <sub>2</sub> CH <sub>2</sub>		0.09 $\pm 0.06$	0.44 $\pm 0.19$	0.53 $\pm 0.17$	0.41 $\pm 0.05$	0.02 $\pm 0.26$
6	<b>7f</b>	CH <sub>2</sub> CH <sub>2</sub> CH <sub>2</sub>		3.22 $\pm 0.17$	2.90 $\pm 0.05$	1.84 $\pm 0.08$	1.05 $\pm 0.04$	0.53 $\pm 0.17$
7	<b>7g</b>	( <i>E</i> )-CHCH		0.22 $\pm 0.06$	1.22 $\pm 0.01$	-0.67 $\pm 0.08$	0.42 $\pm 0.06$	-0.07 $\pm 0.13$
8	<b>7h</b>	CH <sub>2</sub>		0.63 $\pm 0.16$	0.37 $\pm 0.12$	-0.25 $\pm 0.09$	0.05 $\pm 0.02$	-0.04 $\pm 0.13$
9	<b>7i</b>	CH <sub>2</sub>		0.43 $\pm 0.02$	0.31 $\pm 0.07$	-0.01 $\pm 0.21$	0.01 $\pm 0.02$	0.04 $\pm 0.09$
10	<b>7j</b>	CH <sub>2</sub> NH		4.95 $\pm 0.45$	0.88 $\pm 0.01$	0.33 $\pm 0.29$	0.39 $\pm 0.04$	-0.77 $\pm 0.25$
11	<b>7k</b>	CH <sub>2</sub> NH		2.91 $\pm 0.05$	0.65 $\pm 0.22$	-0.23 $\pm 0.18$	0.34 $\pm 0.11$	-1.05 $\pm 0.73$

To reach target compounds **7h** and **i** intermediate **13** was first reacted with KCN to form nitrile **14** (Scheme 4). This was then dissolved in ethanol and treated with acetyl chloride to form an imino ether which was hydrolyzed to ethyl ester **15** upon the addition of water. Target compounds **7h** and **i** were then obtained by direct transamidation of **15**.

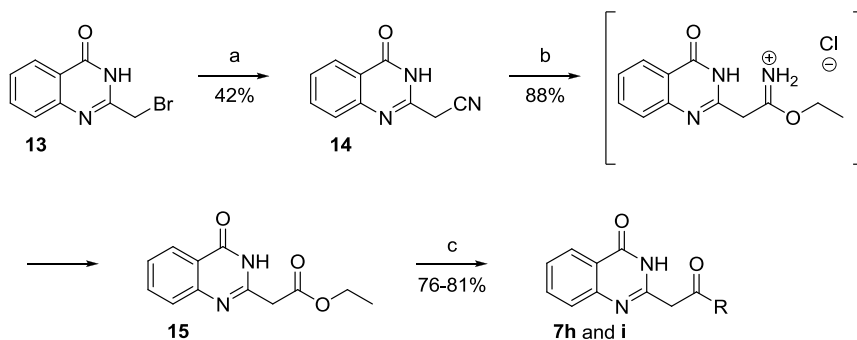
**Scheme 3.** Synthetic route to intermediate **13**<sup>a</sup>.



<sup>a</sup>Reagents and conditions: (a) methoxyacetyl chloride, pyridine, DMF, 20 °C, 24 h; (b) K<sub>2</sub>CO<sub>3</sub>, UHP, H<sub>2</sub>O:acetone 1:1, 82 °C, 22 h; (c) 47% HBr, 120 °C, 5 h; (d) PPh<sub>3</sub>, CBr<sub>4</sub>, DCM, 0 to 20 °C, 20 h.

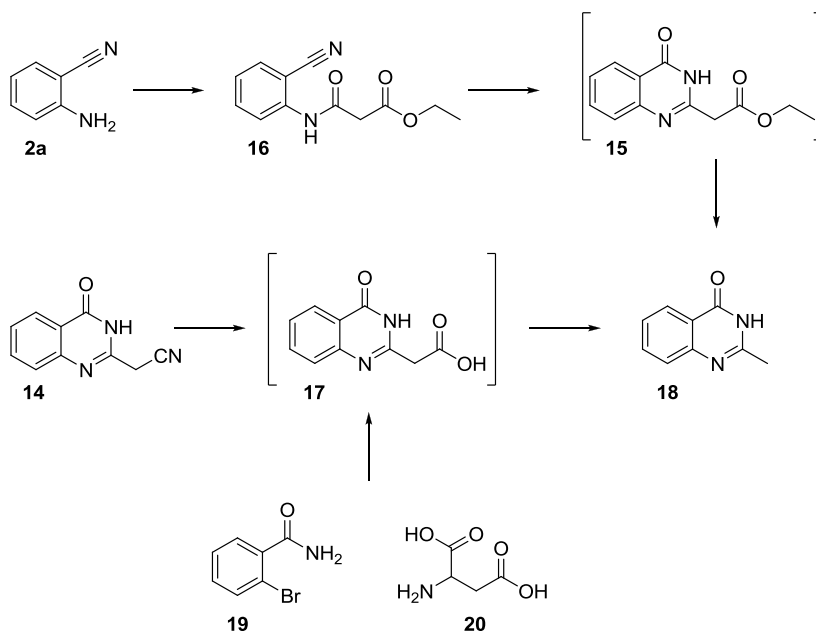
Several other methods of synthesizing **7h** and **i** in fewer reaction steps were also examined. Reacting **2a** with ethyl(chloroformyl) acetate gave anilide **16** which upon cyclization decarboxylated to form **18** instead of **15** (Scheme 5). Acidic hydrolysis of **14** also lead to decarboxylation, as did the CuBr catalyzed one-step synthesis of **17** starting from 2-bromobenzamide (**19**) and aspartic acid (**20**).<sup>116</sup> Palladium catalyzed aminocarbonylation of **13** using Mo(CO)<sub>6</sub> as CO-source,<sup>117,118</sup> successfully produced the target compounds but in less than 5% yield since compound **13** rapidly decomposed under these conditions.

**Scheme 4.** Synthetic route to target compounds **7h** and **i**<sup>a</sup>.



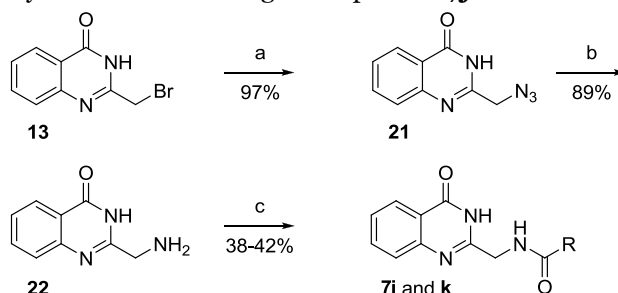
<sup>a</sup>Reagents and conditions: (a) KCN, DMF:H<sub>2</sub>O 2:1, 80 °C, 4 h; (b) AcCl, EtOH, 20 °C, 6 h then H<sub>2</sub>O; (c) amine, 45 °C, 20 h.

**Scheme 5.** Failed attempts at synthesizing **7h** and **i** in fewer reaction steps.



Synthesizing the two urea derivatives, **7j** and **k**, was straightforward starting from intermediate **13** which was treated with  $\text{NaN}_3$  to form **21** (Scheme 6). The azido group was then reduced using Staudinger conditions<sup>112</sup> with  $\text{PPh}_3$  and water to form the corresponding amine, **22**. Compounds **7j** and **k** were obtained by reacting these amines with triphosgene to form their isocyanate analogs which reacted with **22** to give the urea derivatives.

**Scheme 6.** Synthetic route to target compounds **7j** and **k**<sup>a</sup>.



<sup>a</sup>Reagents and conditions: (a)  $\text{NaN}_3$ , Acetone: $\text{H}_2\text{O}$  2:1, 70 °C, 20 min; (b)  $\text{PPh}_3$ ,  $\text{H}_2\text{O}$ , THF, 20 °C, 19 h; (c) amine, triphosgene, EtOAc, 80 °C, 4 h, then THF, 20 °C, 3 h.

The six compounds with an elongated linker, **7a-f**, all displayed reduced affinity for ARTD3. While this reduction was modest for most of these

compounds, **7b** showed a large drop in affinity compared to its analog **5b**. The almost completely abolished affinity for **7g** confirmed the hypothesis that the introduction of a double bond in the linker region would force the ligand into an unfavorable binding pose and thus reduce its ability to stabilize ARTD3. **7h** and **i**, both with a shortened linker, displayed similar results. Replacing the amide with a urea moiety did not seem to produce any additional beneficial interactions since **7k** maintained a similar affinity to its amide analog while **7j** was considerably worse.

## Aromatic Substituents

Modifications to the linker, different substituents at the *meso* position and addition of chlorine to C7 in the quinazolinone all reduced the potency of these compounds. What remained to be investigated was analogs to **5b** with additional substituents on the phenyl ring.

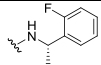
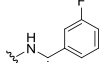
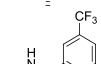
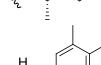
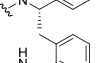
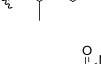
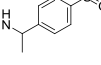
According to the X-ray crystal structure of **5b** in complex with ARTD3 (Figure 13b), substituents larger than fluorine were unlikely to be accepted at the *ortho* position due to steric clashes with the protein. *Meta* substituents larger than chlorine would similarly not fit in the binding pocket without a major change in binding pose. More space was available at the *para* position. However, thermal shift measurements for the two commercial compounds **23h** and **i** (Table 5) suggested that large substituents here would increase ARTD1 affinity. Thus, we decided not to introduce anything larger than a chlorine.

These compounds were all synthesized according to Scheme 1 and were all remarkably difficult to dissolve. Since they also produced low thermal shifts against ARTD3 (Table 5) it was decided not to further investigate aromatic substituents.

**Table 5:** Thermal shift measurements for compounds **23a-i** against five members of the ARTD family.

The structure shows a quinazolinone ring system (a benzene ring fused to a six-membered ring containing a nitrogen and a carbonyl group). A linker consisting of a methylene group, a nitrogen atom, and another methylene group is attached to the nitrogen of the six-membered ring. The terminal methylene group is connected to a carbonyl group, which is further attached to an R substituent.

Entry	ID	R	ARTD3 $\Delta T_m$ (°C)	ARTD1 $\Delta T_m$ (°C)	ARTD2 $\Delta T_m$ (°C)	ARTD5 $\Delta T_m$ (°C)	ARTD8 $\Delta T_m$ (°C)
1	<b>23a</b>		0.20 $\pm 0.08$	0.26 $\pm 0.07$	-0.48 $\pm 0.14$	0.29 $\pm 0.09$	-0.10 $\pm 0.19$
2	<b>23b</b>		0.12 $\pm 0.07$	0.04 $\pm 0.07$	-0.59 $\pm 0.05$	0.18 $\pm 0.04$	0.04 $\pm 0.20$

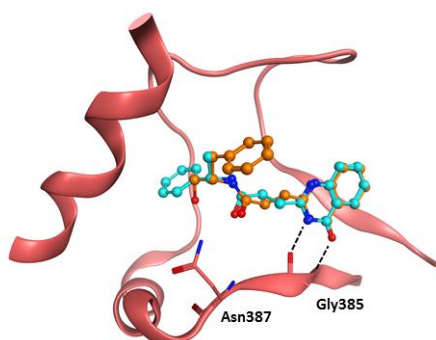
3	<b>23c</b>		0.42 ± 0.24	0.36 ± 0.05	-0.46 ± 0.64	0.12 ± 0.34	0.12 ± 0.16
4	<b>23d</b>		0.75 ± 0.14	1.00 ± 0.57	0.06 ± 0.56	0.13 ± 0.40	-0.18 ± 0.14
5	<b>23e</b>		0.69 ± 0.27	0.25 ± 0.17	-0.60 ± 0.16	0.23 ± 0.09	-0.37 ± 0.10
6	<b>23f</b>		0.74 ± 0.13	0.22 ± 0.16	-0.47 ± 0.19	0.22 ± 0.06	-0.22 ± 0.20
7 <sup>a,b</sup>	<b>23g</b>		3.07 ± 0.19	2.00 ± 0.05	0.87 ± 0.17	0.44 ± 0.05	0.57 ± 0.09
8 <sup>a,b</sup>	<b>23h</b>		6.89 ± 0.35	3.36 ± 0.07	1.49 ± 0.19	1.94 ± 0.06	0.02 ± 0.18
9 <sup>a,b</sup>	<b>23i</b>		7.79 ± 0.19	6.17 ± 0.13	1.61 ± 0.43	0.64 ± 0.10	0.05 ± 0.14

<sup>a</sup>Commercial compound included in the screened library. <sup>b</sup>Racemic mixture.

## Homobenzylic and $\alpha$ -Amino Acid Analogs

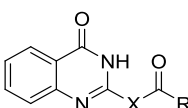
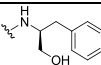
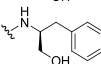
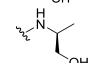
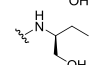
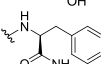
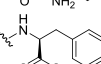
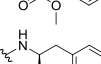
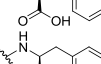
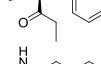
So far, all modifications to **5b** decreased the affinity towards ARTD3. The one exception to this was **6j** which still showed excellent  $\Delta T_m$  values. This required further investigation and after solving the X-ray crystal structure of **6j** in complex with ARTD3 (Figure 15) it was realized that this compound had a very different binding pose compared to **5b** and **d**. The amide part was rotated 180° and the phenyl ring was pointing out of the binding pocket. A final series of ARTD3 inhibitors, using  $\alpha$ -amino acids as building blocks, was synthesized according to Scheme 1 in order to investigate if this discovery could lead to improved inhibitors.

The first four compounds in this series (**24a-d**, Table 6) had reasonable affinity towards ARTD3. Compound **24a** has a similar binding pose to **6j** (180° rotation, Figure 16a) while the smaller **24c** lacks the phenyl ring and instead binds closer to **5b** (Figure 16b). Compound **24e** displayed excellent thermal stabilization of ARTD3 but the ester moiety would likely be converted to the much less active **24f** under physiological conditions. This compound binds similar to **5b** but the ester functionality forces it into a slightly different pose (Figure 16c). To conclude this series, two ester analogs, one ketone (**24g**) and one Weinreb amide (**24h**), were synthesized. While they seemed fairly selective they unfortunately only displayed modest ARTD3 affinity.

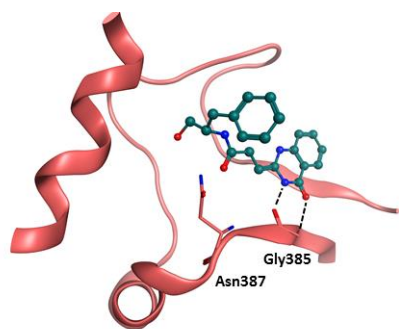


**Figure 15.** X-ray crystal structure of **6j** (brown, PDB ID 4L7L) and **5b** (teal) in ARTD3. The amine part of **6j** binds in a different pose compared to **5b**. The bifurcated interaction between the amide part of the quinazolinone and Gly385 is still present but the phenyl ring is reaching out of the pocket. The watermediated hydrogen bond between the amide group and Asn387 is missing as this water is not present in the X-ray crystal structure of **6j**.

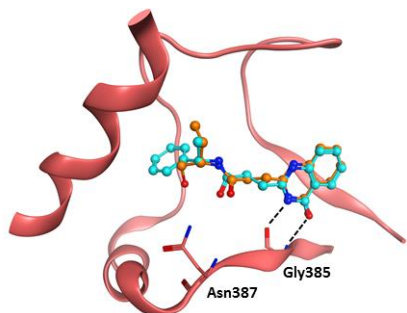
**Table 6:** Thermal shift measurements for compounds **24a-h** against five members of the ARTD family.

Entry	ID	X	R					
				ARTD3 $\Delta T_m$ (°C)	ARTD1 $\Delta T_m$ (°C)	ARTD2 $\Delta T_m$ (°C)	ARTD5 $\Delta T_m$ (°C)	ARTD8 $\Delta T_m$ (°C)
1	<b>6j</b>	CH <sub>2</sub> CH <sub>2</sub>		9.82 ± 0.39	3.59 ± 0.02	1.37 ± 0.17	0.60 ± 0.05	0.08 ± 0.16
2	<b>24a</b>	( <i>E</i> )-CHCH		6.25 ± 0.07	0.41 ± 0.31	-0.17 ± 0.32	0.08 ± 0.33	-0.70 ± 0.08
3	<b>24b</b>	CH <sub>2</sub> CH <sub>2</sub>		7.28 ± 0.19	3.43 ± 0.07	0.94 ± 0.19	0.56 ± 0.14	0.00 ± 0.14
4	<b>24c</b>	CH <sub>2</sub> CH <sub>2</sub>		7.07 ± 0.30	2.88 ± 0.01	0.88 ± 0.34	0.35 ± 0.15	0.01 ± 0.07
5	<b>24d</b>	CH <sub>2</sub> CH <sub>2</sub>		6.58 ± 0.17	3.09 ± 0.03	0.53 ± 0.16	1.08 ± 0.06	0.23 ± 0.04
6	<b>24e</b>	CH <sub>2</sub> CH <sub>2</sub>		10.05 ± 0.70	1.75 ± 0.02	0.35 ± 0.25	0.50 ± 0.10	-0.83 ± 0.20
7	<b>24f</b>	CH <sub>2</sub> CH <sub>2</sub>		1.36 ± 0.10	0.24 ± 0.07	-0.32 ± 0.10	0.22 ± 0.10	-0.37 ± 0.08
8	<b>24g</b>	CH <sub>2</sub> CH <sub>2</sub>		5.71 ± 0.47	1.93 ± 0.23	0.98 ± 0.14	0.07 ± 0.11	0.13 ± 0.21
9	<b>24h</b>	CH <sub>2</sub> CH <sub>2</sub>		5.94 ± 0.57	1.37 ± 0.36	0.33 ± 0.09	0.11 ± 0.11	0.32 ± 0.11

**a**



**b**



**c**

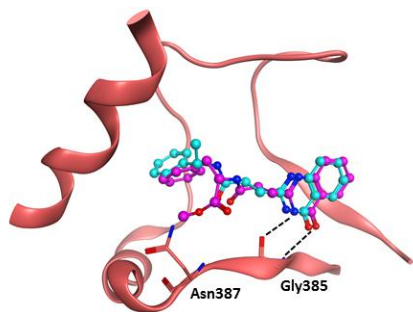


**Figure 16.** X-ray crystal structures of three  $\alpha$ -amino acid analogs in ARTD3. (a) Compound **24a** in ARTD3 (PDB ID 4L7P). The phenyl ring of **24a** is rotated 180° and is pointing out of the binding pocket. (b) Compounds **5b** (teal) and **24c** (brown, PDB ID 4L7R) in ARTD3. **24c** has a similar binding pose as **5b**. (c) Compounds **5b** (teal) and **24e** (purple, PDB ID 4L7U) in ARTD3. The ester functionality forces **24e** into a slightly different binding pose compared to **5b**.

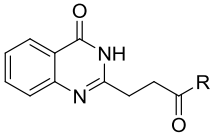
## Further Characterization of Selected Compounds

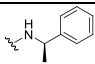
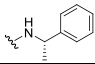
Up to this point all compounds were evaluated exclusively by the previously described thermal shift assay. Since no  $IC_{50}$  values could be obtained in this way, and to further verify the results, an enzymatic assay was used to characterize a subset of the most promising compounds against ARTD3 and ARTD1 (Table 7). These compounds were selected based on their  $\Delta T_m$  values ( $>6.5$  °C), additional compounds with available X-ray crystal structures were also chosen to verify our conclusions about the stereochemistry and the methyl group.

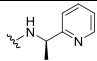
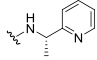
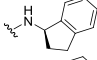
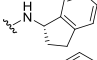
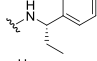
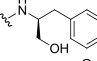
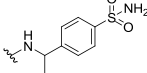
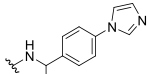
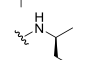
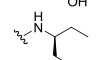
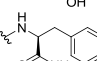
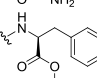
In summary, hexahistidine-tagged ARTD (full length or catalytic domain fragments) and recombinant histone proteins were captured in  $Ni^{2+}$  chelating plates. ADP-ribosylation was then initiated by adding biotinylated  $NAD^+$  and the reaction products were detected by chemiluminescence. The assay was run in the presence of our ARTD inhibitors and with  $[NAD^+]$  close to  $K_m$ .  $IC_{50}$  determinations were conducted with ligand concentrations between 10 nM-450  $\mu M$ .<sup>88</sup>

As can be seen in Table 7, the  $\Delta T_m$  values only provide a rough estimate of the potency and selectivity of a compound. There is a moderately strong correlation between the two assays for ARTD3 but only a weak correlation could be found for ARTD1. The  $\Delta T_m$  values were also generally lower for ARTD1 compared to ARTD3 for compounds with similar  $IC_{50}$  values. The  $IC_{50}$  determinations did however confirm our previous conclusions regarding how selectivity relates to the stereochemistry for **5a-f**. The *S* enantiomers tend to be ARTD3 selective while the *R* enantiomers are preferred by ARTD1. Compound **6j** is the only ARTD3 selective  $\alpha$ -amino acid analog, **24b-d** proved ARTD1 selective and **24e** was unselective, despite their respective  $\Delta T_m$  values.

**Table 7:** Comparison between  $\Delta T_m$  and  $IC_{50}$  values for selected compounds against ARTD3 and ARTD1. Full length ARTD3 was used in all cases. ARTD1 catalytic domain fragment was used for all compounds, and the  $IC_{50}$  determinations for **5a-d** were also expanded with full length ARTD1.



Entry	ID	R	ARTD3 $\Delta T_m$ (°C)	ARTD1 $\Delta T_m$ (°C)	ARTD3 $IC_{50}$ ( $\mu M$ )	ARTD1 $IC_{50}$ ( $\mu M$ )
1	<b>5a</b>		5.97	3.05	15.2	$0.51 \pm 0.16$
		$\pm 0.47$	$\pm 0.03$	$\pm 10.0$	$1.0 \pm 0.10^a$	
2	<b>5b</b>		8.45	1.80	0.9	$3.70 \pm 3.00$
		$\pm 0.59$	$\pm 0.05$	$\pm 0.3$	$6.3 \pm 0.62^a$	

3	<b>5c</b>		4.79 ± 0.21	2.35 ± 0.08	>100 <sup>b</sup>	0.88 ± 0.34 0.9 ± 0.10 <sup>a</sup>
4	<b>5d</b>		9.71 ± 0.39	1.96 ± 0.24	1.3 ± 0.2	2.12 ± 0.46 9.1 ± 2.6 <sup>a</sup>
5	<b>5e</b>		6.84 ± 0.14	2.37 ± 0.01	>100 <sup>b</sup>	0.78 ± 0.26
6	<b>5f</b>		6.72 ± 0.49	2.38 ± 0.05	>100 <sup>b</sup>	0.51 ± 0.11
7	<b>6a</b>		2.80 ± 0.15	1.49 ± 0.02	2.2 ± 0.6	0.14 ± 0.02
8	<b>6j</b>		9.82 ± 0.39	3.59 ± 0.02	1 ± 0.3	6.46 ± 2.30
9	<b>23h</b>		6.89 ± 0.35	3.36 ± 0.07	14.4 ± 4.00	1.50 ± 0.50
10	<b>23i</b>		7.79 ± 0.19	6.17 ± 0.13	13.2 ± 6.00	0.45 ± 0.13
11	<b>24b</b>		7.28 ± 0.19	3.43 ± 0.07	11.1 ± 2.7	1.98 ± 1.40
12	<b>24c</b>		7.07 ± 0.30	2.88 ± 0.01	9.6 ± 1.0	3.10 ± 0.10
13	<b>24d</b>		6.58 ± 0.17	3.09 ± 0.03	3.8 ± 1.4	0.70 ± 0.34
14	<b>24e</b>		10.05 ± 0.70	1.75 ± 0.02	2.2 ± 0.3	2.50 ± 1.60

<sup>a</sup>Full length ARTD1. <sup>b</sup>No curve could be fitted to the data but an IC<sub>50</sub> >100 μM is estimated.

Two of these compounds, **5b** and **d**, were further characterized against 9 additional ARTDs as displayed in Table 8. The data shows that **5b** and **d** selectively inhibit ARTD3 with weaker inhibition against ARTD1 and ARTD2. No significant inhibition for the remaining ARTDs is observed.

Depletion of ARTD3 by RNA interference causes a delay of DNA repair.<sup>79,80</sup> This can be measured by observing the retention of γH2AX protein containing foci in cells after DNA damage is induced by γ-radiation. In order to investigate if these two compounds (**5b** and **d**) could inhibit ARTD3 in a cellular system the retention of γH2AX-foci in human alveolar basal epithelial (A549) cells was measured after 1 hour preincubation with **5b** or **d** followed by γ-irradiation (2 Gy). It was found that both compounds caused a significant delay in DNA repair, proving that they can inhibit ARTD3 in cells (Figure 17a). This delay was significant even at concentrations below 1 μM (Figure 17b) and, importantly, the two opposite enantiomers, **5a** and **c**, did not cause γH2AX-foci retention (Figure 17c). These two compounds are therefore excellent negative controls since they only differ in the stereochemistry of a single methyl group.

**Table 8.** IC<sub>50</sub> values for **5b** and **d** against the ARTD family of proteins.

Name	<b>5b</b> IC50 (μM)	<b>5d</b> IC50 (μM)	Name	<b>5b</b> IC50 (μM)	<b>5d</b> IC50 (μM)
ARTD1	6.3 ± 0.62	9.1 ± 2.6	ARTD10	71.3 ± 22.0	>50
ARTD2	10.8 ± 4.0	n.d.	ARTD11	n.d. <sup>c</sup>	n.d. <sup>c</sup>
ARTD3	0.9 ± 0.3	1.3 ± 0.2	ARTD12	>100	>50
ARTD4	n.d. <sup>a</sup>	n.d. <sup>a</sup>	ARTD13	n.d. <sup>b</sup>	n.d. <sup>b</sup>
ARTD5	47.3 ± 29.0	n.d.	ARTD14	n.d. <sup>c</sup>	n.d. <sup>c</sup>
ARTD6	34.3 ± 17.0	n.d.	ARTD15	n.d. <sup>a</sup>	n.d. <sup>a</sup>
ARTD7	>100	n.d.	ARTD16	n.d. <sup>c</sup>	n.d. <sup>c</sup>
ARTD8	>100	n.d.	ARTD17	n.d. <sup>c</sup>	n.d. <sup>c</sup>
ARTD9	n.d. <sup>b</sup>	n.d. <sup>b</sup>			

<sup>a</sup>Not determined, no transferase activity in presence of DMSO.

<sup>b</sup>Not determined, protein reportedly lacks ADP-ribose transferase activity.<sup>82</sup>

<sup>c</sup>Not determined, transferase domain could not be produced.

Compound **5b** was profiled *in silico* and *in vitro* (in collaboration with AstraZeneca R&D, Mölndal, Sweden) and found to be soluble, cell permeable and metabolically stable in human liver microsomes and rat hepatocytes. Nonirradiated human A549 and mouse MRC5 cells were also cultured in the presence of **5b** and **d** (10 μM), no signs of toxicity were observed after 72 hours. Similar assays with U2Os, 3T3 and Hek293T cells cultured with 50μM compound also did not reveal any toxicity after 96 hours. Finally, control experiments using mouse 3T3 and MRC5 cells with **5b** and **d** (20 μM) showed that neither compound affected ARTD1 activity after H<sub>2</sub>O<sub>2</sub> induced DNA damage.

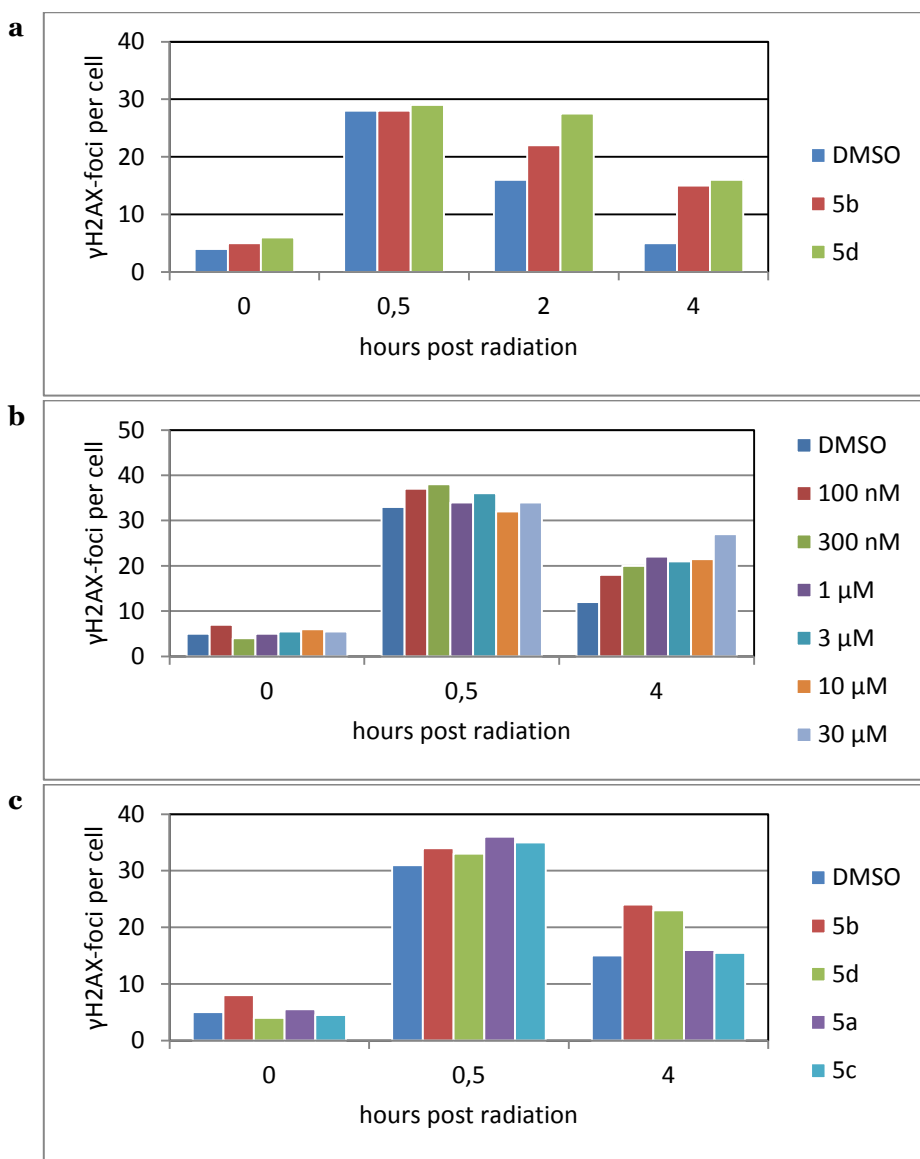


**Figure 17.** Compounds **5b** and **d** are potent inhibitors of ARTD3 in cells while their enantiomers, **5a** and **c**, are inactive. (a) Compounds **5b** and **d** (10 μM) delay DNA repair in human A539 cells as indicated by the retention of γH2AX-foci which serve as markers for DNA double strand break repair. (b) Treating A549 cells with various concentrations of **5b** results in a concentration dependant retention of H2AX-foci. (c) After γ-radiation, H2AX-foci retention could be observed only for **5b** and **d**, not for their respective enantiomers **5a** and **c**.

## Concluding Remarks

The potency and ARTD3 selectivity of compound **1** has been improved by systematically varying different structural features. The stereochemistry at the *meso* position proved important and a substituent at this position was needed. However, anything larger than a methyl group (**5b** and **d**) resulted in lower affinity indicated by the measured thermal shifts. The ethylene linker connecting this part with the quinazolinone scaffold was also investigated but all modifications lowered the affinity, as did the addition of substituents to the phenyl ring.

A series of compounds where the benzyl amine was replaced with  $\alpha$ -amino acid analogs was also synthesized. The X-ray crystal structures of some of these compounds in complex with ARTD3 revealed that they adopt a different binding pose. Except for **6j** they were unfortunately unselective and did not display improved affinity compared to **5b** and **d**.

No robust and reliable assays were available during the earlier stages of this project. Thus, a thermal shift assay was used for initial profiling of all compounds. Selected compounds were then further characterized with IC<sub>50</sub> values once the previously described enzymatic assay became available. Due to limited resources IC<sub>50</sub> values could not be obtained for all compounds. While this is problematic due to the less than ideal correlation between the two assays the thermal shift assay was deemed adequate for a first screening of new compounds.

Finally, two compounds, **5b** and **d**, were tested for inhibition of ARTD3 in cells and were found to be potent and selective inhibitors of ARTD3 *in vivo*. Despite the modest selectivity according to the IC<sub>50</sub> determinations these compounds did not seem to inhibit ARTD1 in cellular systems which make them the first nicotinamide mimicking ARTD3 inhibitors with documented selectivity over other family members. It is noteworthy that most other reported ARTD inhibitors lack any chirality, which according to our study is crucial in order to obtain selectivity. As the first reported selective ARTD3 inhibitors, and due to their favorable physicochemical and metabolic profiles, these compounds are expected to be valuable tools for further elucidating the biological role of the poorly studied ARTD3 in relation to ARTD1 and ARTD2.



## Chapter 2: Development of ARTD7, ARTD8, and ARTD10 Inhibitors (Paper III + IV)

When this project started no good inhibitors of ARTD7 and ARTD8 were described. We decided to adopt a virtual screening approach for finding new inhibitors of these enzymes in order to overcome the throughput limitations of the previously described thermal shift assay. The two proteins had earlier been cocrystallized (ARTD7 with **25** and ARTD8 with **26**, Figure 18) with weak inhibitors identified from the library of 185 NAD<sup>+</sup> mimics (see Chapter 1) and these structures formed the basis for the ensuing virtual screen. Structural similarities in the NAD<sup>+</sup> binding sites and binding modes for the two ligands were revealed by superposing the two X-ray crystal structures. The quinazolinone is stacked between two tyrosines (Tyr569 and Tyr582 for **25** or Tyr1633 and Tyr1646 for **26**) and forms a hydrogen bond to a glycine (Gly538 for **25** and Gly1602 for **26**). A conformational difference can be seen for Tyr576 which is significantly closer to the binding site than Tyr1640. Finally, the triazol of **26** stacks with a tyrosine (Tyr1620) in the donor-site loop. The corresponding interaction is missing for **25** due to structural differences in this loop which is fully visible in the ARTD7•**25** complex whereas no electron density was observed for several residues in the ARTD8•**26** complex. This indicated that the loop is flexible and two structures for each protein were therefore used in the following virtual screening, one with all amino acid residues according to the X-ray crystal structure (ARTD7<sub>long</sub>/ARTD8<sub>long</sub>, modelled for ARTD8) and one with parts of the donor-site loop removed (ARTD7<sub>short</sub>/ARTD8<sub>short</sub>).

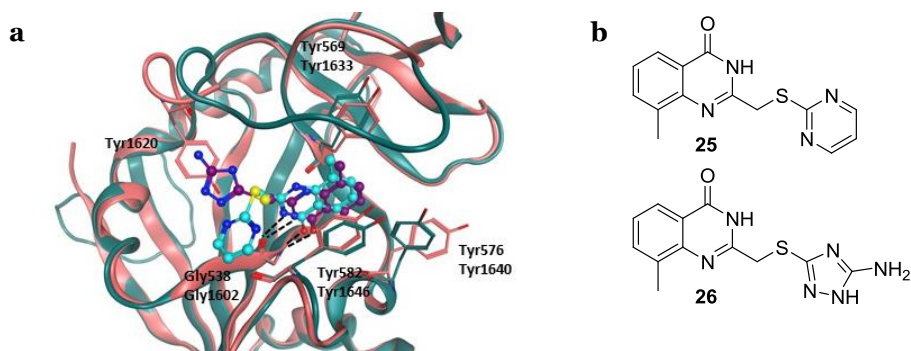


**Figure 18.** Superposition of ARTD7 and ARTD8 with bound ligands. (a) ARTD7 (blue, PDB ID 4FoE) with **25** (teal) and ARTD8 (pink, PDB ID 3SMI) with **26** (purple). The hydrogen bonds between the amide parts of the quinazolinones and the glycines are considered essential. Both ligands are stacked between a pair of tyrosines. (b) Structures of the NAD<sup>+</sup> mimicking ligands **25** and **26**.

## Virtual Screening Procedure

An overview of the virtual screening workflow is presented in Figure 19. A virtual library consisting of 8050 compounds was docked to both the long and short versions of ARTD7 and ARTD8. This resulted in 2904, 4731, 6476 and 6805 remaining compounds, respectively, for ARTD7<sub>long</sub>, ARTD7<sub>short</sub>, ARTD8<sub>long</sub> and ARTD8<sub>short</sub> which were rescored using eight scoring functions (glidescore, chemscore<sup>119</sup>, plp<sup>120</sup>, screenscore<sup>121</sup>, zapbind<sup>122</sup>, chemgauss3, oechemscore and goldscore). The docking results were finally verified using known binders which generally obtained good docking scores. The bioactive binding poses (obtained from the X-ray crystal structures) were also reproduced with low root-mean-square deviation (RMSD) values for both compound **25** and **26**.

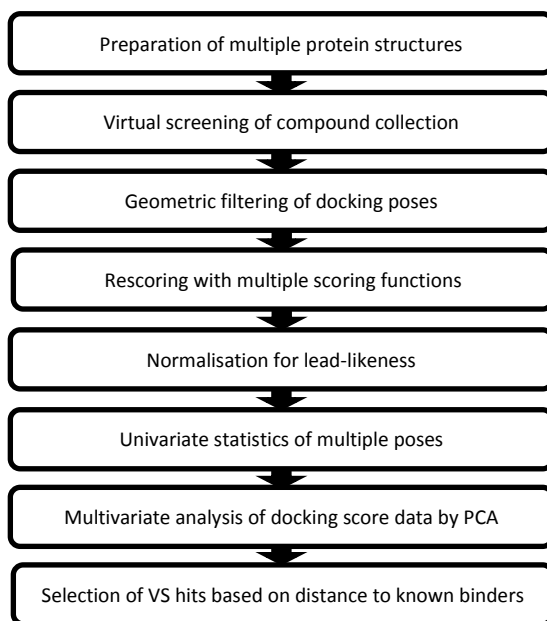


**Figure 19.** Workflow during the virtual screening process.

A multivariate analysis of docking scores produced a PCA model with five principal components (PCs) for each of the four protein structures. PCA is a method used in multivariate data analysis where a large number of variables are reduced to a smaller set of principal components. The first PC describes the largest amount of variability in the data. The second PC then describes the largest possible amount of the remaining data, and so forth. By using PCA it was possible to take both consensus scoring and individual scoring functions into account when selecting a subset of compounds for further evaluation. This subset (set A) was selected by calculating their proximity to

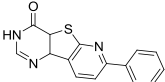
known binders in PC space and included 64 compounds. A second set containing the same number of compounds (set B) was then selected based on their glidescore values. Each set contained 47 unique and 17 shared compounds.

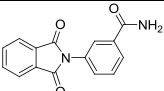
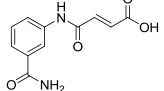
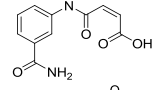
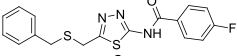
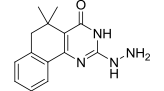
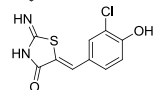
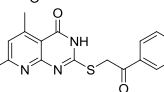
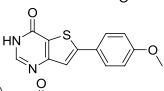
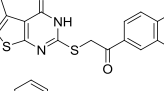
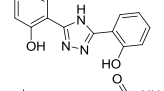
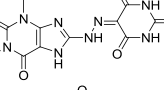
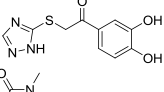
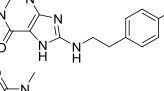
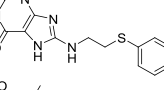
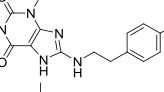
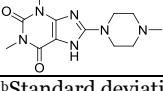
## Evaluation of Hits from the Virtual Screen

These 111 compounds were then evaluated against ARTD7, ARTD8 and ARTD1 in the previously described thermal shift assay. The 16 compounds with a  $\Delta T_m > 1.5$  °C for ARTD7 or ARTD8 are listed in Table 9. The purity and structure of these hits was subsequently verified using HPLC and  $^1\text{H}$ NMR. This process revealed that compound **29** was the *Z*-alkene and not the *E*-alkene as reported in the library database. The reported thermal stabilization is thus for compound **30**. The majority of these hits, 14 compounds, stabilized ARTD8 while only two stabilized ARTD7. The highest  $\Delta T_m$  values were also found against ARTD8. This is consistent with what was seen throughout the virtual screening process where more docking poses were found against ARTD8. A higher number of compounds targeting ARTD8 were thus selected for biological evaluation. This, in turn, can be explained by the fact that Tyr576 is restricting access to parts of the binding site in ARTD7. ARTD8 has a larger binding site since the corresponding amino acid side chain is oriented in a different direction. A final observation is that a majority of the hits (10 out of 16) were identified only from structures with intact donor-site loop, likely since this better represents the true shape of the binding site. However, three compounds were identified exclusively from the “short” versions of the proteins, illustrating that the two methods are complimentary and the importance of using several structures of the same protein in order to maximize the chances of finding new inhibitors.

Most of these 16 compounds have properties similar to what is generally observed for lead-like compounds and, according to reports, chemical probes.<sup>123</sup> The compounds were also analyzed for structural diversity which revealed that the consensus method gave more structurally diverse compounds compared to using solely glidescore.

**Table 9.** Thermal shifts measurements against ARTD7, ARTD8 and ARTD1 for the 16 compounds found in the virtual screen.

Entry	ID	Compound	ARTD7 $\Delta T_m$ (°C)	ARTD8 $\Delta T_m$ (°C)	ARTD1 $\Delta T_m$ (°C)	Set
1	27		1.51 $\pm 0.37$	0.65 $\pm 0.84$	-0.16 $\pm 0.25$	A

2	28		0.06 ± 0.10	2.10 ± 0.12	0.23 ± 0.05	A
3	29		n.d. <sup>a</sup>	n.d. <sup>a</sup>	n.d. <sup>a</sup>	A
4	30		0.80 ± 0.10	3.35 ± 0.67	0.36 ± 0.10	-
5	31		0.36 ± 0.41	1.66 ± 0.83	0.17 ± 0.14	A
6	32		1.38 ± 0.04	2.05 ± 0.60	0.01 ± 0.09	A
7	33		-0.25 ± 0.12	3.89 ± 0.91	0.04 ± 0.27	A
8	34		-0.09 ± 0.09	2.65 ± 0.12	0.89 ± 0.23	A
9	35		1.49 ± 0.10	1.11 ± 0.62	0.13 ± 0.08	A/B
10	36		0.33 ± 0.27	1.63 ± 1.05	3.10 ± 0.26	A/B
11	37		-0.34 ± 0.07	2.65 ± 1.84	-0.46 <sup>b</sup>	B
12	38		-0.08 ± 0.03	2.12 ± 0.00	-0.31 <sup>b</sup>	B
13	39		-0.05 ± 0.14	2.28 ± 0.12	-0.29 <sup>b</sup>	B
14	40		0.66 ± 0.07	3.01 ± 0.67	0.53 <sup>b</sup>	B
15	41		0.09 ± 0.13	2.11 ± 0.69	0.28 <sup>b</sup>	B
16	42		1.09 ± 0.04	2.62 ± 0.02	0.31 <sup>b</sup>	B
17	43		0.19 ± 0.11	1.56 ± 0.06	-0.09 <sup>b</sup>	B

<sup>a</sup>Not determined. <sup>b</sup>Standard deviation not calculated.

## Further Evaluation of Selected Compounds

The compounds in Table 9 were also tested for thermal stabilization of ARTD1 in order to find potentially selective candidates for a medicinal chemistry program. Selectivity was defined as  $\Delta T_m > 3.0$  °C against one of the ARTDs and 1.5 °C higher than against the other two. Two compounds, **30** and **33** fulfilled these criteria with selectivity for ARTD8. Compound **30** was eventually chosen for continued evaluation due to our interest in further investigating the differences between the *E/Z*-alkenes. Compound **29** was thus synthesized in two steps starting from fumaric acid and 2-aminobenzamide.

Isothermal titration calorimetry (ITC) was then used to evaluate the binding of **29** and **30**. ITC is a technique where the ligand is titrated into a cell containing the protein. If the ligand binds to the protein heat is generated which can be measured to determine the enthalpy of binding ( $\Delta H$ ), the dissociation constant ( $K_d$ ) and the stoichiometry. This can in turn be used to calculate changes in entropy ( $\Delta S$ ) and Gibbs Free Energy ( $\Delta G$ ).<sup>124</sup> The ITC measurements of compounds **29** and **30** show that they both bind to ARTD8 with similar dissociation constants and that enthalpy contributes more than entropy (Figure 20).

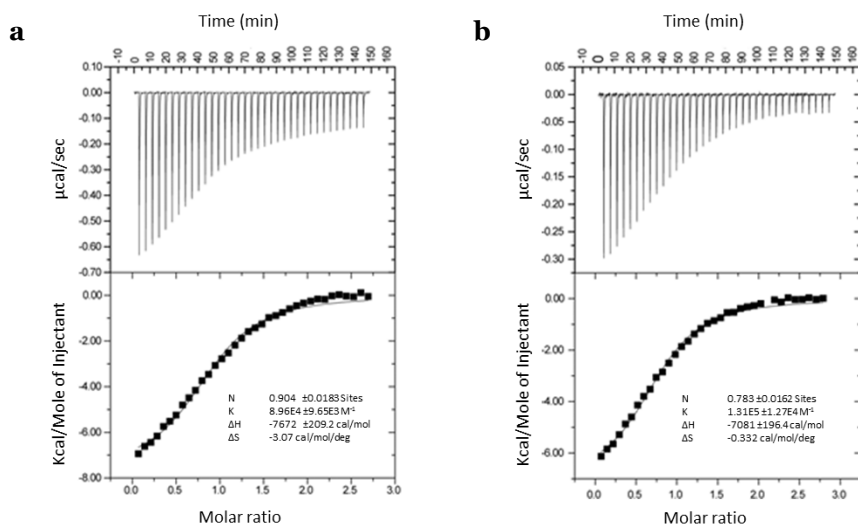


**Figure 20.** Results from the evaluation of compounds **29** and **30** using ITC. The upper panes show raw data after injection and baseline correction and the lower panes show integrated data and regression. N = number of molecules per binding site, K = association constant,  $\Delta H$  = change in enthalpy and  $\Delta S$  = change in entropy. (a) Data for compound **29**.  $K_d = 11.2$   $\mu\text{M}$ ,  $\Delta H = -7.7$  kcal/mol and  $-T\Delta S = 0.92$  kcal/mol (b) Data for compound **30**.  $K_d = 7.6$   $\mu\text{M}$ ,  $\Delta H = -7.1$  kcal/mol and  $-T\Delta S = 0.10$  kcal/mol

These two compounds were cocrystallized with ARTD8 in order to gain further knowledge about their binding modes. The unit cells of **29** and **30** in ARTD8 consisted of two (A-B) and four (A-D) monomers, respectively (Figure 21), which is consistent with previous observations for other ARTD8•ligand complexes.<sup>88</sup> Molecular dynamics (MD) simulations were performed in order to investigate the effects of crystal packing and to select suitable monomers for structure based design of a set of analogs. These simulations showed that the interactions were best preserved in monomer B for compound **30** (Figure 22b). The MD simulations of monomers C and D resulted in lost hydrogen bonds and the ligand was completely dissociated in the simulations of monomer A. For compound **29** all interactions were retained in monomer A while hydrogen bonds were lost in monomer B (Figure 22a).

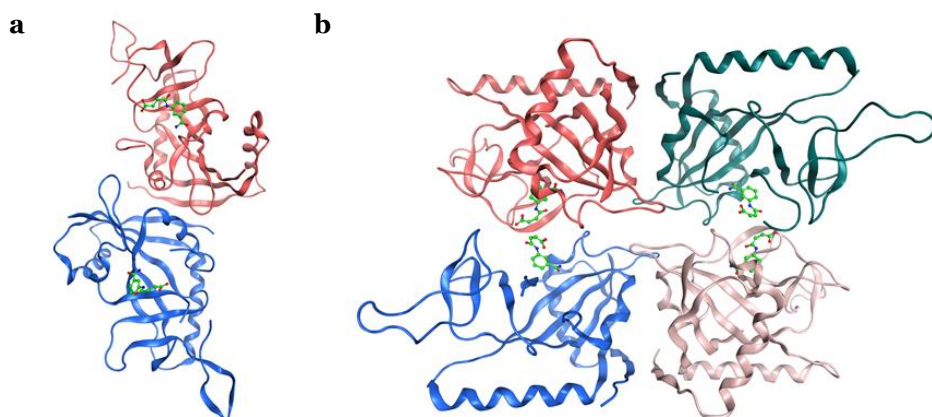
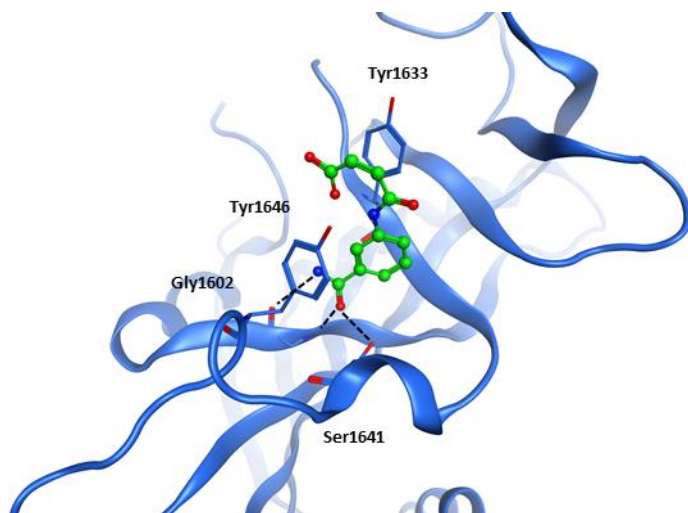


**Figure 21.** The X-ray crystal structures of **29** and **30** in ARTD8. (a) The unit cell of the ARTD8•**29** complex consists of a dimer. (b) The unit cell of the ARTD8•**30** complex consists of a tetramer.

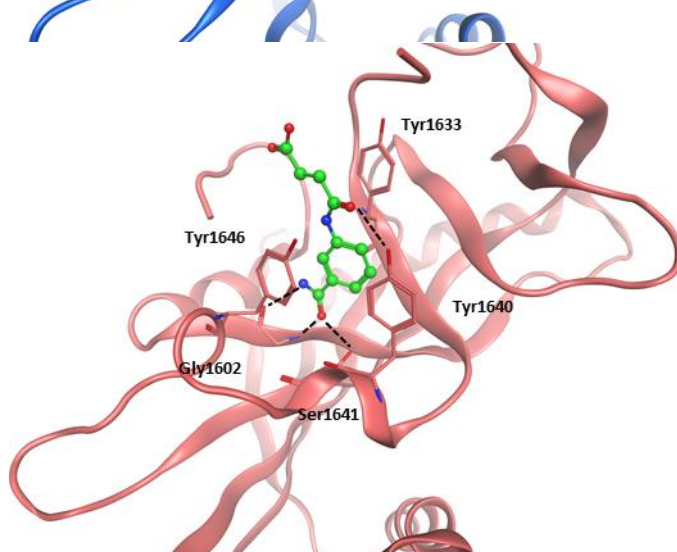
The binding mode for monomer B of the ARTD8•**30** complex is displayed in Figure 22a. The phenyl ring of **30** is stacked between two tyrosines (Tyr1633 and Tyr1646) and the benzamide forms hydrogen bonds to Gly1602 and Ser1641. Figure 22b shows similar interactions for the ARTD8•**29** complex in monomer A. However, an additional hydrogen-bond interaction between the anilide-oxygen and Tyr1640 is observed.

Compared with other known ARTD8 ligands, these two compounds extend into a different, less conserved, part of the binding pocket. For instance, Tyr1640 is replaced by a lysine (Lys903) and Leu1701 is replaced by a glutamate (Glu988) in ARTD1. This difference in binding pose is promising for the purposes of further developing these compounds into potent ARTD8-selective ligands.

**a**



**b**

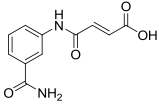
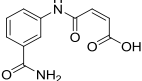
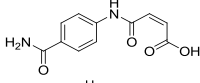
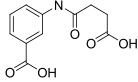
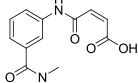
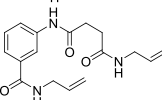
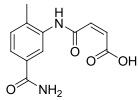
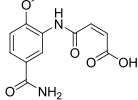
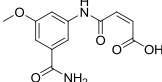


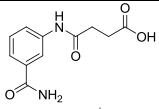
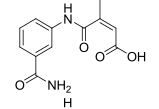
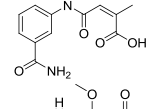
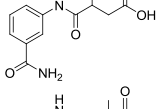
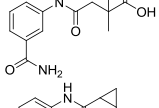
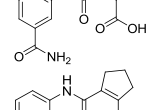
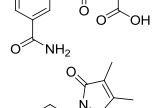
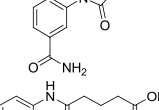
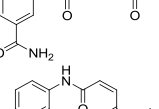
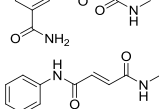
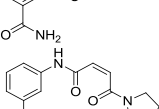
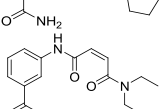
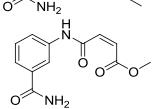

**Figure 22.** The binding poses of compounds **29** and **30** in complex with ARTD8. (a) Compound **30** in ARTD8. The phenyl ring is stacked between two tyrosines (Tyr1633 and Tyr1646) and the benzamide interacts with a glycine and a serine. (b) Compound **29** in ARTD8, similar interactions can be found as for **30** in ARTD8. In addition, the anilide interacts with a third tyrosine (Tyr1640).

## Synthesis of Analogs

When testing these two compounds in the later developed enzymatic assay (described in Chapter 1) against ARTD7, ARTD8, ARTD10, and ARTD1 it was revealed that they are more potent as ARTD10 inhibitors (Table 10). Based on these new results a set of analogs were synthesized in order to establish structure activity relationships (SARs) for these four ARTDs. Most of these analogs were synthesized in one step by reacting aminobenzamides with anhydrides or carboxylic acids in presence of amide coupling reagents. A subset was then further functionalized at the free carboxylic acid according to Scheme 7.

**Table 10.** IC<sub>50</sub> values for compounds **29-30** and **44a-x** against the full length enzymes ARTD1 and ARTD10, and the catalytic domains of ARTD7 and ARTD8.

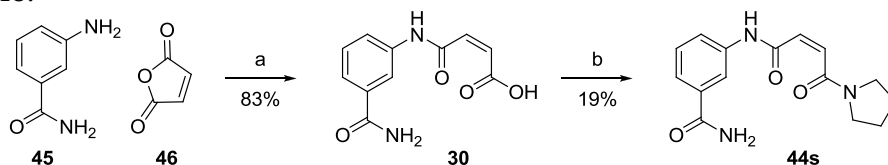
Entry	ID	Compound	ARTD10 IC <sub>50</sub> (μM)	ARTD8 IC <sub>50</sub> (μM)	ARTD7 IC <sub>50</sub> (μM)	ARTD1 IC <sub>50</sub> (μM)
1	<b>29</b>		1.3	> 20	17.8	3.6
2	<b>30</b>		10.6	> 20	15.8	4.4
3	<b>44a</b>		n.i. <sup>a</sup>	n.i. <sup>a</sup>	n.i. <sup>a</sup>	>20
4	<b>44b</b>		n/a <sup>b</sup>	n/a <sup>b</sup>	n/a <sup>b</sup>	n/a <sup>b</sup>
5	<b>44c</b>		n/a <sup>b</sup>	n/a <sup>b</sup>	n/a <sup>b</sup>	n/a <sup>b</sup>
6	<b>44d</b>		n/a <sup>b</sup>	n/a <sup>b</sup>	n/a <sup>b</sup>	n/a <sup>b</sup>
7	<b>44e</b>		n.i. <sup>a</sup>	n.i. <sup>a</sup>	n.i. <sup>a</sup>	>20
8	<b>44f</b>		>20	n.i. <sup>a</sup>	n.i. <sup>a</sup>	>20
9	<b>44g</b>		n.i. <sup>a</sup>	n.i. <sup>a</sup>	n.i. <sup>a</sup>	>20

10	<b>44h</b>		1.9	n.i. <sup>a</sup>	16.3	0.7
11 <sup>c</sup>	<b>44i</b>		>20	>20	>20	8.9
12 <sup>d</sup>	<b>44j</b>		14.0	>20	2.3	2.4
13	<b>44k</b>		7.2	n.i. <sup>a</sup>	n.i. <sup>a</sup>	7.3
14	<b>44l</b>		>20	>20	>20	9.4
15	<b>44m</b>		14.0	>20	>20	5.6
16	<b>44n</b>		2.9	>20	1.6	0.2
17	<b>44o</b>		2,4	>20	11.0	10.5
18	<b>44p</b>		7.4	>20	>20	3.7
19	<b>44q</b>		2.0	>20	>20	9.7
20	<b>44r</b>		2.1	18.7	>20	0.4
21	<b>44s</b>		4.6	>20	16.9	0.6
22	<b>44t</b>		>20	>20	>20	0.8
23	<b>44u</b>		0.8	1.6	1.7	4.4

24	<b>44v</b>		1.9	>20	>20	1.1
25	<b>44w</b>		14.6	n.i. <sup>a</sup>	n.i. <sup>a</sup>	1.1
26	<b>44x</b>		6.9	n.i. <sup>a</sup>	18.0	0.7

<sup>a</sup>n.i., no inhibition at 200  $\mu$ M. <sup>b</sup>n/a, not applicable, the compound was not soluble under assay conditions. <sup>c</sup>**52** contained 5% of **53**. <sup>d</sup>**53** contained 24% of **52**.

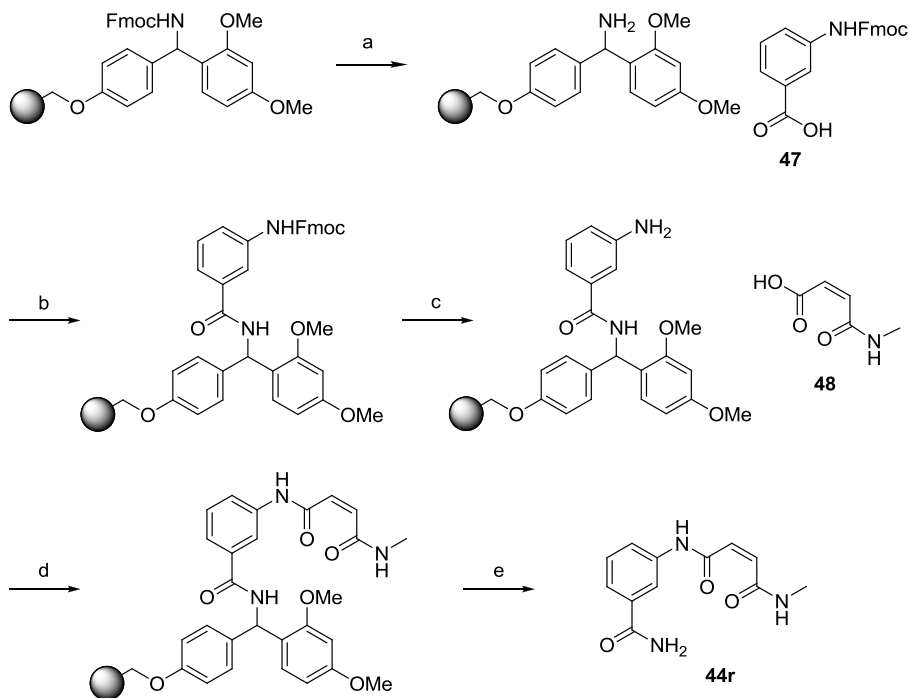
**Scheme 7.** Representative synthetic route to the compounds listed in Table 10.<sup>a</sup>



<sup>a</sup>Reagents and conditions: (a) THF, 20 °C, 18 h; (b) diethyl amine, TBTU, TEA, DMF, 20 °C, 1 w.

The ratio between **44i** and **j** could be controlled by regulating the temperature, at 100 °C a 95:5 mixture was formed (Table 10, entry 11) while at -78 °C a 24:76 mixture was instead obtained (entry 12). The open form of **44o** could not be isolated as it cyclized to the presented imide. Finally, compound **44r** could not be synthesized using the standard methods since it isomerized to compound **44q**. It was instead prepared using solid phase synthesis according to Scheme 8. The RINK-amide resin was deprotected using piperidine in DMF and Fmoc-protected 3-aminobenzoic acid, **47**, was added using DIC and HOAt in DMF. The recently introduced Fmoc was removed using piperidine in DMF and **48** was connected using DIC and HOAt in DMF. Compound **44r** was then cleaved from the resin using TFA in DCM.

**Scheme 8.** Solid phase synthesis of compound **44r**.<sup>a</sup>



<sup>a</sup>Reagents and conditions: (a) 20% piperidine in DMF, 20 °C, 10 + 10 min; (b) DIC, HOAt, DMF, 20 °C, 18 h; (c) 20% piperidine in DMF, 20 °C, 10 + 10 + 10 min; (d) DIC, HOAt, DMF, 20 °C, 18 h; (e) 20% TFA in DCM, 20 °C, 1 h.

Considering the differences in amino acid composition between the mARTDs (ARTD7, ARTD8 and ARTD10) and ARTD1 we believed it would be possible to achieve selectivity between these by slightly modifying the benzamide-part of **29** and **30**. However, moving the amide to *para* position (**44a**) gave a completely inactive compound, indicating that the amide in *meta* position is essential for inhibition of both ARTD1 and the mARTDs. Functionalizing the amide (**44b-d**) produced compounds that were insoluble under the assay conditions. Additional substituents on the phenyl ring (**44e-g**) also abolished inhibition, indicating that there is either a limited amount of space available in the binding pocket around the phenyl ring or that the binding is highly dependant of the electronic properties of the ligands.

The importance of the alkene was also explored by synthesizing a saturated analog (**44h**), analogs with added methyl or methoxy groups (**44i-l**) and analogs with cyclized side chains (**44m-o**). Most of these compounds kept a similar activity as **29** and **30**. The saturated compound and the three with cyclized side-chains were well tolerated while the addition of a methyl group in compound **44j** was beneficial mainly for ARTD7 inhibition. The

side-chain was also elongated by one methylene group (**44p**) which slightly decreased inhibition of ARTD7 and ARTD10. Finally the free carboxylic acid was investigated by transforming it into a methyl ester as well as various amides (**44q-u**). The methyl amides **44q** and **r** proved potent and **44q** also displayed some selectivity for ARTD10 over the other mARTDs. The larger amides (**44s** and **t**) had reduced potency and poor selectivity. The methyl ester, **44u**, proved to be the most potent compound so far, however, it lacked selectivity and the ester would likely be hydrolyzed in a cellular system. Finally, the three methyl ester bioisosteres, **44v-x**, showed selectivity for ARTD10 over the other mARTDs but were unselective with respect to ARTD1.

To summarize these findings, moving the benzamide from *meta* position compared to the anilide moiety or alkylating the benzamide lead to reduced potency. The free carboxylic acid of **29** and **30** was not essential and could be replaced with a methyl ester or methyl amide. Compound **44q** showed promise as a selective inhibitor of ARTD10 and the compound class in general is attractive due to lead-like properties with low molecular weights, LogP values, and number of hydrogen bond acceptors and donors as well as simple synthetic routes.<sup>123,125</sup>

## Merged Compounds

As displayed in Figure 23, compound **30** extends into a different part of the binding pocket compared to compounds **25** and **26**. In order to exploit this and find inhibitors with improved potency and selectivity a set of 20 merged compounds was designed using statistical molecular design (SMD). The six building blocks for the R-position (Figure 24a and b) were selected based on prior knowledge about this part of the binding site. The eight building blocks for the R'-position were manually selected for synthetic feasibility and maximum coverage of chemical space in a PCA model based on commercially available aromatic thiols and alcohols (Figure 24a and c). A D-optimal design was finally used to reduce the 48 resulting possible combinations to the first 20 compounds shown in Table 11 (compounds **49a-t**). Compound **49u** was also included since it would already be synthesized as an intermediate to **49e**, and compound **49v** was added as a direct analog to **25** + **30**. D-optimal design is a method which aims to select the most diverse subset of compounds. This is done by maximizing the volume covered by the subset in property space. In this case, principal components were used to describe the compounds and thus PCA space was used to select a chemically diverse set.

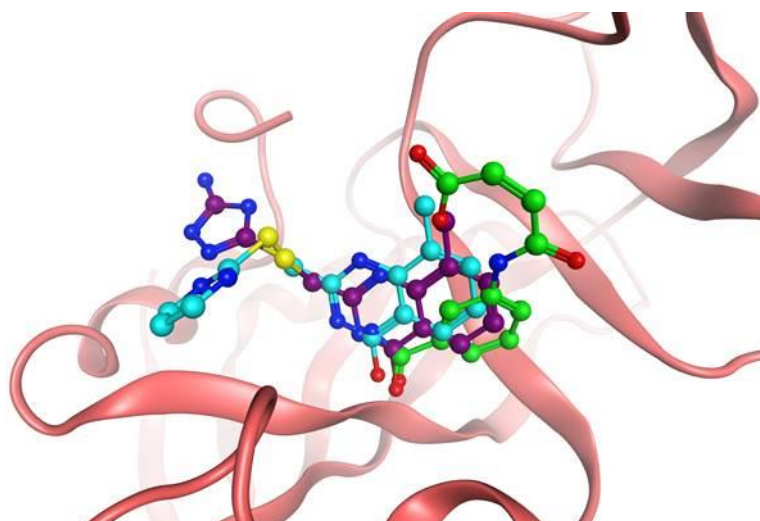
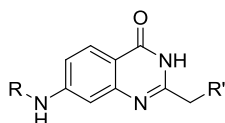
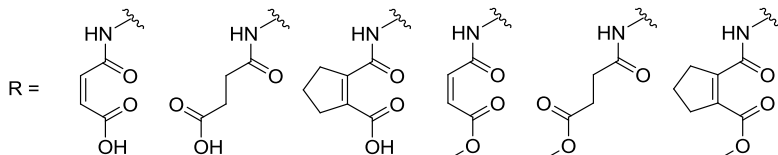


**Figure 23** Superposition of compounds **25** (teal), **26** (purple) and **30** (green) in ARTD8.

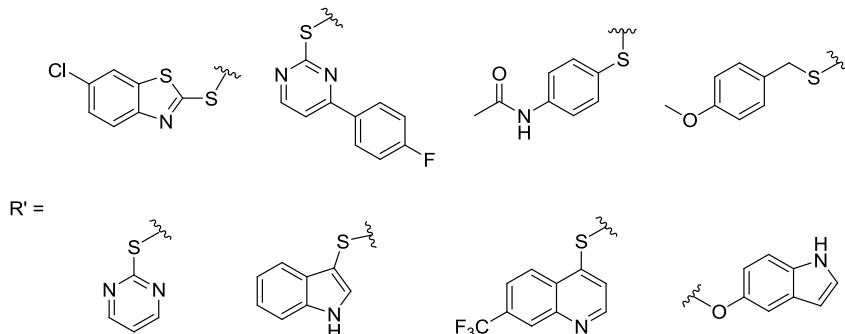
**a**



**b**



**c**

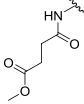
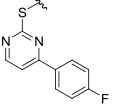
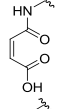
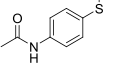
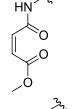
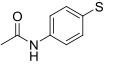
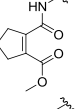
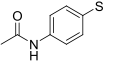
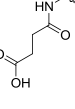
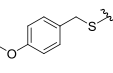
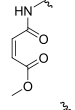
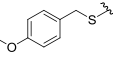
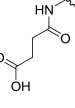
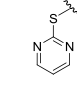
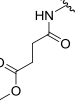
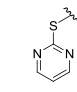
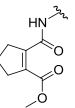
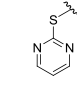
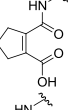
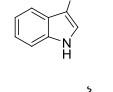
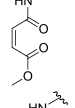
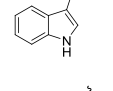
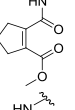
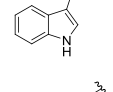
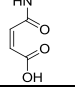
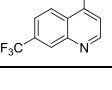


**Figure 24.** Starting point for the D-optimal design. (a) General structure of the merged compounds. (b) Building blocks selected for the R position. (c) Building blocks selected for the R' position.

The synthetic route to these compounds is described in Scheme 9. 2-Bromo-5-nitroaniline **50** was cyanated using CuCN to form compound **51** which was subsequently acylated using methoxyacetyl chloride to form anilide **52**. The quinazolinone, **53**, was then obtained by cyclizing **52** under alkaline condition. The methoxyether was cleaved using 47% HBr to form alcohol **54**, which was finally transformed into the bromide intermediate, **55**, using Appel conditions.<sup>114</sup> This intermediate was then used to synthesize the compounds shown in Table 11. The bromide was first replaced with one of the building blocks in Figure 24c to form compounds **56a-h**. The nitro groups were then reduced to the corresponding anilines **57a-h** using SnCl<sub>2</sub> in EtOAc and subsequently acylated to anilides using a suitable anhydride (Figure 24b). The free carboxylic acid was finally methylated on a subset of these compounds to form the desired methyl esters. Several problems were encountered during these syntheses. Both the reductions and acylations produced several unidentified side products. The acylations were also sluggish and full conversion could generally not be obtained. Finally, getting these compounds in solution was challenging due to their notably poor solubility. Purification was thus difficult and pure material could in several cases not be obtained.

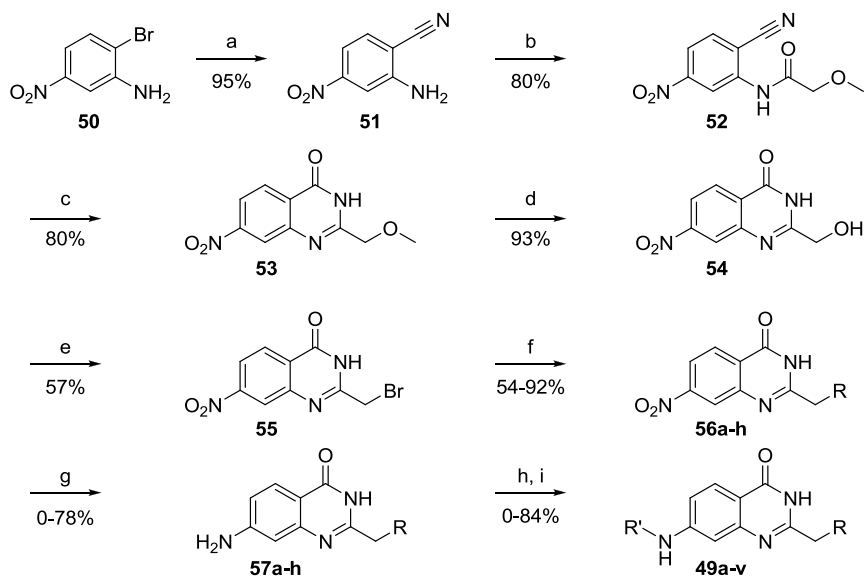
**Table 11.** Structures and preliminary IC<sub>50</sub> values for **49a-v** against the full length enzyme ARTD8, and the catalytic domains of ARTD7, ARTD10 and ARTD1. Only seven compounds were prepared and IC<sub>50</sub> values were only obtained for five of these.

Entry	ID	R	R'	ARTD10 IC <sub>50</sub> (μM)	ARTD8 IC <sub>50</sub> (μM)	ARTD7 IC <sub>50</sub> (μM)	ARTD1 IC <sub>50</sub> (μM)
1 <sup>a</sup>	<b>49a</b>			-	-	-	-
2 <sup>a</sup>	<b>49b</b>			-	-	-	-
3 <sup>a</sup>	<b>49c</b>			-	-	-	-
4 <sup>a</sup>	<b>49d</b>			-	-	-	-

5 <sup>b</sup>	<b>49e</b>			-	-	-	-
6	<b>49f</b>			120.0	61.0	-	-
7 <sup>a</sup>	<b>49g</b>			-	-	-	-
8	<b>49h</b>			85.0	147.0	107.0	-
9 <sup>a</sup>	<b>49i</b>			-	-	-	-
10 <sup>a</sup>	<b>49j</b>			-	-	-	-
11 <sup>b</sup>	<b>49k</b>			-	-	-	-
12 <sup>a</sup>	<b>49l</b>			-	-	-	-
13	<b>49m</b>			72.0	28.0	23.0	22.5
14 <sup>a</sup>	<b>49n</b>			-	-	-	-
15 <sup>a</sup>	<b>49o</b>			-	-	-	-
16 <sup>a</sup>	<b>49p</b>			-	-	-	-
17 <sup>a</sup>	<b>49q</b>			-	-	-	-



## Scheme 9. Synthetic route to compounds **49a-v**<sup>a</sup>



<sup>a</sup>Reagents and conditions: (a) CuCN, NMP, 175 °C, 2 h; (b) methoxyacetyl chloride, pyridine, DMF, 20 °C, 2 h; (c) UHP, K<sub>2</sub>CO<sub>3</sub>, H<sub>2</sub>O:acetone 1:, 82 °C, 24 h; (d) 47% HBr, 120 °C, 5 h; (e) PPh<sub>3</sub>, CBr<sub>4</sub>, DCM, 20 °C, 20 h; (f) thiol or alcohol from Figure 24c, TEA, DMF, 80 °C, 30 min; (g) SnCl<sub>2</sub>, EtOAc, 120 °C, 20-40 min; (h) anhydride from Figure 24b, THF, 90 °C, 2 h - 10 d; (i) (Diazomethyl)trimethylsilane, DCM, MeOH, 20 °C, 30 min.

## Macrocycles

When studying the X-ray crystal structure of **30** in ARTD8 it was observed that a water molecule was present close to the ligand (Figure 25). By expanding the ligand to incorporate the oxygen atom of this water beneficial interactions might be found to improve the potency of the resulting compounds. Figure 26 shows the four macrocyclic analogs to **30** that were considered based on these findings.

These compounds were synthesized in parallel with those displayed in Table 10 and the synthesis started by preparing **44d**. Macrocycle **58d** was then meant to be formed using a ring closing metathesis (RCM).<sup>126,127,128,129</sup> The macrocycle was however never observed, likely due to chelation between the ruthenium in Grubbs 2<sup>nd</sup> generation catalyst<sup>130</sup> and one of the amides in **44d** to form a six-membered ring. There is precedence in the literature that this kind of complex can be avoided by adding Ti(*i*-PrO)<sub>4</sub> to the mixture, however compound **58d** was never obtained despite attempting this procedure.

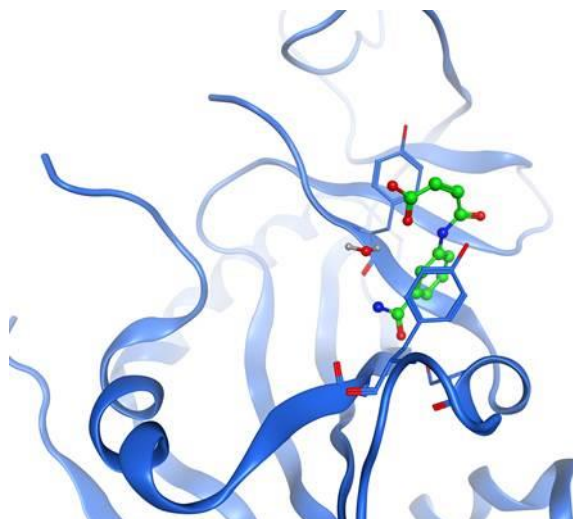


**Figure 25.** Macrocyclic analogs to **30** were considered in order to investigate the implications of incorporating the water displayed in the X-ray crystal structure of **30** in ARTD8 (monomer B).

The synthetic route to macrocycle **58a** is described in Scheme 10. Compound **60** was formed by reacting succinic anhydride with *t*-BuOH in the presence of *N*-hydroxysuccinimide, DMAP and TEA. Weinreb amide<sup>131</sup> **61** was then formed in a TBTU mediated amide coupling and subsequently reacted with vinylmagnesium bromide to produce the  $\alpha,\beta$ -unsaturated ketone **62**. Various conditions were screened for the following reaction where **62** acts as a Michael acceptor for **64** to form compound **65** and it was found that DBU in THF gave the best results. The nitrogroup was then reduced using catalytic transfer hydrogenation. The ester in compound **66** was hydrolyzed using TFA and the resulting intermediate cyclized using HATU to form a 1:1 mixture of **58a** and **67**. These compounds could not be separated and the mixture showed no inhibition of ARTD7, ARTD8, or ARTD10.

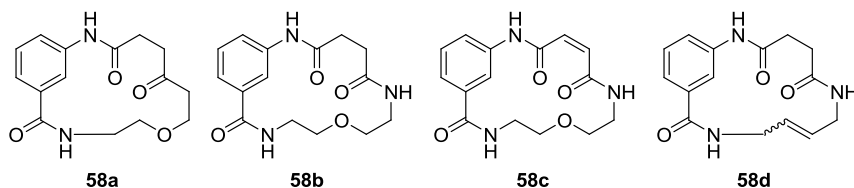
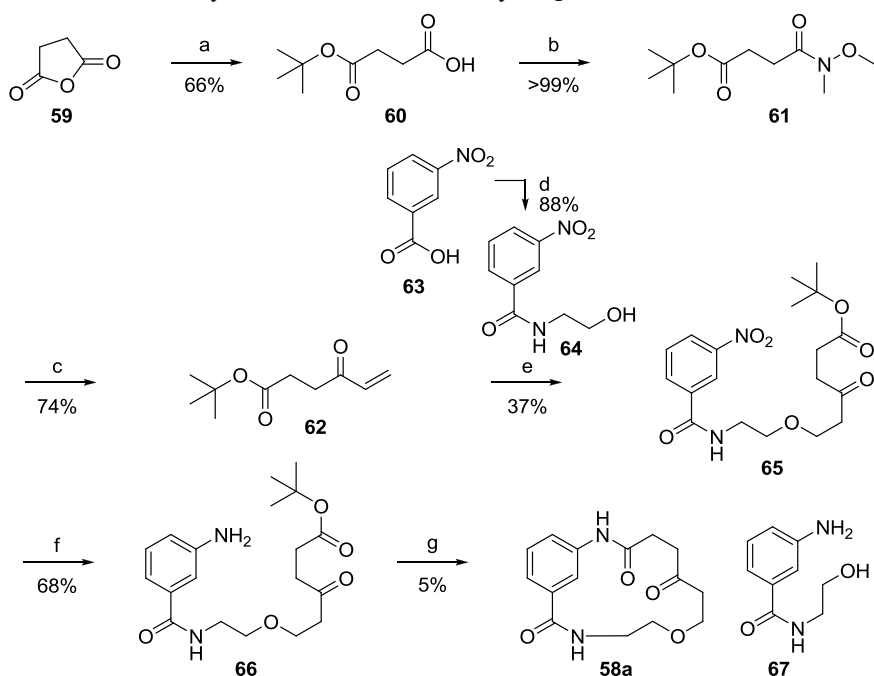


**Figure 26.** The four macrocyclic analogs of **30** that were considered.

**Scheme 10.** The synthetic route to macrocycle **58a**.<sup>a</sup>



<sup>a</sup>Reagents and conditions: (a) *t*-BuOH, *N*-hydroxysuccinimide, DMAP, TEA, toluene, reflux, 18 h; (b) *N,O*-dimethylhydroxylamine, TBTU, TEA, DCM, 20 °C, 18 h; (c) vinylmagnesium bromide, THF, -78 °C, 30 min, then 20 °C, 4 h; (d) DMF, oxalyl chloride, DCM, 0 °C, 30 min, then ethanalamine, TEA, DCM, 20 °C, 18 h; (e) DBU, THF, 20 °C, 21 h; (f) Pd/C 10%, ammonium formate, MeOH, reflux, 1 h; (g) TFA, DCM, 20 °C, 3 h, then HATU, TEA, DCM, DMF, 20 °C, 18 h.

Since macrocycle **58a** was inactive against the mARTDs, and since the compounds in Table 10 indicated that the unsubstituted benzamide was essential, no further attempts were made at synthesizing the remaining macrocyclic compounds. Experimental procedures for synthesized and characterized compounds are presented in Appendix 2.

## Concluding Remarks

Virtual screening was used to find novel inhibitors of ARTD7 and ARTD8. Multiple X-ray crystal structures and scoring functions were used in order to find the sixteen inhibitors presented in Table 9. Subsequent IC<sub>50</sub> evaluations using an enzymatic assay revealed that compounds **29** and **30** were more potent against ARTD10. These compounds then served as a starting point for a medicinal chemistry program aimed at developing inhibitors with improved potency and selectivity for the mARTDs. During this process a set of 25 analogs was synthesized. These analogs all have lead-like properties (small size, low lipophilicity, relatively high water solubility) and simple synthetic routes which make them attractive starting points for further development of selective ARTD inhibitors.

Attempts at this were made both with the merged compounds and with the macrocycles. However, due to the problematic synthesis, low solubility and poor IC<sub>50</sub> values, the merged compounds (**48a-v**) were abandoned before the full set was completed. New knowledge about structure activity relationships (the unsubstituted benzamide seemed essential) became available during the process of synthesizing the macrocyclic compounds (**58a-d**). Due to this, and since the first synthesized compound was inactive, the remaining macrocyclic analogs of **30** were also abandoned.

## Chapter 3: Biotinylated ARTD7, ARTD8, and ARTD10 Inhibitors for AlphaScreen

During the early stages of these projects, before the enzymatic assay was available (see Chapter 1), attempts were made to develop an Amplified Luminescent Proximity Homogeneous Assay<sup>132</sup> (AlphaScreen) as an alternative to the thermal shift measurements, and in order to better evaluate the activity of new ARTD inhibitors (see Chapter 1). Figure 27 gives a schematic representation of this assay. The protein of interest is attached to a donor bead and avidin is attached to an acceptor bead. The idea is that a biotinylated analog of a known binder will bind to both of these proteins and thus keep the two beads in close proximity to each other. When excited by laser at a wavelength of 680 nm the donor beads release singlet oxygen. If an acceptor bead is nearby (within 200 nm) it will absorb this singlet oxygen and in turn emit light with a wavelength between 520-620 nm. A second ligand can be used to break this complex, causing the two beads to drift away from each other. The amount of light emitted by the acceptor beads is thus reduced since the reactive singlet oxygen will decay before reaching an acceptor bead.

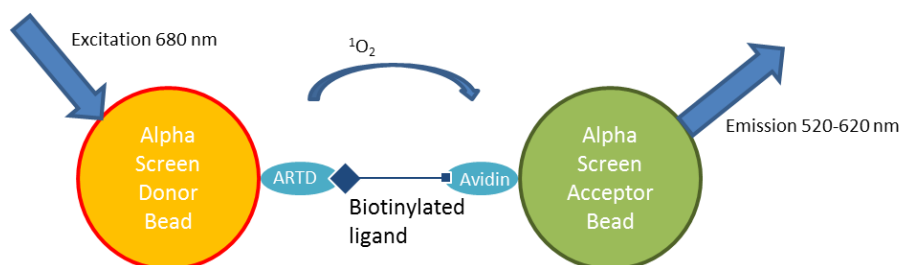


**Figure 27.** Schematic representation of AlphaScreen.

The previously mentioned screen of 185 compounds against 13 of the ARTDs had already identified compound **26** as an inhibitor of ARTD8 (Figure 28). Three biotinylated analogs to **26** with different attachment points for the biotin moiety were envisaged (Figure 29). Compound **68** is a simplified version of **26** with the entire triazol region removed and replaced by an amide and a hydrophilic spacer. Compound **69** includes the same hydrophilic spacer but also maintains a modified version of the triazol moiety. Compound **70** has a different attachment point for the biotin and is thus structurally more similar to **26**.

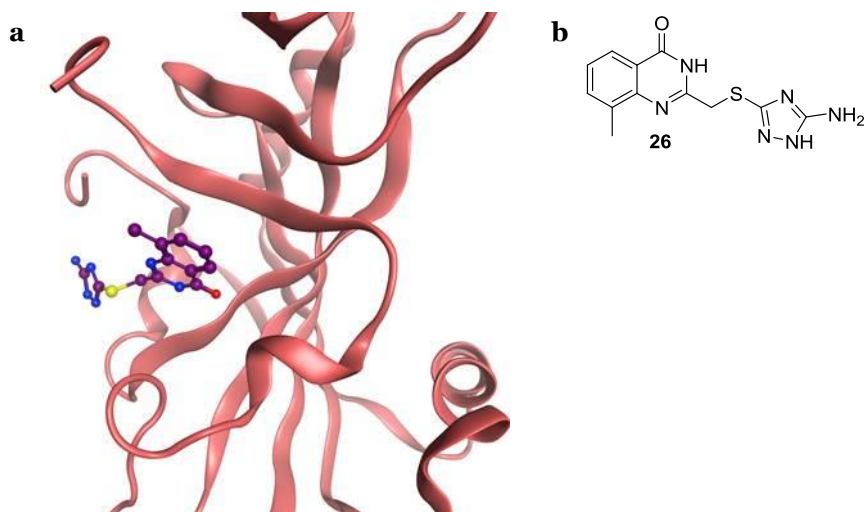


**Figure 28.** X-ray crystal structure of **26** in ARTD8. (a) The best attachment points for the biotin moiety are either at the methyl group on the quinazolinone or at the triazole, both of which are pointing out from the protein. (b) The structure of compound **26**.

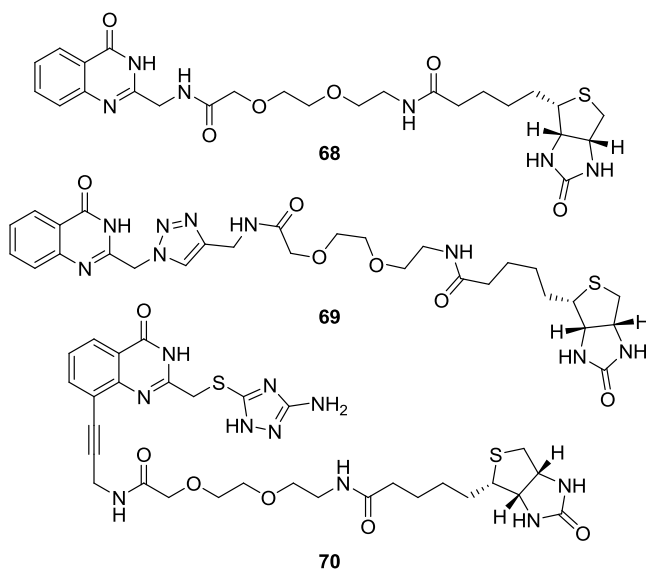
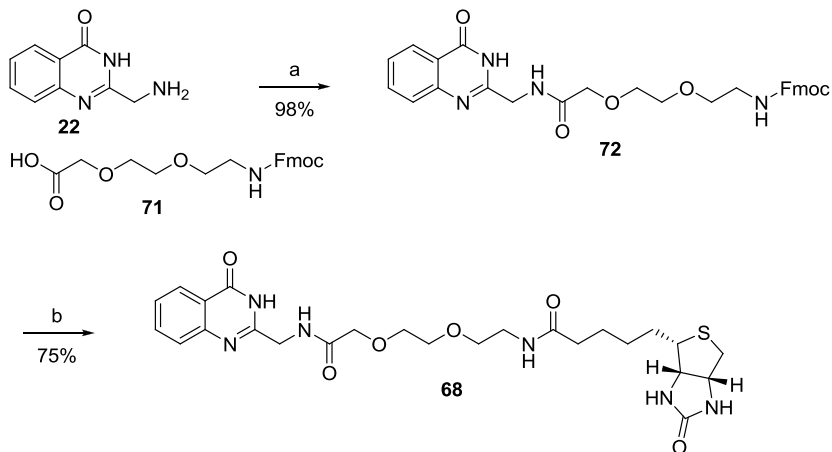


**Figure 29.** The structures of the three synthesized biotinylated analogs of compound **26**.

## Synthesis of Biotinylated Ligands

The synthesis of the first biotinylated analog, **68**, started by preparing compound **22** (See Chapter 1). Compound **22** was then acylated with an Fmoc protected hydrophilic spacer, **71**, using DIC/HOAt. The Fmoc group was subsequently removed using TBAF and (+)-biotin was attached using DIC/HOAt to form compound **68** (Scheme 11).

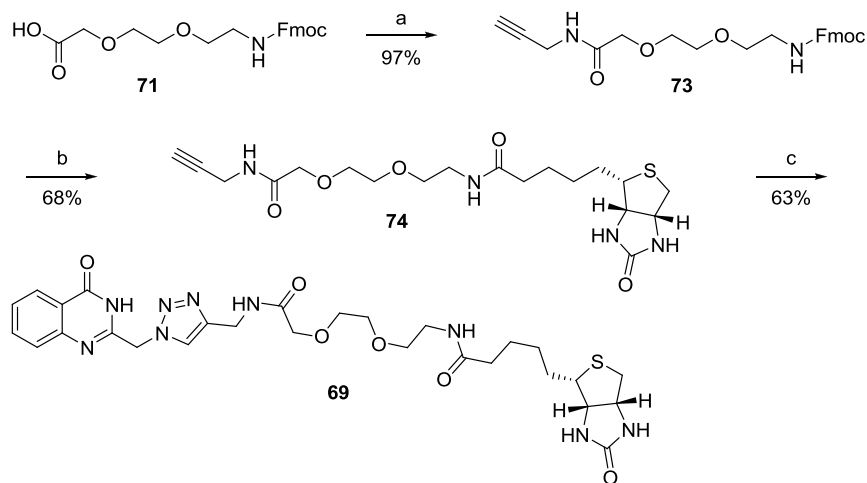
**Scheme 11.** Synthesis of the biotinylated compound **68**.



<sup>a</sup>Reagents and conditions: (a) DIC, HOAt, DMF, 20 °C, 16 h; (b) TBAF, DMF, 20 °C, 4 h, then DIC, HOAt, (+)-biotin, 70 °C, 1 h.

The same Fmoc protected hydrophilic spacer was used for the second biotinylated compound, **69**. Propargylamide **73** was first prepared starting from propargylamine hydrochloride and the previously mentioned linker (Scheme 12). The protecting group was then removed and (+)-biotin attached to form compound **74**. Compounds **21** (See Chapter 1) and **74** were finally combined using a Huisgen 1,3-dipolar cycloaddition<sup>133,134,135</sup> to form the triazole moiety present in **69**.

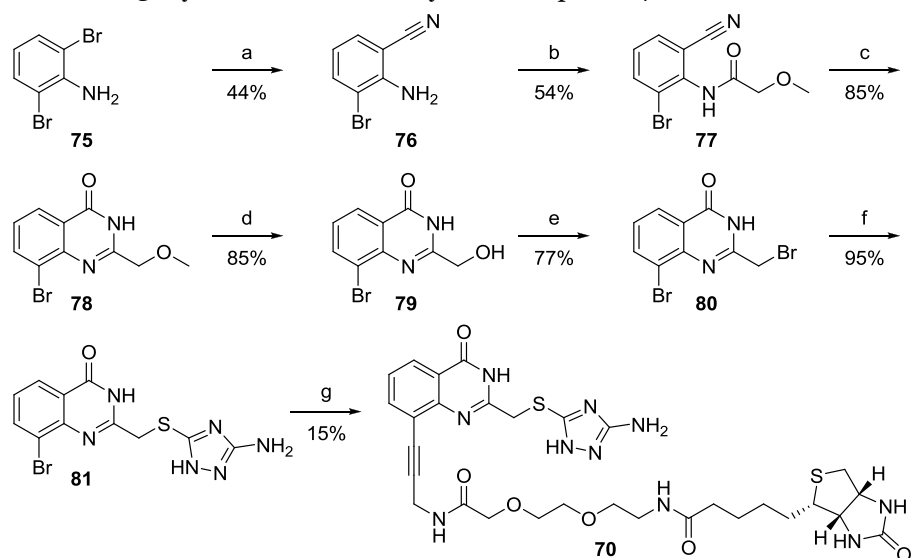
**Scheme 12.** Synthesis of the biotinylated compound **69**.



\*Reagents and conditions: (a) propargylamine hydrochloride, DIC, HOAt, TEA, DCM, 20 °C, 90 min; (b) KF, DMF, 70 °C, 30 min, then DIC, HOAt, 70 °C, 30 min; (c) **21**, sodium ascorbate, CuSO<sub>4</sub>, DMF, H<sub>2</sub>O, 20 °C, 30 min.

In order to reach the third biotinylated analog, compound **76** was first prepared by monocyanting dibromoaniline **75** under Rosenmund-von Braun conditions<sup>136,137</sup> using CuCN in NMP (Scheme 13). 20% of the dicyanated side product was also isolated using this method. Compound **80** was then prepared analogously to **13** (See Chapter 1). Large amounts of diacylation were observed when reacting **76** with methoxyacetyl chloride, causing low yields in this reaction step. Different conditions were investigated but this diacylation could not be completely avoided. Once obtained, **80** was reacted with the appropriate thiol to produce compound **81**. Finally, compound **74** was attached using a Sonogashira coupling<sup>138</sup> to produce the third biotinylated compound, **70**. This final reaction step proceeded with excellent conversion to the product but purification was troublesome due to low solubility, thus an isolated yield of only 15% was achieved.

### Scheme 13. Synthesis of the biotinylated compound **70**.



<sup>a</sup>Reagents and conditions: (a) CuCN, NMP, 165 °C, 4 h; (b) methoxyacetyl chloride, pyridine, DMF, 20 °C, 18 h; (c) K<sub>2</sub>CO<sub>3</sub>, UHP, Acetone, H<sub>2</sub>O, 82 °C, 48 h; (d) 47% HBr, 120 °C, 5 h; (e) CBr<sub>4</sub>, PPh<sub>3</sub>, DCM, 0 °C, 1 h, then 20 °C, 20 h; (f) 3-amino-4-mercapto-1,2,4-triazole, DMF, 80 °C, 15 min; (g) PdCl<sub>2</sub>(PPh<sub>3</sub>)<sub>2</sub>, CuI, Cs<sub>2</sub>CO<sub>3</sub>, **74**, DMF, 125 °C, 30 min.

These three biotinylated ligands were evaluated against ARTD8 and ARTD10 in the previously mentioned thermal shift assay (See Chapter 1). Compound **70** displayed a low thermal shift (0.27 °C) against ARTD8 while the other two biotinylated ligands produced statistically insignificant results against both enzymes. Despite this, attempts were made at developing an AlphaScreen assay using these three compounds. A weak signal was eventually observed (data not shown), however, it was concluded to be caused by unspecific binding and the project was abandoned when the enzymatic assay became available.

### Concluding Remarks

An AlphaScreen assay was considered in order to obtain qualitative inhibition data for novel ARTD inhibitors. Three biotinylated analogs to a known binder, **26**, were synthesized and efforts were made to adjust the previously described AlphaScreen assay to work with these compounds. Unfortunately these attempts failed as only unspecific binding was observed. The compounds did not seem to bind to any of the ARTDs and AlphaScreen was eventually abandoned in favor of the recently developed enzymatic assay described in Chapter 1.



## Chapter 4: Total Synthesis of Polyphenol Based Natural Products (Paper V)

The interest in polyphenol based natural products is increasing.<sup>93</sup> In order to further the scientific community's knowledge about this class of compounds, and to investigate if the entire tetrameric structure of (-)-hopeaphenol is required to inhibit the T3SS<sup>96,97</sup>, we decided to develop a total synthesis for  $\epsilon$ -viniferin, **82**, and ampelopsin B, **83** (Figure 30), using a strategy that would also allow the preparation of structural analogs with altered substitution patterns. The total syntheses of several related natural products are already described in the literature<sup>111,139,140,141,142,143,144,145</sup>, and after investigating several options<sup>146,147,148,149,150,151</sup> it was decided to prepare  $\epsilon$ -viniferin using methods inspired by Kim's synthesis of pentamethylated viniferifuran, **84**.<sup>152</sup> The synthetic route is presented in Scheme 14. Compound **85** was first monoprotected using iodomethane in DMF, producing a 12:37:31 mixture of substrate, monomethylated, and dimethylated products. No attempts at improving this ratio were made. In parallel, acetophenone **87** was brominated using  $\text{CuBr}_2$  to produce  $\alpha$ -bromo ketone **88**. These two compounds were then combined to give **89** which was subsequently cyclized to benzofurane **90** using  $\text{Bi}(\text{OTf})_3$ .

A direct arylation using  $\text{Pd}(\text{OAc})_2$ ,  $\text{P}(t\text{-Bu})_3 \cdot \text{HBF}_4$  and pivalic acid was then employed to introduce a benzyl protected phenol at the benzofurane C2 position.<sup>153,154</sup> Oxygen free conditions were of utmost importance during this reaction and yields around 70% could reliably be achieved when using meticulously freeze-thaw-degassed reagents and solvents. If this process was neglected the yields decreased to 20-60% with considerable amounts of dimerized **90** instead being formed. Compound **91** was then subjected to catalytic transfer hydrogenation in order to saturate the furane moiety and remove the benzyl protecting group to form cis-dihydrobenzofurane **92** in one step. When treated with TFA, compound **92** epimerized to trans-isomer **93** as detailed in Scheme 15. Separating these two diastereomers proved difficult but baseline separation was eventually achieved using column chromatography on silica gel with a toluene:MeCN eluent.

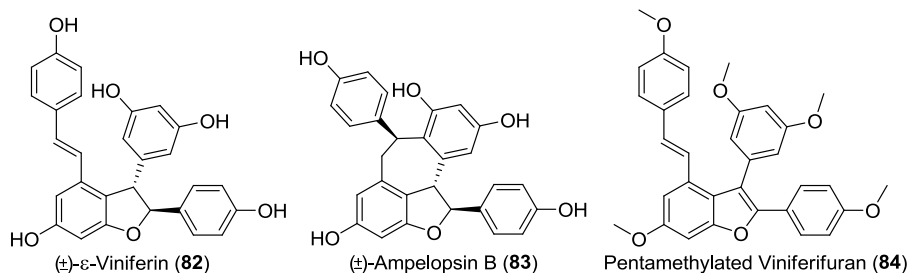
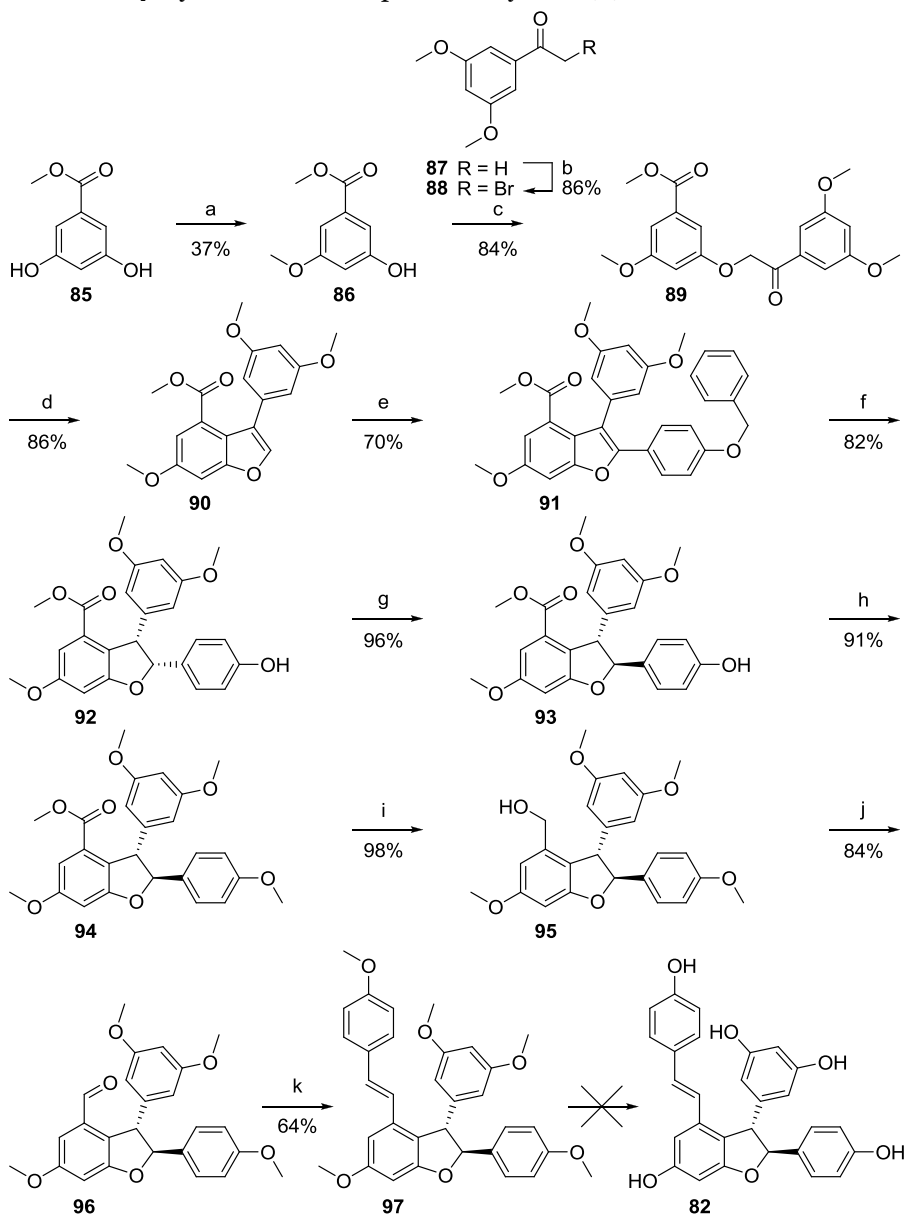


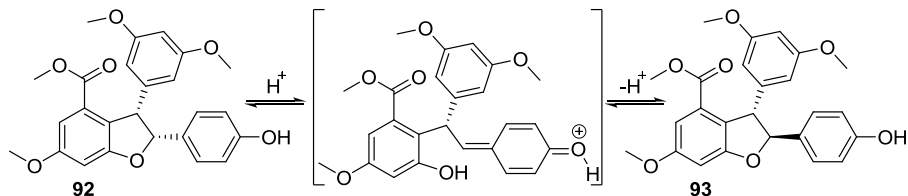
**Figure 30.** The structures of  $\epsilon$ -viniferin, ampelopsin B, and pentamethylated viniferifuran.

**Scheme 14.** Synthetic route to pentamethylated ( $\pm$ )- $\epsilon$ -viniferin.<sup>a,b</sup>



<sup>a</sup>Reagents and conditions: (a) MeI, K<sub>2</sub>CO<sub>3</sub>, DMF, 20 °C, 46 h; (b) CuBr<sub>2</sub>, EtOAc:CHCl<sub>3</sub> 1:1, reflux, 23 h; (c) K<sub>2</sub>CO<sub>3</sub>, acetone, reflux, 16 h; (d) Bi(OTf)<sub>3</sub>, DCM, reflux, 16 h; (e) Pd(OAc)<sub>2</sub>, 4-benzyloxybromobenzene, P(Cy)<sub>3</sub>•HBF<sub>4</sub>, K<sub>2</sub>CO<sub>3</sub>, pivalic acid, DMA, 100 °C, 27 h; (f) H-Cube, 10% Pd/C, EtOAc, 1 bar H<sub>2</sub>, 70 °C; (g) TFA, DCM, 80 °C, 30 min; (h) MeI, K<sub>2</sub>CO<sub>3</sub>, acetone, reflux, 5 h; (i) DIBAL, DCM, -78 °C, 1 h; (j) DMP, DCM, 0 °C, 15 min, 20 °C, 90 min; (k) Diethyl 4-methoxybenzylphosphonate, KOt-Bu, THF, -78 °C, 16 h. <sup>b</sup>All chiral compounds are racemic mixtures.

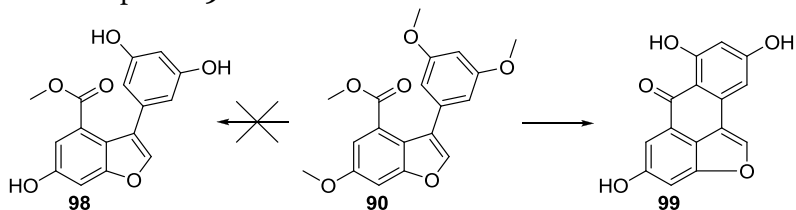
**Scheme 15.** Putative mechanism for the acid mediated epimerization of **92** to form compound **93**.



Next followed some routine reactions where the free phenol was first methyl protected and the methyl ester then reduced and reoxidized to aldehyde **96** using DIBAL followed by Dess-Martin periodinane.<sup>155</sup> The final fragment was then installed using Horner-Wadsworth-Emmons conditions<sup>156,157,158</sup> to form pentamethylated  $\epsilon$ -viniferin, **97**. This reaction produced exclusively the *E*-alkene when applied to the unsaturated benzofurane<sup>152</sup>, however, a mixture of the two isomers (64% *E* and 19% *Z*, isolated yields) was obtained when dihydrobenzofurane **96** was instead used. These isomers could fortunately be separated using flash column chromatography to yield pure pentamethylated  $\epsilon$ -viniferin, **97**, as a racemic mixture.

Despite considerable efforts, the global deprotection of **97** to form  $\epsilon$ -viniferin, **82**, was never successful. Several well established methods for ether cleavage were investigated but the methyl groups could not be removed without also decomposing  $\epsilon$ -viniferin. Boron tribromide showed promising preliminary results on TLC and LC-MS but crude <sup>1</sup>HNMR revealed complex mixtures without traces of  $\epsilon$ -viniferin.

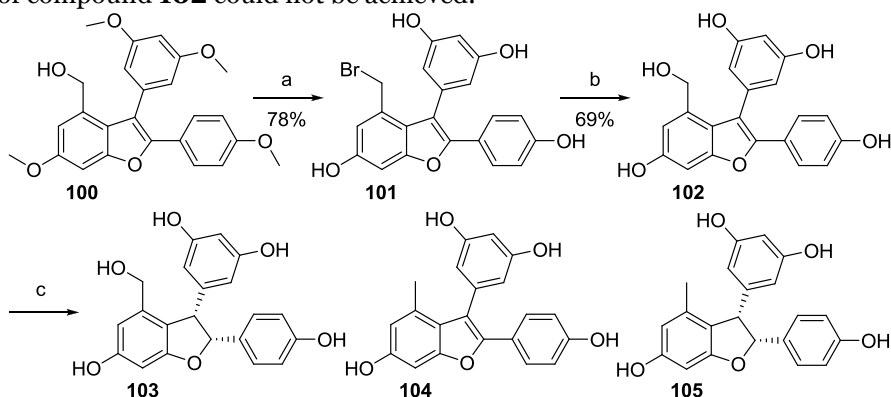
**Scheme 16.** Deprotection of compound **90** produced the cyclized analog **99** instead of compound **98**.



Attempts were also made to remove the methyl groups at an earlier stage. Deprotection of compound **90** also induced an intramolecular Friedel-Crafts acylation to form the Diptoinonesin G<sup>159</sup> analog **99** instead of compound **98** (Scheme 16). Deprotection of dihydrobenzofurane **95** produced a complex mixture. However, the unsaturated analog, **100** (Scheme 17 and Appendix 4), could be deprotected to produce **101** in good yield (78%) on a

100 mg scale, unfortunately this yield dropped considerably (to ca. 30%) when the reaction was scaled up to 500 mg or more. The alcohol could be reintroduced to form compound **102** by treating **101** with NaNO<sub>3</sub> in dioxane, but the following hydrogenation produced a mixture of **103-105**. Several catalysts and solvents were investigated in order to avoid reducing the benzylic alcohol but no selectivity could be obtained. Subsequent attempts to refunctionalize this position on protected analogs to compound **104** and **105** by oxidations or radical brominations also failed.

**Scheme 17.** Deprotection of **100** followed by reintroduction of the benzylic alcohol produced good results only on a small scale. Selective hydrogenation of compound **102** could not be achieved.<sup>a,b</sup>

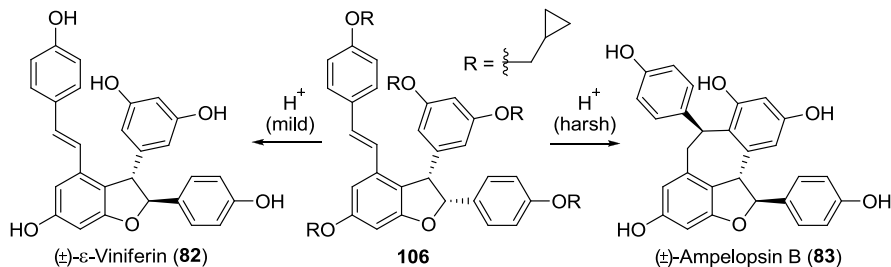


<sup>a</sup>Reagents and conditions: (a) BBr<sub>3</sub>, DCM, -78 °C to 20 °C, 17 h; (b) 20% NaNO<sub>3</sub> (aq), dioxane, 80 °C, 30 min; (c) hydrogenation, various conditions. <sup>b</sup>All chiral compounds are racemic mixtures.

## Cyclopropylmethyl, an Unconventional Protecting Group

Eventually it became obvious that a different protecting group was necessary. Several options were considered before it was decided to synthesize the cyclopropylmethyl (cPrMe) protected compound **106** (Scheme 18). Cyclopropylmethyl ethers have been reported as being stable to a wide range of reaction conditions while still being easy to selectively remove under acidic conditions.<sup>160</sup> If a balance could be found where compound **106** is selectively deprotected and epimerized to  $\epsilon$ -viniferin, **82**, under mild acidic conditions, and under harsher conditions also cyclized to ampelopsin B, **83**, it would be possible to selectively prepare both these natural products from a common precursor.

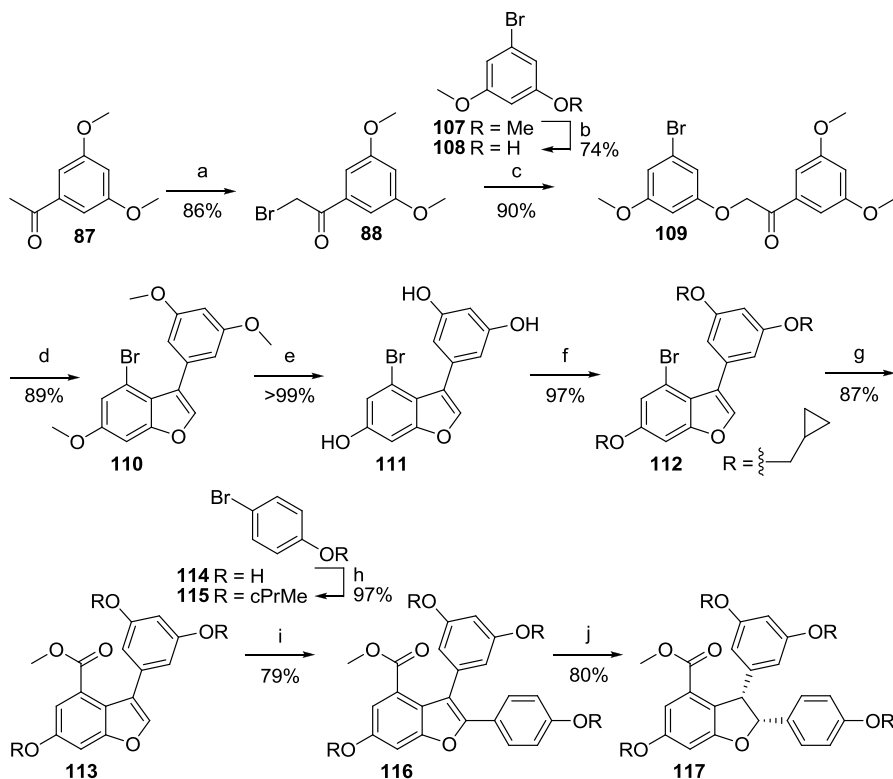
**Scheme 18.** If conditions could be found where compound **106** is deprotected and epimerized but not cyclized it would be possible to selectively prepare  $\epsilon$ -viniferin, **82**, or Ampelopsin B, **83**.



The synthetic route to compound **106** is presented in Scheme 19 and Scheme 20. Unfortunately the cPrMe protected benzofurane **113** could not be prepared directly since these protecting groups were incompatible with the cyclization conditions. Several other protecting groups were also investigated but only methyl protected phenols produced good results. The ester functionality therefore had to be introduced after a protecting group switch since previous experience had proved that the methyl groups could not be removed from compound **90** (Scheme 16). Hence, the synthetic route started by preparing phenol **108** by mono-deprotecting compound **107** in unexpectedly good yield. The phenol was then combined with  $\alpha$ -bromo ketone **88** to give compound **109** which was cyclized to benzofurane **110** using  $\text{Bi}(\text{OTf})_3$  as previously described. The methoxy ethers could then be cleaved using  $\text{BBr}_3$  and replaced with cPrMe equivalents to form compound **112**.

A palladium catalyzed carbonylation using  $\text{Mo}(\text{CO})_6$  as carbon monoxide source<sup>117,118</sup> was then used to introduce the ester functionality. This reaction had previously been tweaked to work well on compound **110** using  $\text{Pd}(\text{dppf})\text{Cl}_2$ , DBU, and MeOH in a MeCN/toluene mixture at 100 °C for 30 minutes. However, when these conditions were applied to cPrMe analog **112** the reaction was sluggish. Increasing the reaction time and temperature produced large amounts of the dehalogenated side product (Table 12, Entry 10). Replacing DBU with  $\text{K}_2\text{CO}_3$  improved the conversion but the product to dehalogenation ratio was still unfavorable (Entry 14). However, this ratio could be reversed by changing the solvent to DMF (Entry 9). Other catalyst systems were also investigated but produced worse results than  $\text{Pd}(\text{OAc})_2/\text{dppf}$ . Using an electron rich ligand improved the reaction rate but produced mainly the dehalogenated side product (Entry 5).<sup>161</sup> Curiously, using  $\text{Pd}(\text{dppf})\text{Cl}_2$  instead of  $\text{Pd}(\text{OAc})_2/\text{dppf}$  gave similar results (Entry 15). Other catalysts showed poor conversion.

**Scheme 19.** Synthetic route to intermediate **117**.<sup>a,b</sup>



<sup>a</sup>Reagents and conditions: (a) CuBr<sub>2</sub>, EtOAc:CHCl<sub>3</sub> 1:1, reflux, 23 h; (b) BBr<sub>3</sub>, DCM, 0 to 20 °C, 23 h; (c) K<sub>2</sub>CO<sub>3</sub>, acetone, reflux, 2 h; (d) Bi(OTf)<sub>3</sub>, DCM, reflux, 22 h; (e) BBr<sub>3</sub>, DCM, -78 to 20 °C, 18 h; (f) (bromomethyl)cyclopropane, K<sub>2</sub>CO<sub>3</sub>, acetone, reflux, 22 h; (g) Pd(OAc)<sub>2</sub>, K<sub>2</sub>CO<sub>3</sub>, Mo(CO)<sub>6</sub>, MeOH, dppe, DMF, 120 °C, 15 h; (h) 4-bromophenol, (bromomethyl)cyclopropane, K<sub>2</sub>CO<sub>3</sub>, acetone, reflux, 24 h; (i) Pd(OAc)<sub>2</sub>, P(Cy)<sub>3</sub>·HBF<sub>4</sub>, K<sub>2</sub>CO<sub>3</sub>, pivalic acid, DMA, 100 °C, 20 h; (j) Pd/C 10%, H<sub>2</sub>, EtOAc:MeOH 1:9, 20 °C, 3 d. <sup>b</sup>All chiral compounds are racemic mixtures.

Other methods to introduce the carbonyl group were also investigated, including cyanations using CuCN under Rosenmund-von Braun conditions<sup>136,137</sup>, and lithiation followed by quenching with DMF or CO<sub>2</sub>. The former successfully gave the nitrile, which unfortunately failed at later stages in the envisioned synthetic strategy, and the latter functionalized the benzofurane C2 position. Blocking this position by performing the direct arylation on bromide **112** gave low yields and several unidentified side products were formed.

The following direct arylation of **113** to form compound **116** proceeded in good yields when using meticulously degassed solvents and an aryl bromide coupling partner. Aryl iodides were also investigated but showed slow conversion to **116** and large amounts of the dimerized side product. Subsequent hydrogenation of the furane to form compound **117** followed by reduction and reoxidation of the methyl ester to aldehyde **119** proceeded

smoothly (Scheme 20). Compound **106** could then be obtained using Horner-Wadsworth-Emmons conditions after preparing phosphonate **120** in four separate steps.

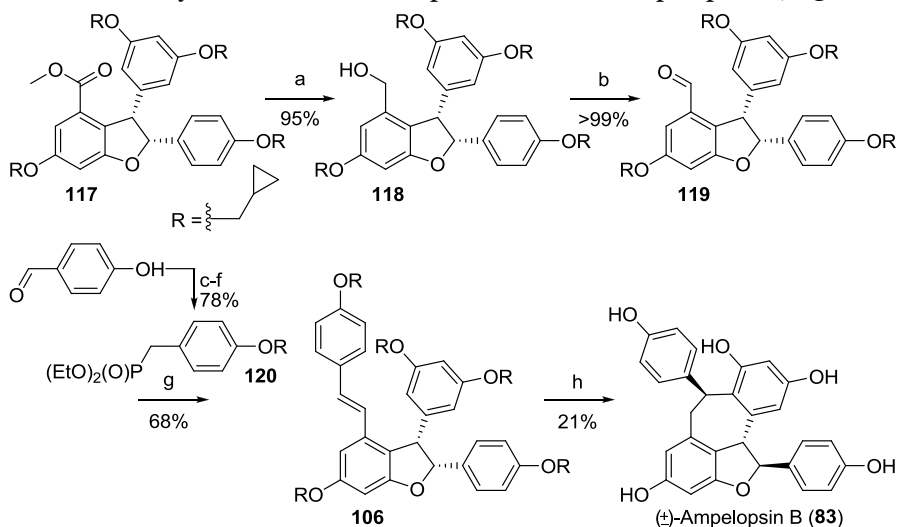
**Table 12.** Various reaction conditions for the transformation of **112** to compound **113**.

Entry	Catalyst/Ligand	Base	Solvent	Additives	Time (h)	Temp (°C)	Product (%) <sup>a</sup>	-Br (%) <sup>a</sup>
1	Hermann-Beller	DBU	MeCN/Tol	MeOH + Mo(CO) <sub>6</sub>	2	120	5	35
2	Rh(PPh <sub>3</sub> ) <sub>3</sub> Cl	DBU	MeCN/Tol	MeOH + Mo(CO) <sub>6</sub>	2	120	10	1
3	Pd(PPh <sub>3</sub> ) <sub>2</sub> Cl <sub>2</sub>	DBU	MeCN/Tol	MeOH + Mo(CO) <sub>6</sub>	2	120	10	20
4	Pd(PPh <sub>3</sub> ) <sub>4</sub>	DBU	MeCN/Tol	MeOH + Mo(CO) <sub>6</sub>	2	120	10	15
5	Pd(OAc) <sub>2</sub> /PCy <sub>3</sub>	DBU	MeCN/Tol	MeOH + Mo(CO) <sub>6</sub>	2	120	20	80
6	Hermann-Beller	DBU	DMF	MeOH + Mo(CO) <sub>6</sub>	2	120	5	3
7	Hermann-Beller	K <sub>2</sub> CO <sub>3</sub>	DMF	MeOH + Mo(CO) <sub>6</sub>	2	120	5	3
8	Pd(OAc) <sub>2</sub> /dppf	DBU	DMF	MeOH + Mo(CO) <sub>6</sub>	2	120	30	20
9	Pd(OAc) <sub>2</sub> /dppf	K <sub>2</sub> CO <sub>3</sub>	DMF	MeOH + Mo(CO) <sub>6</sub>	2	120	80	20
10	Pd(dppf)Cl <sub>2</sub>	DBU	MeCN/Tol	MeOH + Mo(CO) <sub>6</sub>	2	120	15	25
11	Rh(PPh <sub>3</sub> ) <sub>3</sub> Cl	K <sub>2</sub> CO <sub>3</sub>	MeCN/Tol	MeOH + Mo(CO) <sub>6</sub>	2	120	5	1
12	Rh(PPh <sub>3</sub> ) <sub>3</sub> Cl	K <sub>2</sub> CO <sub>3</sub>	DMF	MeOH + Mo(CO) <sub>6</sub>	2	120	1	15
13	Pd(OAc) <sub>2</sub> /dppf	K <sub>2</sub> CO <sub>3</sub>	DMF	MeOH + Mo(CO) <sub>6</sub>	2	100	30	5
14	Pd(OAc) <sub>2</sub> /dppf	K <sub>2</sub> CO <sub>3</sub>	MeCN/Tol	MeOH + Mo(CO) <sub>6</sub>	2	120	20	80
15	Pd(dppf)Cl <sub>2</sub>	K <sub>2</sub> CO <sub>3</sub>	DMF	MeOH + Mo(CO) <sub>6</sub>	2	120	10	50

<sup>a</sup>Yields were approximated from the relative area of the peaks in the LC-MS UV-trace.

Unfortunately, no conditions were found where  $\epsilon$ -viniferin, **82**, could be isolated from the following multistep reaction. The cyclization was taking place at milder conditions than what was required to remove the cPrMe protecting groups. However, Ampelopsin B, **83**, could be isolated through a noteworthy three-step-one-pot deprotection-cyclization-epimerization to produce this natural product in 5% overall yield over 12 reaction steps in the longest linear sequence. This is the first reported total synthesis of Ampelopsin B which does not involve a dimerization of resveratrol.

**Scheme 20.** Synthetic route to compound **106** and ampelopsin B, **83**.<sup>a,b</sup>



<sup>a</sup>Reagents and conditions: (a) DIBAL, DCM,  $-78\text{ }^{\circ}\text{C}$ , 1 h; (b) DMP, DCM,  $20\text{ }^{\circ}\text{C}$ , 90 min; (c) 4-hydroxybenzaldehyde, (bromomethyl)cyclopropane,  $\text{K}_2\text{CO}_3$ , acetone, reflux, 24 h; (d)  $\text{NaBH}_4$ , MeOH,  $20\text{ }^{\circ}\text{C}$ , 1 h; (e)  $\text{SOCl}_2$ ,  $\text{Et}_2\text{O}$ ,  $20\text{ }^{\circ}\text{C}$ , 2 h; (f)  $\text{P}(\text{OEt})_3$ ,  $130\text{ }^{\circ}\text{C}$ , 22 h; (g)  $\text{KOt-Bu}$ , THF,  $-78\text{ }^{\circ}\text{C}$ , 16 h; (h) 12M HCl (aq), THF,  $80\text{ }^{\circ}\text{C}$ , 1 h. <sup>b</sup>All chiral compounds are racemic mixtures.

It was realized that a different protecting group, preferably one removable under alkaline conditions, was required in order to reach  $\epsilon$ -viniferin, **82**. Compound **117** could be deprotected and epimerized in one step to form trans dihydrobenzofurane **121** (Scheme 21). During this reaction, a small amount of ester hydrolysis to form the corresponding carboxylic acid was also observed. This hydrolysis could not be avoided but the side product could be reesterified back to **121**. Compound **121** was subsequently reprotected with cPrMe in order to verify the isomerization at C2. A shift in coupling constant between the protons at C2 and C3 from  $J = 8.0\text{ Hz}$  to  $J = 4.8\text{ Hz}$  was observed, proving the reversed stereochemistry (Figure 31). Unsuccessful attempts were also made to deprotect the cPrMe protected analogs of **122**, **123**, and **125**, only side products were formed during these reactions.

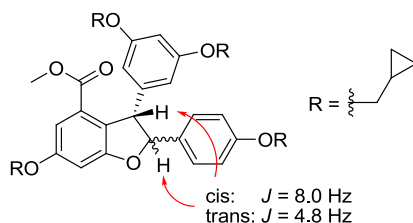
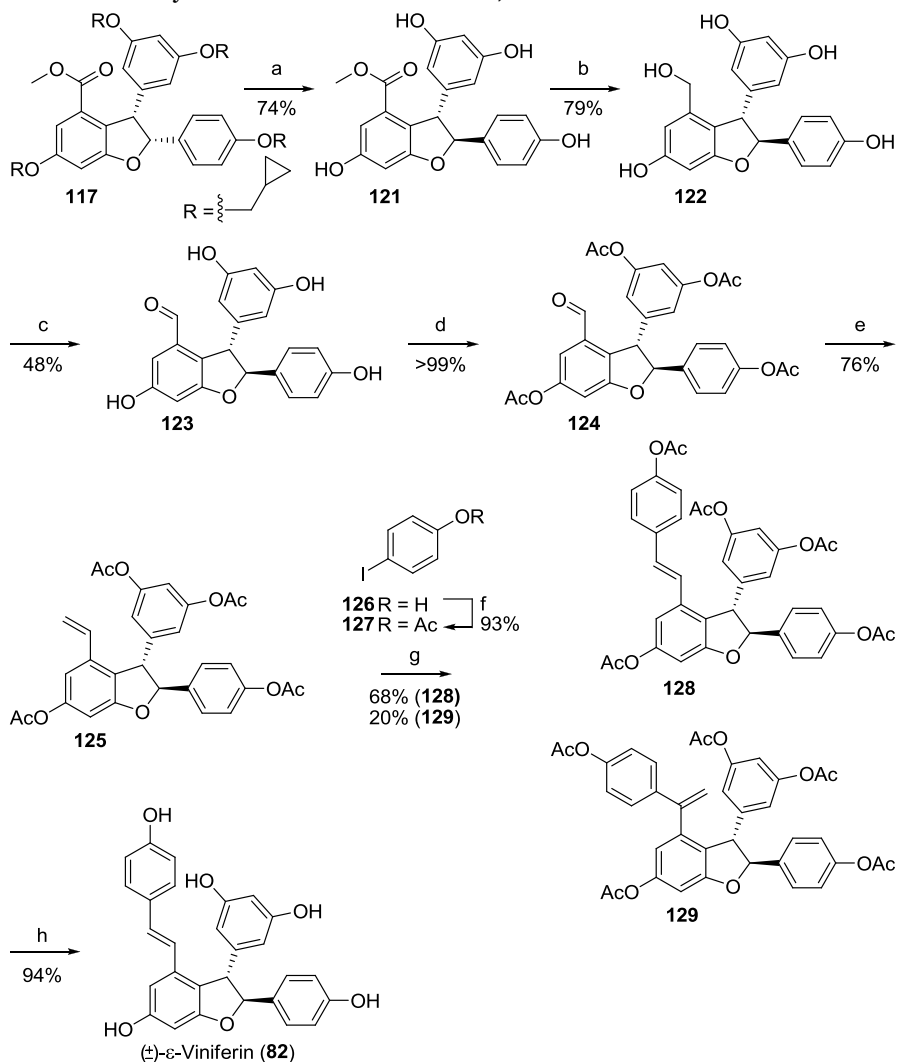


**Figure 31.** The coupling constant ( $J$ ) was measured to 8.0 Hz for the cis isomer, **117**, and 4.8 Hz for the trans isomer.

**Scheme 21.** Synthetic route to  $\epsilon$ -viniferin, **82**.<sup>a,b</sup>



<sup>a</sup>Reagents and conditions: (a) 12 M HCl, DCM, MeOH, 100 °C, 1 h; (b) LiAlH<sub>4</sub>, -78 to 20 °C, 5 d; (c) PDC, THF, 20 °C, 17 h; (d) Ac<sub>2</sub>O, TEA, THF, 20 °C, 17 h; (e) methyltriphenylphosphonium bromide, K<sub>2</sub>CO<sub>3</sub>, THF, reflux, 20 h; (f) 4-iodophenol, Ac<sub>2</sub>O, pyridine, 20 °C, 18 h; (g) P(*t*-Bu)<sub>3</sub>·HBF<sub>4</sub>, Pd(OAc)<sub>2</sub>, TEA, MeCN, 120 °C, 3 h; (h) KOH, MeOH, 0 °C, 70 min. <sup>b</sup>All chiral compounds are racemic mixtures.

Selective reduction of the methyl ester on pivaloyl protected **121** failed, NaBH<sub>4</sub> and DIBAL selectively reduced the pivaloyl protecting groups and LiAlH<sub>4</sub> displayed no selectivity between the different esters. Borane reduction of the corresponding carboxylic acid was not investigated since the required substrate could not be prepared. The methyl ester of compound **121** was instead reduced directly using LiAlH<sub>4</sub>, reoxidized to aldehyde **123** using PDC, and acetyl protected to form compound **124**. Spot to spot conversion was observed during the PDC oxidation and the low yield can therefore most

likely be contributed to workup or purification issues. The following Horner-Wadsworth-Emmons reaction<sup>155,156,157,158</sup> to transform aldehyde **124** directly to acetyl protected  $\epsilon$ -viniferin, **128** was unsuccessful. It was also attempted with pivaloyl protected phenols but the desired product was not observed. Instead a single carbon was added using standard Wittig conditions<sup>162,163</sup> to form the styrene derivative **125**. A Heck coupling<sup>164,165</sup> was then used to introduce then final phenyl ring, forming a mixture of acetyl protected  $\epsilon$ -viniferin, **128**, and gem-diaryl alkene **129**. A variety of reaction conditions were investigated in order to improve the yield and minimize the amount of regioisomer **129**, these experiments are summarized in Table 13.

**Table 13.** Summary of reaction conditions for the Heck coupling between compounds **125** and **127**.

Entry	Catalyst/Ligand	Base	Halide	solvent	Time (h)	Temp (°C)	N <sub>2</sub>	Rating <sup>a</sup>
1	Pd(OAc) <sub>2</sub> / P(O-Tol) <sub>3</sub>	TEA	1 eq Br	DMF	20	80	-	+
2	Pd(OAc) <sub>2</sub> / P(O-Tol) <sub>3</sub>	TEA	2 eq Br	DMF	20	80	-	+
3	Pd(OAc) <sub>2</sub> / P(O-Tol) <sub>3</sub>	K <sub>2</sub> CO <sub>3</sub>	1 eq Br	DMF	20	80	-	+
4	Pd(OAc) <sub>2</sub> / P(O-Tol) <sub>3</sub>	K <sub>2</sub> CO <sub>3</sub>	1 eq Br	MeCN	20	80	-	+
5	Pd(OAc) <sub>2</sub> / P(O-Tol) <sub>3</sub>	TEA	10 eq Br	TEA	20	80	-	-
6	Pd(PPh <sub>3</sub> ) <sub>4</sub>	TEA	1 eq Br	DMF	20	80	-	+
7	PEPPSI-IPr	TEA	1 eq Br	DMF	20	80	-	+
8	PEPPSI-IPr	TEA	1 eq Br	MeCN	20	80	-	+
9	Pd(OAc) <sub>2</sub> /P( <i>t</i> -Bu) <sub>3</sub> HBF <sub>4</sub>	TEA	1 eq Br	DMF	20	80	-	++
10	Herrmann-Beller	TEA	1 eq Br	DMF	20	80	-	+
11	Pd(OAc) <sub>2</sub> /P( <i>t</i> -Bu) <sub>3</sub> HBF <sub>4</sub>	K <sub>2</sub> CO <sub>3</sub>	1 eq I	DMF	20	80	-	+
12	Pd(OAc) <sub>2</sub> /P(Cy) <sub>3</sub> HBF <sub>4</sub>	TEA	1 eq I	DMF	20	80	-	++
13	Pd(OAc) <sub>2</sub> /P( <i>t</i> -Bu) <sub>3</sub> HBF <sub>4</sub>	TEA	1 eq I	DMF	20	80	-	++
14	Pd(OAc) <sub>2</sub> /P( <i>t</i> -Bu) <sub>3</sub> HBF <sub>4</sub>	TEA	1 eq I	MeCN	20	80	-	+++
15	Pd(OAc) <sub>2</sub> /P( <i>t</i> -Bu) <sub>3</sub> HBF <sub>4</sub>	TEA	2 eq I	MeCN	20	80	-	+
16	Pd(OAc) <sub>2</sub> /P( <i>t</i> -Bu) <sub>3</sub> HBF <sub>4</sub>	TEA	2 eq I	MeCN	20	80	yes	++
17	Pd(OAc) <sub>2</sub> /P( <i>t</i> -Bu) <sub>3</sub> HBF <sub>4</sub>	TEA	2 eq I	DMF	20	80	-	++
18	Pd(OAc) <sub>2</sub> /P( <i>t</i> -Bu) <sub>3</sub> HBF <sub>4</sub>	TEA	2 eq I	DMF	20	80	yes	++
19	Pd(OAc) <sub>2</sub> /P( <i>t</i> -Bu) <sub>3</sub> HBF <sub>4</sub>	TEA	2 eq I	DMF	20	100	-	++++
20	Pd(OAc) <sub>2</sub> /P( <i>t</i> -Bu) <sub>3</sub> HBF <sub>4</sub>	TEA	2 eq I	DMF	20	120	-	++++
21	Pd(OAc) <sub>2</sub> /P( <i>t</i> -Bu) <sub>3</sub> HBF <sub>4</sub>	TEA	2 eq I	MeCN	3	120	-	+++++

<sup>a</sup>Reactions were subjectively rated (from (-) = no product observed to (+++++) = full conversion, clean reaction) from the relative area of the peaks in the LC-MS UV-trace.

In general, TEA is preferable to  $K_2CO_3$ , the aryl iodide gives better results than the corresponding bromide, an electron rich ligand is needed, and  $N_2$  atmosphere is not beneficial. Conversion could not be objectively calculated from the LC-MS chromatogram due to severe overlap between different peaks, different conditions were instead subjectively rated according to the rating column. The conditions presented in entry 21 were eventually used to obtain a 78:22 mixture of **128** and **129** according to crude  $^1H$ NMR, no further attempts were made to improve this ratio.

## Alkene Isomerization, *E* to *Z*

Despite investigating several eluent systems the mixture of **128** and **129** could not be separated using neither flash column chromatography on silica gel nor reverse phase HPLC. In addition, Compound **128** unexpectedly isomerized to *Z*-alkene **130** when subjected to the HPLC conditions and the  $^1H$ NMR spectra afterwards showed a 58:25:17 mixture of the three regioisomers (Figure 32). The resulting gem-diaryl alkene could be separated from  $\epsilon$ -viniferin, **82**, if the mixture of **128** and **129** was first deprotected using KOH in MeOH. However, pure  $\epsilon$ -viniferin could not be obtained since a 35:65 mixture of  $\epsilon$ -viniferin and “*Z*- $\epsilon$ -viniferin” was observed after HPLC purification.

Alternative ways to purify the mixture were investigated and it was realized that separation of **128** and **129** was possible using preparatory TLC. This way, the two isomers could be fully separated with less than 1% of the *Z*-alkene observed in the  $^1H$ NMR spectra. The crude mixture also slowly (2-3%) isomerized when left concentrated at room temperature overnight. However, no further isomerization of the alkene was observed after pure **128** was obtained. The final global deprotection of **128** proceeded smoothly using KOH in MeOH to produce pure  $\epsilon$ -viniferin, **82**, in 5% overall yield over 15 reaction steps in the longest linear sequence.

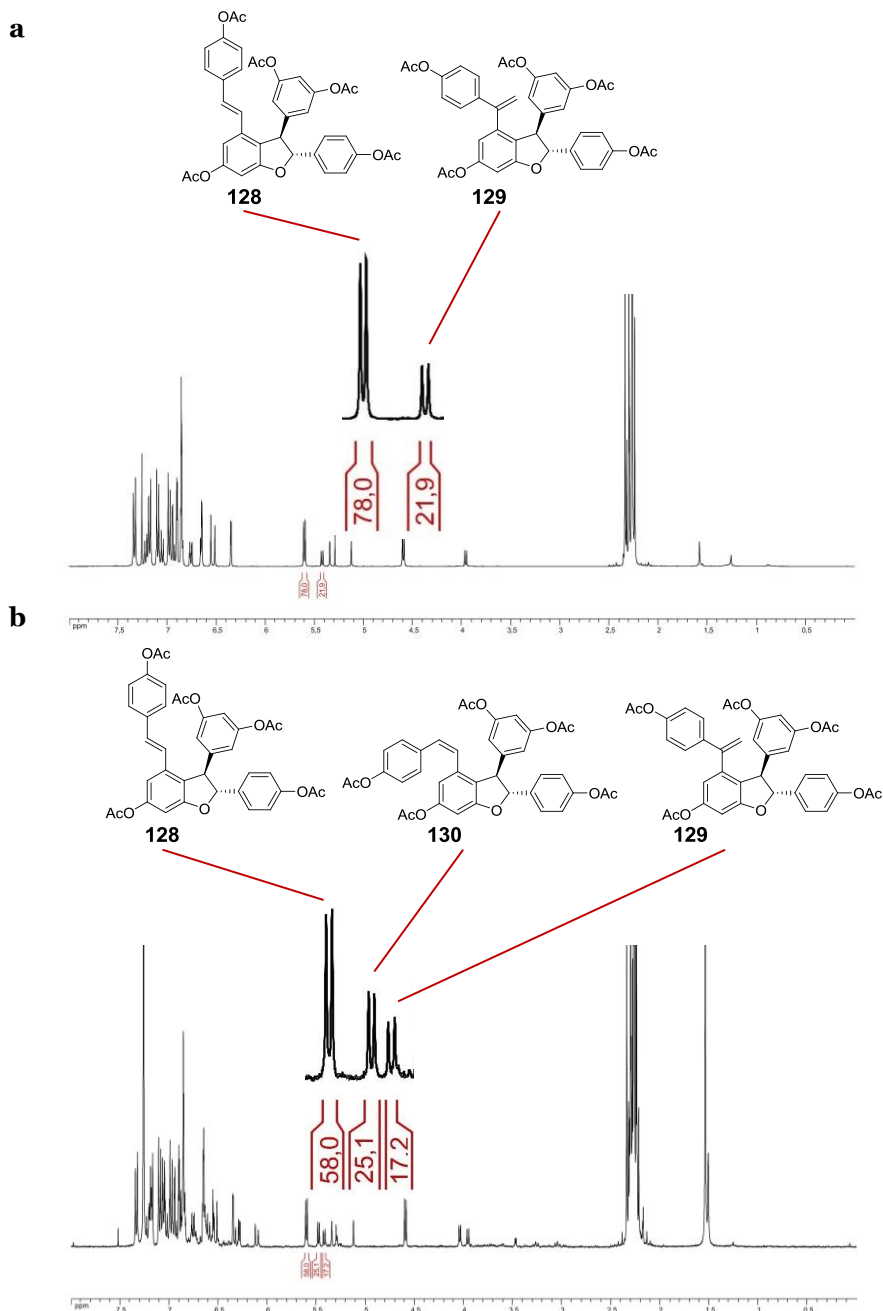


**Figure 32.**  $^1\text{H}$ NMR spectra before and after HPLC. Integrals correspond to the proton at C2 on the dihydrobenzofuranes. (a) Before HPLC a 78:22 mixture of the two regioisomers is observed. (b) After HPLC the *Z*-alkene, **130**, is formed and a 58:25:17 mixture of the three regioisomers is observed.

## Concluding Remarks

A flexible synthetic route to the two natural products  $\epsilon$ -viniferin, **82**, and ampelopsin B, **83**, has been developed. The strategy employs a rarely used protecting group, cyclopropylmethyl, to achieve a three-step-one-pot reaction where Ampelopsin B is obtained through a sequence containing deprotection of five phenol ethers, epimerization to form a trans dihydrobenzofurane, and an intramolecular Friedel-Crafts alkylation. Using this strategy the two natural products were prepared in 15 steps with 5% overall yield, and 12 steps with 5% overall yield, respectively. These are the first reported total syntheses of  $\epsilon$ -viniferin and ampelopsin B which does not involve a dimerization of resveratrol and an important advantage with this strategy is the possibility to synthesize structural analogs with specific alterations to the substitution patterns. Future work includes investigating the scope and limitations of this strategy by synthesizing a library of analogs to these two natural products in order to identify novel inhibitors of various infectious microorganisms.



# Conclusions and Outlook

## Diphtheria Toxin-like ADP-Ribosyltransferases

A combination of synthetic organic chemistry, computational chemistry, and structural biology has been used to develop inhibitors of the human diphtheria toxin-like ADP-ribosyl transferase family of proteins. A potent and selective inhibitor of ARTD3 was identified. This compound can selectively inhibit ARTD3 in cells and is thus a suitable chemical probe for elucidating the biological function of this enzyme.

A set of inhibitors targeting ARTD7, ARTD8, and ARTD10 were also developed. Due to their lead-like properties, these compounds are excellent starting points for medicinal chemistry programmes aimed at finding potent and selective inhibitors of the mARTDs. Attempts at this were made with both the merged compounds and the macrocycles. For different reasons these two compound classes unfortunately proved unsuitable as mARTD inhibitors.

With the exception of ARTD1, the ARTD family of proteins is still poorly understood, many of the enzymes are not fully characterized and their substrates are not known. New methods to probe the biological function of individual family members are thus needed. The compounds described in this thesis can hopefully help alleviate this situation by acting as chemical probes and thus allow scientists to individually study these proteins.

## Total Synthesis of Polyphenol Based Natural Products

Polyphenols is an interesting and often challenging class of compounds. This thesis describes the total synthesis of two related polyphenolic natural products using a flexible synthetic strategy that allows alterations to their substitution patterns and therefore the synthesis of structural analogs. The strategy makes use of an unconventional protecting group to enable a noteworthy three-step-one-pot deprotection-epimerization-cyclization to reach the first of these natural products. The second natural products was subsequently obtained after a protecting group switch.

With antibacterial resistance on the rise the need for new ways of combating this threat is increasing. Natural products continue to be important for the development of new pharmaceuticals and our ability to synthesize and modify these challenging compounds is therefore essential. While large amounts of natural products can usually be isolated from nature, structure activity relationships for various pathogens cannot be established without structural analogs, which are not readily available in this way.



# Appendix 1

## Experimental Procedures for the Compounds Presented in Scheme 9.

**2-Amino-4-nitrobenzonitrile (51).** 2-Bromo-5-nitroaniline (4.0 g, 18.43 mmol) and CuCN (2.0 g, 22.13 mmol) in NMP (15 ml) were heated to 175 °C for 1 hour. CuCN (0.5 g, 5.53 mmol) was added and heating was continued for 1 hour. Diluted with EtOAc and washed with 0.1 M NaOH. The organic phase was dried (Na<sub>2</sub>SO<sub>4</sub>), filtered and concentrated. Purified using column chromatography on silica gel (Heptane:EtOAc 75:25) to give **51** (3.0 g, 95%). <sup>1</sup>H NMR (400MHz, SO(CD<sub>3</sub>)<sub>2</sub>) δ 7.70 (d, *J* = 8.6 Hz, 1H), 7.64 (d, *J* = 2.3 Hz, 1H), 7.32 (dd, *J* = 8.6, 2.3 Hz, 1H), 6.74 (s, 2H); <sup>13</sup>C NMR (100 MHz, SO(CD<sub>3</sub>)<sub>2</sub>) δ 162.3, 150.9, 134.5, 116.5, 109.4, 109.3, 98.4.

**N-(2-cyano-5-nitrophenyl)-2-methoxyacetamide (52).** Compound **51** (2650 mg, 16.24 mmol), methoxyacetyl chloride (2.23 ml, 26.37 mmol) and pyridine (3.94 ml, 48.74 mmol) were dissolved in DMF (11 ml) and stirred at room temperature for 2 hours. The solution was diluted with EtOAc and washed with 1M HCl followed by brine. The organic layer was dried (Na<sub>2</sub>SO<sub>4</sub>), filtered and concentrated. Purified using column chromatography on silica gel (Heptane:EtOAc 75:25) to give **52** (3050 mg, 80%). <sup>1</sup>H NMR (400MHz, CDCl<sub>3</sub>) δ 9.43 (d, *J* = 2.2 Hz, 1H), 9.21 (s, 1H), 8.06 (dd, *J* = 8.5, 2.2 Hz, 1H), 7.82 (d, *J* = 8.5 Hz, 1H), 4.16 (s, 2H), 3.61 (s, 3H); <sup>13</sup>C NMR (100 MHz, CDCl<sub>3</sub>) δ 168.4, 151.2, 141.2, 133.4, 118.8, 115.6, 114.5, 107.0, 71.8, 59.8.

**2-(Methoxymethyl)-7-nitroquinazolin-4(3H)-one (53).** Compound **52** (10170 mg, 43.24 mmol), UHP (8140 mg, 86.51 mmol) and K<sub>2</sub>CO<sub>3</sub> (1195 mg, 8.65 mmol) were dissolved in acetone (150 ml) and water (150 ml). The mixture was heated to 82 °C for 24 hours. The mixture was then allowed to reach room temperature and concentrated until product started to precipitate. This precipitate was collected by filtration, washed with water and dried *in vacuo* to give **53** (8160 mg, 80%). <sup>1</sup>H NMR (400MHz, SO(CD<sub>3</sub>)<sub>2</sub>) δ 12.62 (s, 1H), 8.35 (d, *J* = 2.3 Hz, 1H), 8.32 (d, *J* = 8.9 Hz, 1H), 8.22 (dd, *J* = 8.9, 2.3 Hz, 1H), 4.38 (s, 2H), 3.39 (s, 3H); <sup>13</sup>C NMR (100 MHz, SO(CD<sub>3</sub>)<sub>2</sub>) δ 160.7, 156.4, 151.2, 148.7, 128.2, 125.8, 122.0, 120.3, 71.4, 58.5.

**2-(Hydroxymethyl)-7-nitroquinazolin-4(3H)-one (54).** Compound **53** (1000 mg, 4.25 mmol) was dissolved in 47% HBr (80 ml) and heated to 120 °C for 5 hours. The pH was adjusted to ~8 by addition of NaOH (s) and the waterphase was extracted with EtOAc. The organic phase was dried (Na<sub>2</sub>SO<sub>4</sub>), filtered and concentrated to give **54** (873 mg, 93%). <sup>1</sup>H NMR

(400MHz, SO(CD<sub>3</sub>)<sub>2</sub>) δ 12.41 (s, 1H), 8.33 (d, *J* = 2.3 Hz, 1H), 8.32 (d, *J* = 8.7 Hz, 1H), 8.20 (dd, *J* = 8.7, 2.3 Hz, 1H), 5.72 (s, 1H), 4.44 (s, 2H); <sup>13</sup>C NMR (100 MHz, SO(CD<sub>3</sub>)<sub>2</sub>) δ 160.1, 159.0, 150.7, 148.3, 127.7, 125.1, 121.2, 119.4, 61.0.

**2-(Bromomethyl)-7-nitroquinazolin-4(3H)-one (55).** Compound **54** (5980 mg, 27.4 mmol) was suspended in dry DCM (200 ml) and PPh<sub>3</sub> (4255 mg, 16.22 mmol) and CBr<sub>4</sub> (5380 mg, 16.22 mmol) were added at 0 °C. The reaction was stirred at 0 °C for 1 hour. PPh<sub>3</sub> (4255 mg, 16.22 mmol) and CBr<sub>4</sub> (5380 mg, 16.22 mmol) were added and the reaction was stirred at 0 °C for 1 hour and then at room temperature for 20 hours. Purified using column chromatography on silica gel (DCM:MeOH 96:4) followed by trituration with DCM to give **55** (285 mg, 88%). <sup>1</sup>H NMR (400MHz, SO(CD<sub>3</sub>)<sub>2</sub>) δ 13.00 (s, 1H), 8.38 (d, *J* = 2.2 Hz, 1H), 8.35 (d, *J* = 8.7 Hz, 1H), 8.27 (dd, *J* = 8.7, 2.2 Hz, 1H), 4.44 (s, 2H).

**N-(4-((7-nitro-4-oxo-3,4-dihydroquinazolin-2-yl)methylthio)phenyl)acetamide (56a).** Compound **55** (100 mg, 0.35 mmol), 4-acetamidothiophenol (64.7 mg, 0.39 mmol) and TEA (0.054 ml, 0.39 mmol) were dissolved in DMF (1.5 ml) and heated to 80 °C for 30 minutes using microwave irradiation. Diluted with EtOAc and washed with NaHCO<sub>3</sub> (sat, aq) and brine. The organic layer was dried (Na<sub>2</sub>SO<sub>4</sub>), filtered and concentrated. Purified using column chromatography on silica gel (Heptane:EtOAc 75:25) to give **56a** (105 mg, 81%, 85% pure). <sup>1</sup>H NMR (400MHz, SO(CD<sub>3</sub>)<sub>2</sub>) δ 12.75 (s, 1H), 9.99 (s, 1H), 8.30 (d, *J* = 8.8 Hz, 1H), 8.25 (d, *J* = 2.2 Hz, 1H), 8.20 (dd, *J* = 8.8, 2.2 Hz, 1H), 7.52 (d, *J* = 8.5 Hz, 2H), 7.38 (d, *J* = 8.5 Hz, 2H), 4.05 (s, 2H), 2.02 (s, 3H).

**2-((4-(4-Fluorophenyl)pyrimidin-2-ylthio)methyl)-7-nitroquinazolin-4(3H)-one (56b).** Compound **55** (100 mg, 0.35 mmol), 4-(4-fluorophenyl)-2-pyrimidinethiol (79.9 mg, 0.39 mmol) and TEA 0.054 ml, 0.39 mmol) were dissolved in DMF (1.5 ml) and heated to 80 °C for 30 minutes using microwave irradiation. The precipitate was filtered off and washed with cold EtOAc to give **56b** (105 mg, 73%). <sup>1</sup>H NMR (400MHz, SO(CD<sub>3</sub>)<sub>2</sub>) δ 12.95 (s, 1H), 8.69 (d, *J* = 5.3 Hz, 1H), 8.38-8.28 (m, 4H), 8.20 (dd, *J* = 8.8, 2.3 Hz, 1H), 7.81 (d, *J* = 5.3 Hz, 1H), 7.38 (t, *J* = 8.8 Hz, 2H), 4.55 (s, 2H).

**2-((4-Methoxybenzylthio)methyl)-7-nitroquinazolin-4(3H)-one (56c).** Compound **55** (100 mg, 0.35 mmol), 4-methoxybenzyl mercaptan (0.054 ml, 0.39 mmol) and TEA (0.054 ml, 0.39 mmol) were dissolved in DMF (1.5 ml) and heated to 80 °C for 30 minutes using microwave irradiation. Diluted with EtOAc and washed with NaHCO<sub>3</sub> (sat, aq) and

brine. The organic layer was dried (Na<sub>2</sub>SO<sub>4</sub>), filtered and concentrated. Purified using column chromatography on silica gel (Heptane:EtOAc 40:60) to give **56c** (105 mg, 81%, 92% pure). <sup>1</sup>H NMR (400MHz, SO(CD<sub>3</sub>)<sub>2</sub>) δ 12.68 (s, 1H), 8.36 (d, *J* = 2.3 Hz, 1H), 8.31 (d, *J* = 8.7 Hz, 1H), 8.22 (dd, *J* = 8.8, 2.3 Hz, 1H), 7.30 (d, *J* = 8.6 Hz, 2H), 6.83 (d, *J* = 8.5 Hz, 2H), 3.81 (s, 2H), 3.69 (s, 3H), 3.56 (s, 2H).

**7-Nitro-2-((7-(trifluoromethyl)quinolin-4-ylthio)methyl)quinazolin-4(3H)-one (56d)**. Compound **55** (100 mg, 0.35 mmol), 7-(trifluoromethyl)quinoline-4-thiol (88.7 mg, 0.39 mmol) and TEA 0.054 ml, 0.39 mmol) were dissolved in DMF (1.5 ml) and heated to 80 °C for 30 minutes using microwave irradiation. The precipitate was filtered off and washed with cold EtOAc to give **56d** (82 mg, 54%, 90% pure). <sup>1</sup>H NMR (400MHz, SO(CD<sub>3</sub>)<sub>2</sub>) δ 12.99 (s, 1H), 8.94 (d, *J* = 4.8 Hz, 1H), 8.38-8.28 (m, 4H), 8.22 (dd, *J* = 8.6, 2.3 Hz, 1H), 7.93 (d, *J* = 4.8 Hz, 1H), 7.91 (dd, *J* = 9.0, 1.4 Hz, 1H), 4.54 (s, 2H).

**2-((6-Chlorobenzod[d]thiazol-2-ylthio)methyl)-7-nitroquinazolin-4(3H)-one (56e)**. Compound **55** (100 mg, 0.35 mmol), 5-chloro-2-mercaptobenzothiazole (78.1 mg, 0.39 mmol) and TEA (0.054 ml, 0.39 mmol) were dissolved in DMF (1.5 ml) and heated to 80 °C for 30 minutes using microwave irradiation. The precipitate was filtered off and washed with cold EtOAc to give **56e**. <sup>1</sup>H NMR (400MHz, SO(CD<sub>3</sub>)<sub>2</sub>) δ 12.80 (s, 1H), 8.34 (d, *J* = 9.0 Hz, 1H), 8.30 (d, *J* = 2.3 Hz, 1H), 8.23 (dd, *J* = 9.0, 2.3 Hz, 1H), 8.08 (d, *J* = 8.0 Hz, 1H), 7.92 (d, *J* = 2.3 Hz, 1H), 7.44 (dd, *J* = 8.0, 2.3 Hz, 1H), 4.71 (s, 2H).

**7-Nitro-2-((pyrimidin-2-ylthio)methyl)quinazolin-4(3H)-one (56f)**. Compound **55** (250 mg, 0.88 mmol), 2-mercaptopyrimidine (108.6 mg, 0.97 mmol) and TEA (0.135 ml, 0.97 mmol) were dissolved in DMF (3.75 ml) and heated to 80 °C for 35 minutes using microwave irradiation. Diluted with EtOAc and washed with NaHCO<sub>3</sub> (sat, aq) and brine. The organic layer was dried (Na<sub>2</sub>SO<sub>4</sub>), filtered and concentrated. Purified using column chromatography on silica gel (Heptane:EtOAc 25:75) to give **56f** (215 mg, 78%). <sup>1</sup>H NMR (400MHz, SO(CD<sub>3</sub>)<sub>2</sub>) δ 12.86 (s, 1H), 8.66 (d, *J* = 4.9 Hz, 2H), 8.32 (d, *J* = 8.7 Hz, 1H), 8.28 (d, *J* = 2.3 Hz, 1H), 8.21 (dd, *J* = 8.7, 2.3 Hz, 1H), 7.26 (d, *J* = 4.9 Hz, 1H), 4.48 (s, 2H); <sup>13</sup>C NMR (100 MHz, SO(CD<sub>3</sub>)<sub>2</sub>) δ 170.3, 161.1, 158.4 (2C), 156.8, 151.7, 149.4, 128.6, 125.8, 122.4, 120.6, 118.2, 34.0.

**N-(4-((7-amino-4-oxo-3,4-dihydroquinazolin-2-yl)methylthio)phenyl)acetamide (57a)**. Compound **56a** (100 mg, 0.27 mmol) and tin chloride dihydrate (201 mg, 0.89 mmol) were suspended in

EtOAc (5 ml) and heated to 120 °C for 20 minutes using microwave irradiation. Tin chloride dihydrate (150 mg, 0.22 mmol) was added and heating continued for 20 minutes. Diluted with EtOAc and washed with NaHCO<sub>3</sub> (sat, aq). Purified using column chromatography on silica gel (DCM:MeOH 90:10) to give **57a** (72 mg, 78%, 90% pure). <sup>1</sup>H NMR (400MHz, SO(CD<sub>3</sub>)<sub>2</sub>) δ 11.68 (s, 1H), 9.99 (s, 1H), 7.71 (d, *J* = 8.6 Hz, 1H), 7.52 (d, *J* = 8.5 Hz, 1H), 7.37 (d, *J* = 8.7 Hz, 1H), 6.67 (dd, *J* = 8.6, 2.2 Hz, 1H), 6.52 (d, *J* = 2.2 Hz, 1H), 6.05 (s, 2H), 5.76 (s, 1H), 3.94 (s, 2H), 2.03 (s, 3H).

**7-Amino-2-((4-(4-fluorophenyl)pyrimidin-2-ylthio)methyl)quinazolin-4(3H)-one (57b)**. Compound **56b** (126 mg, 0.31 mmol) and tin chloride dihydrate (347 mg, 1.54 mmol) were suspended in EtOAc (5 ml) and heated to 120 °C for 40 minutes using microwave irradiation. Diluted with EtOAc and washed with NaHCO<sub>3</sub> (sat, aq). Purified using column chromatography on silica gel (DCM:MeOH 90:10) to give **57b** (60 mg, 51%). <sup>1</sup>H NMR (400MHz, SO(CD<sub>3</sub>)<sub>2</sub>) δ 11.82 (s, 1H), 8.69 (d, *J* = 5.3 Hz, 1H), 8.40-8.34 (m, 2H), 7.81 (d, *J* = 5.3 Hz, 1H), 7.72 (d, *J* = 8.6 Hz, 1H), 7.39 (t, *J* = 8.9 Hz, 2H), 6.66 (dd, *J* = 8.7, 2.2 Hz, 1H), 6.59 (d, *J* = 2.2 Hz, 1H), 6.06 (s, 2H), 4.39 (s, 2H).

**7-Amino-2-((7-(trifluoromethyl)quinolin-4-ylthio)methyl)quinazolin-4(3H)-one (57d)**. Compound **56d** (82 mg, 0.19 mmol) and tin chloride dihydrate (141 mg, 0.63 mmol) were suspended in EtOAc (5 ml) and heated to 120 °C for 40 minutes using microwave irradiation. Diluted with EtOAc and washed with NaHCO<sub>3</sub> (sat, aq). Purified using column chromatography on silica gel (DCM:MeOH 90:10) to give **57d** (23 mg, 30%). <sup>1</sup>H NMR (400MHz, SO(CD<sub>3</sub>)<sub>2</sub>) δ 11.96 (s, 1H), 9.01 (d, *J* = 4.5 Hz, 1H), 8.49 (d, *J* = 8.8 Hz, 1H), 8.39 (s, 1H), 7.92 (dd, *J* = 8.9, 2.2 Hz, 1H), 7.72 (d, *J* = 8.5 Hz, 1H), 7.66 (d, *J* = 4.5 Hz, 1H), 6.65 (dd, *J* = 8.9, 2.2 Hz, 1H), 6.40 (d, *J* = 2.2 Hz, 1H), 5.98 (s, 2H), 4.46 (s, 2H).

**7-Amino-2-((6-chlorobenzo[d]thiazol-2-ylthio)methyl)quinazolin-4(3H)-one (57e)**. Compound **56e** (143 mg, 0.35 mmol) and tin chloride dihydrate (263 mg, 1.17 mmol) were suspended in EtOAc (5 ml) and heated to 120 °C for 40 minutes using microwave irradiation. Diluted with EtOAc and washed with NaHCO<sub>3</sub> (sat, aq). Purified using column chromatography on silica gel (DCM:MeOH 90:10) to give **57e** (25 mg, 19%). <sup>1</sup>H NMR (400MHz, SO(CD<sub>3</sub>)<sub>2</sub>) δ 11.91 (s, 1H), 8.08 (d, *J* = 8.6 Hz, 1H), 7.93 (d, *J* = 2.0 Hz, 1H), 7.73 (d, *J* = 8.6 Hz, 1H), 7.43 (dd, *J* = 8.6, 2.0 Hz, 1H), 6.69 (dd, *J* = 8.7, 2.1 Hz, 1H), 6.56 (d, *J* = 2.1 Hz, 1H), 6.09 (s, 2H), 4.57 (s, 2H).

**7-Amino-2-((pyrimidin-2-ylthio)methyl)quinazolin-4(3H)-one (57f).** Compound **56f** (148 mg, 0.47 mmol) and tin chloride dihydrate (349 mg, 1.55 mmol) were suspended in EtOAc (10 ml) and heated to 120 °C for 20 minutes using microwave irradiation. Diluted with EtOAc and washed with NaHCO<sub>3</sub> (sat, aq). Purified using column chromatography on silica gel (DCM:MeOH 90:10) to give **57f** (82 mg, 61%). <sup>1</sup>H NMR (400MHz, SO(CD<sub>3</sub>)<sub>2</sub>) δ 11.80 (s, 1H), 8.67 (d, *J* = 4.9 Hz, 2H), 7.73 (d, *J* = 8.6 Hz, 1H), 7.26 (t, *J* = 4.9 Hz, 1H), 6.68 (dd, *J* = 8.6, 2.2 Hz, 1H), 6.55 (d, *J* = 2.2 Hz, 1H), 6.06 (s, 2H), 4.33 (s, 2H); <sup>13</sup>C NMR (100 MHz, SO(CD<sub>3</sub>)<sub>2</sub>) δ 170.3, 161.1, 158.4 (2C), 156.8, 151.7, 149.4, 128.6, 125.8, 122.4, 120.6, 118.2, 34.0.

**Methyl 4-(2-((4-(4-fluorophenyl)pyrimidin-2-ylthio)methyl)-4-oxo-3,4-dihydroquinazolin-7-ylamino)-4-oxobutanoate (49e).** Compound **49u** (9 mg, 0.019 mmol) was dissolved in DCM (0.6 ml) and MeOH (0.2 ml) and (diazomethyl)trimethylsilane (0.015 ml, 0.028 mmol) was added. The reaction was stirred at room temperature for 30 minutes. Diluted with DCM and washed with NaHCO<sub>3</sub> (sat, aq), water and brine. The organic layer was dried (Na<sub>2</sub>SO<sub>4</sub>), filtered and concentrated to give **49e** (5 mg, 54%). <sup>1</sup>H NMR (400MHz, SO(CD<sub>3</sub>)<sub>2</sub>) δ 12.34 (s, 1H), 10.41 (s, 1H), 8.68 (d, *J* = 5.3 Hz, 1H), 8.38-8.32 (m, 2H), 8.00 (s, 1H), 7.99 (d, *J* = 6.0 Hz, 1H), 7.79 (d, *J* = 5.3 Hz, 1H), 7.54 (dd, *J* = 8.8, 2.1 Hz, 1H), 7.38 (t, *J* = 8.8 Hz, 2H), 4.46 (s, 2H), 3.59 (s, 3H), 2.71-2.58 (m, 4H).

**(Z)-4-(2-((4-acetamidophenylthio)methyl)-4-oxo-3,4-dihydroquinazolin-7-ylamino)-4-oxobut-2-enoic acid (49f).** Compound **57a** (50 mg, 0.15 mmol) and maleic anhydride (18.2 mg, 0.19 mmol) were dissolved in THF (2 ml) and the reaction was heated to 90 °C for 2 hours using microwave irradiation. Purified using HPLC (H<sub>2</sub>O:MeCN 85:15) to give **49f** (15 mg, 23%, 85% pure). <sup>1</sup>H NMR (400MHz, SO(CD<sub>3</sub>)<sub>2</sub>) δ 12.88 (s, 1H), 12.21 (s, 1H), 10.68 (s, 1H), 9.99 (s, 1H), 8.02 (d, *J* = 8.8 Hz, 1H), 7.91 (d, *J* = 1.9 Hz, 1H), 7.63 (dd, *J* = 8.8 Hz, 1.9 Hz, 1H), 7.52 (d, *J* = 8.3 Hz, 2H), 7.38 (d, *J* = 8.7 Hz, 2H), 6.52 (d, *J* = 12.0 Hz, 1H), 6.34 (d, *J* = 12.0 Hz, 1H), 4.02 (s, 2H), 2.03 (s, 3H).

**Methyl 2-(2-((4-acetamidophenylthio)methyl)-4-oxo-3,4-dihydroquinazolin-7-ylcarbamoyl)cyclopent-1-enecarboxylate (49h).** Compound **57a** (30 mg, 0.09 mmol) and 1-cyclopentene-1,2-dicarboxylic anhydride (14.6 mg, 0.11 mmol) were dissolved in THF (1 ml) and the reaction was heated to 90°C for 90 minutes using microwave irradiation. 1-cyclopentene-1,2-dicarboxylic anhydride (14.6 mg, 0.11 mmol) was added and the mixture was heated to 100 °C for 1 hour. A precipitate formed which was filtered off and washed with cold THF to give **49h** (15 mg, 36%). <sup>1</sup>H NMR (400MHz, SO(CD<sub>3</sub>)<sub>2</sub>) δ 12.66 (s, 1H), 12.21 (s, 1H), 10.67 (s,

1H), 9.99 (s, 1H), 8.00 (d,  $J = 8.8$  Hz, 1H), 7.92 (d,  $J = 1.9$  Hz, 1H), 7.63 (dd,  $J = 8.8$  Hz, 1.9, 1H), 7.52 (d,  $J = 8.3$  Hz, 2H), 7.37 (d,  $J = 8.7$  Hz, 2H), 4.02 (s, 2H), 2.83-2.76 (m, 2H), 2.71-2.61 (m, 2H), 2.03 (s, 3H), 1.94 (p,  $J = 7.7$  Hz, 2H).

**4-Oxo-4-(4-oxo-2-((pyrimidin-2-ylthio)methyl)-3,4-dihydroquinazolin-7-ylamino)butanoic acid (49k).** Compound **57f** (42 mg, 0.15 mmol) and succinic anhydride (59 mg, 0.59 mmol) were dissolved in THF (1.5 ml) and heated to 90 °C for 1 day. Succinic anhydride (29 mg, 0.29 mmol) and DMSO (0.4 ml) were added and heating continued for 1 day. The precipitate was filtered off and washed with cold MeOH to give **49k** (27 mg, 48%). <sup>1</sup>H NMR (400MHz, SO(CD<sub>3</sub>)<sub>2</sub>) δ 12.38 (s, 1H), 12.15 (s, 1H), 10.50 (s, 1H), 8.75 (d,  $J = 4.9$  Hz, 2H), 8.09 (d,  $J = 8.6$  Hz, 1H), 8.02 (d,  $J = 2.0$  Hz, 1H), 7.66 (dd,  $J = 8.6, 2.0$  Hz, 1H), 7.34 (t,  $J = 4.9$  Hz, 1H), 4.49 (s, 2H), 2.75-2.61 (m, 4H); <sup>13</sup>C NMR (100 MHz, SO(CD<sub>3</sub>)<sub>2</sub>) δ 170.3, 161.1, 158.4 (2C), 156.8, 151.7, 149.4, 128.6, 125.8, 122.4, 120.6, 118.2, 34.0.

**2-(4-Oxo-2-((pyrimidin-2-ylthio)methyl)-3,4-dihydroquinazolin-7-ylcarbamoyl)cyclopent-1-enecarboxylic acid (49m).** Compound **57f** (20 mg, 0.07 mmol) and 1-cyclopentene-1,2-dicarboxylic anhydride (29 mg, 0.21 mmol) were dissolved in THF (1 ml) and heated to 90 °C for 1 day. 1-Cyclopentene-1,2-dicarboxylic anhydride (20 mg, 0.20 mmol) and DMSO (0.4 ml) were added and heating continued for 1 day. Purified using HPLC (H<sub>2</sub>O:MeCN 85:15 to 30:70 over 50 minutes) to give **49m** (5 mg, 17%). <sup>1</sup>H NMR (400MHz, SO(CD<sub>3</sub>)<sub>2</sub>) δ 12.27 (s, 1H), 8.66 (d,  $J = 4.9$  Hz, 2H), 8.01 (d,  $J = 8.7$  Hz, 1H), 7.97 (d,  $J = 2.1$  Hz, 1H), 7.59 (dd,  $J = 8.7, 2.1$  Hz, 1H), 7.25 (t,  $J = 4.8$  Hz, 1H), 4.41 (s, 2H), 2.80-2.72 (m, 2H), 2.71-2.64 (m, 2H), 1.86 (p,  $J = 7.5$  Hz, 2H), Carboxylic acid and anilide protons are not observed; <sup>13</sup>C NMR (100 MHz, SO(CD<sub>3</sub>)<sub>2</sub>) δ 170.3, 161.1, 158.4 (2C), 156.8, 151.7, 149.4, 128.6, 125.8, 122.4, 120.6, 118.2, 34.0.

**(Z)-4-(2-((4-(4-fluorophenyl)pyrimidin-2-ylthio)methyl)-4-oxo-3,4-dihydroquinazolin-7-ylamino)-4-oxobut-2-enoic acid (49u).** Compound **57b** (30 mg, 0.079 mmol) and succinic anhydride (9.5 mg, 0.095 mmol) were dissolved in THF (1 ml) and heated to 90°C for 1 day. Succinic anhydride (15.8 mg, 0.16 mmol) was added together with DMSO (0.5 ml) and heating continued for 3 days. MeOH was then added until a precipitate formed. The precipitate was collected to give **49u** (25 mg, 66%). <sup>1</sup>H NMR (400MHz, SO(CD<sub>3</sub>)<sub>2</sub>) δ 12.38 (s, 1H), 12.22 (s, 1H), 10.44 (s, 1H), 8.79-8.71 (m, 1H), 8.48-8.36 (m, 2H), 8.12-8.00 (m, 2H), 7.90-7.82 (m, 1H), 7.67-7.58 (m, 1H), 7.51-7.39 (m, 2H), 4.53 (s, 2H), 2.78-2.63 (m, 4H).

**(Z)-4-oxo-4-(4-oxo-2-((pyrimidin-2-ylthio)methyl)-3,4-dihydroquinazolin-7-ylamino)but-2-enoic acid (49v).** Compound **57f** (15 mg, 0.053 mmol) and maleic anhydride (6.2 mg, 0.063 mmol) were dissolved in THF (0.5 ml) heated to 90 °C for 4 hours. The reaction was then stirred at room temperature for 11 days. Purified using HPLC (H<sub>2</sub>O:MeCN 90:10 to 20:80 over 40 minutes. Not pure, repurified using the same system) to give **49v** (17 mg, 84%). <sup>1</sup>H NMR (400MHz, SO(CD<sub>3</sub>)<sub>2</sub>) δ 12.86 (s, 1H), 12.35 (s, 1H), 10.73 (s, 1H), 8.67 (d, *J* = 4.9 Hz, 2H), 8.04 (d, *J* = 9.3 Hz, 1H), 7.96 (s, 1H), 7.62 (d, *J* = 9.7 Hz, 1H), 7.26 (t, *J* = 4.8 Hz, 1H), 6.52 (d, *J* = 11.9 Hz, 1H), 6.34 (t, *J* = 11.9 Hz, 1H), 4.42 (s, 2H); <sup>13</sup>C NMR (100 MHz, SO(CD<sub>3</sub>)<sub>2</sub>) δ 170.3, 161.1, 158.4 (2C), 156.8, 151.7, 149.4, 128.6, 125.8, 122.4, 120.6, 118.2, 34.0.



## Appendix 2

### Experimental Procedures for the Compounds Presented in Scheme 10.

**4-Tert-butoxy-4-oxobutanoic acid (60).** Succinic anhydride (5.0 g, 50.0 mmol), *t*-BuOH (4.8 g, 64.9 mmol), N-hydroxysuccinimide (1.7 g, 15.0 mmol), DMAP (610 mg, 5.0 mmol) and TEA (2.09 ml, 15.0 mmol) were suspended in toluene (25 ml) and refluxed for 18 hours. Diluted with EtOAc and washed with 10% citric acid (aq) followed by brine. Dried (Na<sub>2</sub>SO<sub>4</sub>), filtered and concentrated. Purified using column chromatography on silica gel (Heptane:Et<sub>2</sub>O 50:50) to give **60** (5.79g, 66%). <sup>1</sup>H NMR (400MHz, CDCl<sub>3</sub>) δ 11.58 (s, 1H), 2.64 (t, *J* = 6.6 Hz, 2H), 2.56 (t, *J* = 6.6 Hz, 2H), 1.46 (s, 9H); <sup>13</sup>C NMR (100 MHz, CDCl<sub>3</sub>) δ 178.2, 171.4, 81.0, 30.1, 29.1, 28.0 (3C).

**Tert-butyl 4-(methoxy(methyl)amino)-4-oxobutanoate (61).** Compound **60** (3.0 g, 17.2 mmol), *N,O*-dimethylhydroxylamine (2.0 g, 20.7 mmol), TBTU (6.7 g, 20.7 mmol) and TEA (7.2 ml, 51.7 mmol) were dissolved in DCM (100 ml) and stirred at room temperature for 18 hours. The mixture was washed with 0.1 M HCl and the organic layer was dried (Na<sub>2</sub>SO<sub>4</sub>), filtered and concentrated. Purified using column chromatography on silica gel (Heptane:EtOAc 75:25) to give **61** (3.75 g, 100%). <sup>1</sup>H NMR (400MHz, CDCl<sub>3</sub>) δ 3.73 (s, 3H), 3.20 (s, 3H), 2.72 (t, *J* = 6.9 Hz, 2H), 2.58 (t, *J* = 6.9 Hz, 2H), 1.47 (s, 9H); <sup>13</sup>C NMR (100 MHz, CDCl<sub>3</sub>) δ 173.1, 172.3, 80.4, 61.2, 32.3, 29.8, 28.1 (3C), 27.0.

**Tert-butyl 4-oxohex-5-enoate (62).** Compound **61** (3.7 g, 17.0 mmol) was dissolved in dry THF (150 ml) and vinylmagnesium bromide (1M in THF, 20.8 ml) was added dropwise at -78 °C. The mixture was stirred at -78 °C for 30 minutes and then at room temperature for 4 hours. Poured into cold NH<sub>4</sub>Cl (sat, aq) and extracted with DCM. The organic layer was washed with brine and dried (Na<sub>2</sub>SO<sub>4</sub>), filtered, and concentrated. Purified using column chromatography on silica gel (DCM) to give **62** (2320 mg, 74%). <sup>1</sup>H NMR (400MHz, CDCl<sub>3</sub>) δ 6.37 (dd, *J* = 17.7, 10.4 Hz, 1H), 6.25 (d, *J* = 17.7 Hz, 1H), 5.85 (d, *J* = 10.4 Hz, 1H), 2.86 (t, *J* = 6.7 Hz, 2H), 2.55 (t, *J* = 6.7 Hz, 2H), 1.43 (s, 9H); <sup>13</sup>C NMR (100 MHz, CDCl<sub>3</sub>) δ 198.7, 172.0, 136.3, 128.3, 80.6, 34.2, 29.1, 28.0 (3C).

***N*-(2-hydroxyethyl)-3-nitrobenzamide (64).** 3-nitrobenzoic acid (500 mg, 3.0 mmol) and DMF (1 drop) were dissolved in DCM (15 ml) and oxalyl chloride (0.39 ml, 4.5 mmol) was added at 0 °C. Stirred at 0 °C for 30

minutes and then at room temperature for 2 hours. Solvents were removed under vacuum and the residue was redissolved in DCM (9 ml). Ethanolamine (0.22 ml, 3.6 mmol) and TEA (0.83 ml, 6.0 mmol) were dissolved in DCM (10 ml) and the previously prepared acid chloride was added dropwise at 0 °C. The mixture was stirred at room temperature for 18 hours after which the solvents were removed under vacuum. Purified using column chromatography on silica gel (DCM:MeOH 96:4) to give **64** (551 mg, 88%). <sup>1</sup>H NMR (400MHz, SO(CD<sub>3</sub>)<sub>2</sub>) δ 8.86 (t, *J* = 5.8 Hz, 1H), 8.70 (dd, *J* = 2.3, 1.6 Hz, 1H), 8.41-8.37 (m, 1H), 8.33-8.29 (m, 1H), 7.79 (dd, *J* = 8.2, 7.8 Hz, 1H), 4.78 (t, *J* = 5.7 Hz, 1H), 3.55 (q, *J* = 5.9 Hz, 2H), 3.37 (q, *J* = 5.9 Hz, 2H); <sup>13</sup>C NMR (100 MHz, SO(CD<sub>3</sub>)<sub>2</sub>) δ 164.7, 148.2, 136.5, 134.2, 130.5, 126.2, 122.4, 60.0, 42.9.

**Tert-butyl 6-(2-(3-nitrobenzamido)ethoxy)-4-oxohexanoate (65).** Compound **62** (1260 mg, 6.85 mmol) and compound **64** (480 mg, 2.28 mmol) were dissolved in dry THF (24 ml) under N<sub>2</sub> and DBU (0.17 ml, 1.14 mmol) was added. The reaction was stirred at room temperature for 21 hours, concentrated, and purified using column chromatography on silica gel (Heptane:EtOAc 35:65) to give **65** (331 mg, 37%). <sup>1</sup>H NMR (400MHz, CDCl<sub>3</sub>) δ 8.80 (t, *J* = 2.0 Hz, 1H), 8.40-8.36 (m, 1H), 8.35-8.31 (m, 1H), 7.67 (t, *J* = 8.0 Hz, 1H), 7.51-7.39 (m, 1H), 3.79 (t, *J* = 5.5 Hz, 2H), 3.74-3.66 (m, 4H), 2.81-2.73 (m, 4H), 2.59-2.53 (m, 2H), 1.40 (s, 9H); <sup>13</sup>C NMR (100 MHz, CDCl<sub>3</sub>) δ 208.4, 172.2, 165.0, 148.3, 136.2, 133.5, 129.6, 125.9, 122.4, 80.8, 69.2, 65.0, 42.5, 39.6, 38.0, 29.0, 28.0 (3C).

**Tert-butyl 6-(2-(3-aminobenzamido)ethoxy)-4-oxohexanoate (66).** Compound **65** (75 mg, 0.19 mmol) and Pd/C 10% (20 mg) were suspended in MeOH (7.5 ml) and ammonium formate (120 mg, 1.9 mmol) was added. The mixture was refluxed for 1 hour, filtered, and concentrated. Purified using column chromatography on silica gel (Heptane:EtOAc 25:75) to give **66** (47 mg, 68%). <sup>1</sup>H NMR (400MHz, CDCl<sub>3</sub>) δ 7.22-7.15 (m, 3H), 6.93-6.88 (m, 1H), 6.79-6.76 (m, 1H), 3.77 (br s, 2H), 3.73 (t, *J* = 5.8 Hz, 2H), 3.62-3.58 (m, 4H), 2.74-2.68 (m, 4H), 2.52-2.48 (m, 2H), 1.41 (s, 9H); <sup>13</sup>C NMR (100 MHz, CDCl<sub>3</sub>) δ 207.7, 172.0, 167.7, 146.8, 135.6, 129.3, 117.8, 116.8, 113.8, 80.8, 69.5, 65.2, 42.6, 39.4, 37.9, 29.1, 28.0 (3C).

**9-Oxa-2.12-diazabicyclo[12.3.1]octadeca-1(18),14,16-triene-3,6,13-trione (58a).** Compound **66** (35 mg, 0.19 mmol) was dissolved in DCM (3 ml) and TFA (3 ml) and stirred at room temperature for 3 hours. Solvents were removed under vacuum and the residue was redissolved in DCM (10 ml) and DMF (5 ml). HATU (73 mg, 0.192 mmol) and TEA (0.067 ml, 0.48 mmol) were added and the mixture was stirred at room temperature for 18 hours. The solvents were removed under vacuum and the residue was

purified using preparatory HPLC (H<sub>2</sub>O:MeCN 90:10 to 30:70 over 40 minutes) to give a 1:1 mixture of **58a** and **67** (1.5 mg, 5%). <sup>1</sup>H NMR (400MHz, CDCl<sub>3</sub>) δ 10.14 (s, 1H), 8.37 (t, *J* = 6.0 Hz, 1H), 8.24 (t, *J* = 6.0 Hz, 1H), 8.02 (t, *J* = 1.8 Hz, 1H), 7.74 (dd, *J* = 7.6, 2.2 Hz, 1H), 7.51-7.47 (m, 1H), 7.36 (t, *J* = 7.9 Hz, 1H), 7.13 (t, *J* = 7.9 Hz, 1H), 7.03-6.99 (m, 2H), 6.72-6.67 (m, 1H), 5.71 (t, *J* = 5.4 Hz, 1H), 4.73 (br s, 2H), 3.56-3.44 (m, 4H), 3.36-3.23 (m, 6H), 2.84-2.73 (m, 4H), 2.58 (t, *J* = 6.8 Hz, 2H); <sup>13</sup>C NMR (100 MHz, SO(CD<sub>3</sub>)<sub>2</sub>) δ 208.9, 171.0, 167.4, 166.8, 149.1, 139.8, 135.9, 135.8, 129.1, 129.0, 121.9, 121.8, 118.7, 115.3, 115.0, 111.0, 60.3, 60.2, 42.7, 42.6, 41.9, 38.3, 37.6, 30.5.



## Appendix 3

### Experimental Procedures for Previously Unpublished Compounds Presented in Scheme 11, 12, and 13.

**(9H-fluoren-9-yl)methyl 2-(2-(2-oxo-2-((4-oxo-3,4-dihydroquinazolin-2-yl)methylamino)ethoxy)ethoxy)ethylcarbamate (72).** Compound **22** (150 mg, 0.86 mmol), compound **71** (396 mg, 1.03 mmol), DIC (0.16 ml, 1.03 mmol) and HOAt (140 mg, 1.03 mmol) were dissolved in DMF (6 ml) and the reaction was stirred at room temperature for 16 hours. The mixture was diluted with EtOAc and washed with NaHCO<sub>3</sub> (sat, aq). The organic layer was dried (Na<sub>2</sub>SO<sub>4</sub>), filtered and concentrated. Purified using column chromatography on silica gel (DCM:Acetone 67:33 followed by DCM:MeOH 96:4) to give **72** (453 mg, 98%). <sup>1</sup>H NMR (400MHz, CDCl<sub>3</sub>) δ 10.55 (br s, 1H), 8.27 (dd, *J* = 7.9, 1.4 Hz, 1H), 8.07 (t, *J* = 6.6 Hz, 1H), 7.76-7.67 (m, 3H), 7.65-7.61 (m, 1H), 7.56 (d, *J* = 7.8 Hz, 1H), 7.48 (ddd, *J* = 8.1, 6.9, 1.3 Hz, 1H), 7.36 (t, *J* = 7.4 Hz, 2H), 7.28-7.22 (m, 2H), 6.33 (t, *J* = 5.6 Hz, 1H), 4.46 (d, *J* = 6.7 Hz, 2H), 4.40 (d, *J* = 6.0 Hz, 2H), 4.18 (t, *J* = 6.5 Hz, 1H), 4.12 (s, 2H), 3.73-3.68 (m, 2H), 3.67-3.59 (m, 4H), 3.45-3.37 (m, 4H); <sup>13</sup>C NMR (100 MHz, CDCl<sub>3</sub>) δ 172.4, 161.8, 157.0, 153.4, 147.5, 144.0 (2C), 141.4 (2C), 134.9, 127.8 (2C), 127.5, 127.1 (2C), 126.8 (2C), 125.0 (2C), 121.5, 120.0 (2C), 71.4, 70.4 (2C), 70.2, 66.6, 47.4, 42.4, 41.2.

**N-(2-(2-(2-oxo-2-((4-oxo-3,4-dihydroquinazolin-2-yl)methylamino)ethoxy)ethoxy)ethyl)-5-((3aS,4S,6aR)-2-oxohexahydro-1H-thieno[3,4-d]imidazol-4-yl)pentanamide (68).** Compound **72** (50 mg, 0.092 mmol) was dissolved in DMF (1 ml) and TBAF (0.14 ml, 1 M in THF) was added. The reaction was stirred at room temperature for 4 hours. DIC (0.022 ml, 0.138 mmol), HOAt (18.8 mg, 0.138 mmol) and (+)-biotin (27 mg, 0.11 mmol) were added and the mixture was heated to 70 °C for 1 hour. The solid material was filtered off and purified using column chromatography on silica gel (DCM:MeOH 90:10) to give **68** (38 mg, 75%). <sup>1</sup>H NMR (400MHz, SO(CD<sub>3</sub>)<sub>2</sub>) δ 12.23 (s, 1H), 8.19 (t, *J* = 7.2 Hz, 1H), 8.09 (d, *J* = 8.1 Hz, 1H), 7.90-7.74 (m, 2H), 7.60 (d, *J* = 8.4 Hz, 1H), 7.49 (t, *J* = 7.4 Hz, 1H), 6.40 (s, 1H), 6.35 (s, 1H), 4.37-4.25 (m, 3H), 4.15-4.08 (m, 1H), 3.99 (s, 2H), 3.74-3.65 (m, 2H), 3.64-3.57 (m, 2H), 3.44 (t, *J* = 5.3 Hz, 2H), 3.25-3.16 (m, 2H), 3.11-3.03 (m, 1H), 2.80 (dd *J* = 13.2, 4.0 Hz, 1H), 2.57 (d, *J* = 13.2 Hz, 1H), 2.04 (t, *J* = 7.0 Hz, 2H), 1.68-1.53 (m, 1H), 1.53-1.37 (m, 3H), 1.33-1.20 (m, 2H); <sup>13</sup>C NMR (100 MHz, SO(CD<sub>3</sub>)<sub>2</sub>) δ 172.1, 169.8, 162.7, 161.4, 154.0, 148.3, 134.5, 126.9, 126.4, 125.8, 121.2, 70.3, 70.0, 69.4, 69.2, 61.0, 59.2, 55.4, 40.9, 39.9, 38.5, 35.1, 28.2, 28.0, 25.2.

**(9H-fluoren-9-yl)methyl-2-(2-(2-oxo-2-(prop-2-ynylamino)ethoxy)ethoxy)ethylcarbamate (73)**. Compound **71** (500 mg, 1.30 mmol), DIC (0.22 ml, 1.43 mmol), HOAt (194 mg, 1.43 mmol), TEA (0.22 ml, 1.56 mmol) and propargylamine hydrochloride (142 mg, 1.56 mmol) were dissolved in DCM (12 ml) and stirred at room temperature for 90 minutes. The mixture was then diluted with DCM and washed with brine. Dried (Na<sub>2</sub>SO<sub>4</sub>), filtered and concentrated. Purified using column chromatography on silica gel (Heptane:EtOAc 25:75) to give **73** (530 mg, 97%). <sup>1</sup>H NMR (400MHz, CDCl<sub>3</sub>) δ 7.78 (d, *J* = 7.6 Hz, 2H), 7.61 (d, *J* = 7.5 Hz, 2H), 7.42 (t, *J* = 7.4 Hz, 2H), 7.33 (td, *J* = 7.4, 1.1 Hz, 2H), 7.19 (s, 1H), 5.33 (t, *J* = 5.2 Hz, 1H), 4.46 (d, *J* = 6.9 Hz, 2H), 4.23 (t, *J* = 6.6 Hz, 1H), 4.09 (dd, *J* = 5.3, 2.3 Hz, 2H), 4.03 (s, 2H), 3.71-3.65 (m, 2H), 3.65-3.60 (m, 2H), 3.60-3.56 (m, 2H), 3.47-3.40 (m, 2H), 2.18 (s, 1H); <sup>13</sup>C NMR (100 MHz, CDCl<sub>3</sub>) δ 169.8, 156.5, 144.0 (2C), 141.4 (2C), 127.8 (2C), 127.1 (2C), 125.0 (2C), 120.0 (2C), 79.6, 71.7, 71.1, 70.4, 70.3, 70.1, 66.6, 47.3, 40.9, 28.4.

**N-(2-(2-(2-oxo-2-(prop-2-ynylamino)ethoxy)ethoxy)ethyl)-5-((3a*S*,4*S*,6a*R*)-2-oxohexahydro-1*H*-thieno[3,4-*d*]imidazol-4-yl)pentanamide (74)**. Compound **73** (220 mg, 0.52 mmol) and KF (31.8 mg, 0.55 mmol) were suspended in DMF (2 ml) and heated to 70 °C for 30 minutes using microwave irradiation. (+)-Biotin (140 mg, 0.57 mmol), DIC (0.09 ml, 0.57 mmol) and HOAt (78 mg, 0.57 mmol) were added and the mixture was heated to 70 °C for 30 minutes using microwave irradiation. Concentrated and purified using column chromatography on silica gel (DCM:MeOH 90:10) to give **74** (151 mg, 68%). <sup>1</sup>H NMR (400MHz, CDCl<sub>3</sub>) δ 7.22 (t, *J* = 4.9 Hz, 1H), 6.60 (t, *J* = 5.4 Hz, 1H), 6.53 (s, 1H), 5.67 (s, 1H), 4.49 (dd, *J* = 7.8, 4.8 Hz, 1H), 4.30 (dd, *J* = 7.8, 4.8 Hz, 1H), 4.10 (dd, *J* = 5.3, 2.7 Hz, 2H), 4.03 (s, 2H), 3.72-3.62 (m, 4H), 3.58 (t, *J* = 5.0 Hz, 2H), 3.46 (q, *J* = 5.2 Hz, 2H), 3.13 (td, *J* = 7.3, 4.5 Hz, 1H), 2.90 (dd, *J* = 12.9, 4.9 Hz, 1H), 2.72 (d, *J* = 12.8 Hz, 1H), 2.28 (t, *J* = 2.5 Hz, 1H), 2.23 (t, *J* = 7.5 Hz, 2H), 1.79-1.60 (m, 4H), 1.49-1.38 (m, 2H); <sup>13</sup>C NMR (100 MHz, CDCl<sub>3</sub>) δ 173.5, 170.0, 164.2, 79.7, 71.8, 71.1, 70.6, 70.2, 70.1, 61.9, 60.3, 55.8, 40.7, 39.2, 36.1, 28.7, 28.3, 28.2, 25.7.

**N-(2-(2-(2-oxo-2-((1-((4-oxo-3,4-dihydroquinazolin-2-yl)methyl)-1*H*-1,2,3-triazol-4-yl)methylamino)ethoxy)ethoxy)ethyl)-5-((3a*S*,4*S*,6a*R*)-2-oxohexahydro-1*H*-thieno[3,4-*d*]imidazol-4-yl)pentanamide (69)**. Compound **74** (53.4 mg, 0.125 mmol), compound **21** (23 mg, 0.114 mmol), sodium ascorbate (10.1 mg, 0.051 mmol) and CuSO<sub>4</sub> (2.7 mg, 0.017 mmol) were dissolved in H<sub>2</sub>O (1 ml) and DMF (1 ml). The reaction was stirred at room temperature for 30 minutes. The mixture was then concentrated and purified using column chromatography on silica gel (DCM:MeOH 90:10) to give **69** (45 mg, 63%). <sup>1</sup>H NMR (400MHz, SO(CD<sub>3</sub>)<sub>2</sub>)

$\delta$  12.66 (br s, 1H), 8.26 (t,  $J = 5.9$  Hz, 1H), 8.12 (dd,  $J = 8.2, 1.8$  Hz, 1H), 8.10 (s, 1H), 7.87 (t,  $J = 5.7$  Hz, 1H), 7.79 (ddd,  $J = 8.0, 7.3, 1.6$  Hz, 1H), 7.58-7.48 (m, 2H), 6.43 (s, 1H), 6.38 (s, 1H), 5.58 (s, 2H), 4.41 (d,  $J = 5.9$  Hz, 2H), 4.31 (dd,  $J = 7.7, 5.0$  Hz, 1H), 4.16-4.10 (m, 1H), 3.94 (s, 2H), 3.64-3.50 (m, 4H), 3.40 (t,  $J = 6.0$  Hz, 2H), 3.22-3.16 (m, 2H), 3.12-3.05 (m, 1H), 2.82 (dd,  $J = 12.4, 5.1$  Hz, 1H), 2.58 (d,  $J = 12.4$  Hz, 1H), 2.07 (t,  $J = 7.3$  Hz, 2H), 1.66-1.54 (m, 1H), 1.54-1.39 (m, 3H), 1.35-1.22 (m, 2H);  $^{13}\text{C}$  NMR (100 MHz,  $\text{SO}(\text{CD}_3)_2$ )  $\delta$  172.2, 169.3, 162.7, 161.5, 151.3, 148.1, 144.8, 134.5, 127.0, 126.9, 125.9, 124.3, 121.3, 70.2, 69.9, 69.3, 69.2, 61.0, 59.2, 55.4, 51.3, 48.6, 38.4, 35.1, 33.8, 28.2, 28.0, 25.3.

**2-Amino-3-bromobenzonitrile (76).** 2,6-Dibromoaniline (4.0 g, 15.9 mmol) and CuCN (1.57 g, 17.5 mmol) were suspended in NMP and the mixture was heated to 165 °C for 4 hours. Diluted with 1 M NaOH and extracted with EtOAc. The organic layer was dried ( $\text{Na}_2\text{SO}_4$ ), filtered and concentrated. Purified using column chromatography on silica gel (Heptane:EtOAc 90:10) to give **76** (1390 mg, 44%).  $^1\text{H}$  NMR (400MHz,  $\text{CDCl}_3$ )  $\delta$  7.57 (dd,  $J = 8.0, 1.5$  Hz, 1H), 7.34 (dd,  $J = 7.7, 1.6$  Hz, 1H), 6.59 (t,  $J = 7.9$  Hz, 1H), 4.89 (s, 2H);  $^{13}\text{C}$  NMR (100 MHz,  $\text{CDCl}_3$ )  $\delta$  147.1, 137.3, 131.8, 118.4, 116.9, 109.1, 96.9.

**N-(2-bromo-6-cyanophenyl)-2-methoxyacetamide (77).** Compound **76** (1285 mg, 6.52 mmol), methoxyacetyl chloride (0.60 ml, 6.52 mmol) and pyridine (1.05 ml, 13.0 mmol) were dissolved in DMF at 0 °C. The solution was allowed to reach room temperature and was then stirred for 18 hours under nitrogen. Diluted with EtOAc and washed with 1 M HCl and brine. The organic layer was dried ( $\text{Na}_2\text{SO}_4$ ), filtered and concentrated. Purified using column chromatography on silica gel (Heptane:EtOAc 75:25) to give **77** (955 mg, 54%).  $^1\text{H}$  NMR (400MHz,  $\text{CDCl}_3$ )  $\delta$  8.46 (s, 1H), 7.75 (dt,  $J = 8.2, 1.7$  Hz, 1H), 7.56 (dt,  $J = 7.8, 1.4$  Hz, 1H), 7.17 (td,  $J = 8.0, 1.9$  Hz, 1H), 4.06 (s, 2H), 3.48 (s, 3H);  $^{13}\text{C}$  NMR (100 MHz,  $\text{CDCl}_3$ )  $\delta$  168.0, 137.1, 136.9, 132.3, 128.1, 121.4, 115.6, 113.1, 71.7, 59.5.

**8-Bromo-2-(methoxymethyl)quinazolin-4(3H)-one (78).** Compound **77** (915 mg, 3.4 mmol),  $\text{K}_2\text{CO}_3$  (60 mg, 0.43 mmol) and UHP (640 mg, 6.8 mmol) were suspended in acetone (13 ml) and water (13 ml). The reaction was heated to 82 °C for 24 hours. The mixture was diluted with acetone (5 ml) and water (5 ml) and  $\text{K}_2\text{CO}_3$  (60 mg, 0.43 mmol) and UHP (320 mg, 3.4 mmol) were added. Heating continued for 24 hours after which the solution was cooled until a precipitate formed. The precipitate was collected by filtration, washed with water and dried *in vacuo*. The filtrate was extracted 3 times with EtOAc and the organic extracts were concentrated. The residue was triturated with water and dried *in vacuo* to give **78** (779 mg, 85%).  $^1\text{H}$

NMR (400MHz, SO(CD<sub>3</sub>)<sub>2</sub>) δ 10.38 (s, 1H), 8.24 (d, *J* = 7.9 Hz, 1H), 8.01 (dt, *J* = 7.8, 1.5 Hz, 1H), 7.31 (t, *J* = 7.8 Hz, 1H), 4.58 (s, 2H), 3.56 (s, 3H); <sup>13</sup>C NMR (100 MHz, SO(CD<sub>3</sub>)<sub>2</sub>) δ 161.5, 153.9, 146.5, 138.5, 127.3, 126.3, 123.2, 122.2, 71.3, 59.5.

**8-Bromo-2-(hydroxymethyl)quinazolin-4(3H)-one (79).** Compound **78** (751 mg, 2.79 mmol) was dissolved in 47% HBr (aq) and the solution was heated to 120 °C for 5 hours. The pH was set to ~8 using NaOH (s) with cooling. A precipitate formed which was collected by filtration, washed with water and dried. Purified using column chromatography on silica gel to give **79** (602 mg, 85%). <sup>1</sup>H NMR (400MHz, SO(CD<sub>3</sub>)<sub>2</sub>) δ 12.14 (s, 1H), 8.14-8.05 (m, 2H), 7.37 (t, *J* = 7.7 Hz, 1H), 5.69 (s, 1H), 4.43 (s, 2H); <sup>13</sup>C NMR (100 MHz, SO(CD<sub>3</sub>)<sub>2</sub>) δ 161.0, 157.9, 146.0, 137.9, 127.1, 125.7, 123.0, 121.5, 61.8.

**8-Bromo-2-(bromomethyl)quinazolin-4(3H)-one (80).** Compound **79** (543 mg, 2.13 mmol), CBr<sub>4</sub> (424 mg, 1.28 mmol) and PPh<sub>3</sub> (335 mg, 1.28 mmol) were dissolved in DCM (17 ml). The reaction was stirred at 0 °C for 1 hour. CBr<sub>4</sub> (424 mg, 1.28 mmol) and PPh<sub>3</sub> (335 mg, 1.28 mmol) were added and the mixture was stirred at 0 °C for 1 hour and then at room temperature for 20 hours. Concentrated and purified using column chromatography on silica gel (DCM:MeOH 97:3) to give **80** (519 mg, 77%). <sup>1</sup>H NMR (400MHz, SO(CD<sub>3</sub>)<sub>2</sub>) δ 12.81 (s, 1H), 8.15 (dd, *J* = 7.6, 1.7 Hz, 1H), 8.11 (dd, *J* = 8.0, 1.7 Hz, 1H), 7.44 (t, *J* = 7.8 Hz, 1H), 4.42 (s, 2H); <sup>13</sup>C NMR (100 MHz, SO(CD<sub>3</sub>)<sub>2</sub>) δ 161.1, 153.9, 145.9, 138.1, 128.1, 125.7, 122.9, 121.8, 29.7.

**2-((3-Amino-1H-1,2,4-triazol-5-ylthio)methyl)-8-bromoquinazolin-4(3H)-one (81).** Compound **80** (180 mg, 0.57 mmol) and 3-amino-5-mercapto-1,2,4-triazole (72.3 mg, 0.62 mmol) were dissolved in DMF (2 ml) and heated to 80°C for 15 minutes using microwave irradiation. Diluted with EtOAc and washed with NaHCO<sub>3</sub> (sat, aq). The organic layer was dried (Na<sub>2</sub>SO<sub>4</sub>), filtered and concentrated to give **81** (190 mg, 95%). <sup>1</sup>H NMR (400MHz, SO(CD<sub>3</sub>)<sub>2</sub>) δ 12.59 (s, 1H), 12.16 (s, 1H), 8.15-8.06 (m, 2H), 7.39 (t, *J* = 7.6 Hz, 1H), 6.16 (s, 2H), 4.21 (s, 2H); <sup>13</sup>C NMR (100 MHz, SO(CD<sub>3</sub>)<sub>2</sub>) δ 161.0, 157.6, 155.2, 155.1, 145.9, 138.0, 127.4, 125.6, 122.7, 121.6, 34.7.

**N-(2-(2-(2-(3-(2-((3-amino-1H-1,2,4-triazol-5-ylthio)methyl)-4-oxo-3,4-dihydroquinazolin-8-yl)prop-2-ynylamino)-2-oxoethoxy)ethoxy)ethyl)-5-((3a*S*,4*S*,6a*R*)-2-oxohexahydro-1H-thieno[3,4-*d*]imidazol-4-yl)pentanamide (70).** Compound **81** (20 mg, 0.057 mmol), compound **74** (48.3 mg, 0.11 mmol), CuI (4.3 mg, 0.023 mmol), Cs<sub>2</sub>CO<sub>3</sub> (129 mg, 0.40 mmol) and Pd(PPh<sub>3</sub>)<sub>2</sub>Cl<sub>2</sub> (8.0 mg, 0.011 mmol) were dissolved in DMF (1.5 ml) and heated to 125 °C for 30 minutes using

microwave irradiation. The resulting mixture was filtered and concentrated. Purified using preparatory HPLC (H<sub>2</sub>O:MeCN 90:10 to 50:50 over 40 minutes) to give **70** (6 mg, 15%). <sup>1</sup>H NMR (400MHz, CDCl<sub>3</sub>) δ 12.52-11.92 (m, 2H), 8.02 (dd, *J* = 7.9, 1.5 Hz, 1H), 7.82 (t, *J* = 5.7 Hz, 1H), 7.67 (dd, *J* = 7.5, 1.5 Hz, 1H), 7.45 (t, *J* = 7.6 Hz, 1H), 6.87 (s, 1H), 6.41 (s, 1H), 6.36 (s, 1H), 6.16 (s, 2H), 4.48 (s, 2H), 4.38 (s, 2H), 4.34-4.27 (m, 1H), 4.23 (s, 2H), 4.15-4.09 (m, 1H), 3.60-3.54 (m, 2H), 3.54-3.47 (m, 2H), 3.40-3.34 (m, 2H), 3.21-3.13 (m, 2H), 3.12-3.05 (m, 1H), 2.82 (dd, *J* = 12.4, 5.1 Hz, 1H), 2.58 (d, *J* = 12.4 Hz, 1H), 2.06 (t, *J* = 7.4 Hz, 2H), 1.67-1.55 (m, 1H), 1.55-1.40 (m, 3H), 1.37-1.21 (m, 2H).



## Appendix 4

### Experimental Procedures for Previously Unpublished Compounds Presented in Chapter 4.

**Methyl 3-(3,5-dimethoxyphenyl)-6-methoxy-2-(4-methoxyphenyl)benzofuran-4-carboxylate (A1).** Compound **90** (2.0 g, 5.84 mmol), 4-bromoanisole (1.46 ml, 11.68 mmol), Pd(OAc)<sub>2</sub> (82 mg, 0.37 mmol), tricyclohexylphosphonium tetrafluoroborate (269 mg, 0.73 mmol), K<sub>2</sub>CO<sub>3</sub> (1.2 g, 8.76 mmol) and pivalic acid (1.8 g, 17.52 mmol) were mixed together in a Schlenk tube and nitrogen atmosphere was established. Meticulously freeze-thaw-degassed DMA (35 ml) was added and the reaction was stirred at 100 °C for 27 hours under nitrogen atmosphere. The mixture was diluted with EtOAc and washed brine. The organic layer was dried (Na<sub>2</sub>SO<sub>4</sub>), filtered and concentrated. Purified using column chromatography on silica gel (Heptane:EtOAc 80:20) to give **A1** (1860 mg, 71%). <sup>1</sup>H NMR (400MHz, CDCl<sub>3</sub>) δ 7.51 (d, *J* = 8.8 Hz, 2H), 7.26 (dd, *J* = 15.7, 2.7 Hz, 2H), 6.84 (d, *J* = 8.8 Hz, 2H), 6.57-6.53 (m, 3H), 3.91 (s, 3H), 3.84-3.77 (m, 9H), 3.28 (s, 3H); <sup>13</sup>C NMR (100 MHz, CDCl<sub>3</sub>) δ 168.0, 161.1 (2C), 159.7, 157.1, 155.3, 151.7, 136.6, 128.2 (2C), 125.2, 123.0, 121.6, 115.7, 113.9 (2C), 112.3, 107.5 (2C), 100.1, 99.6, 56.1, 55.5 (2C), 55.3, 51.5.

**(3-(3,5-Dimethoxyphenyl)-6-methoxy-2-(4-methoxyphenyl)benzofuran-4-yl)methanol (100).** Compound **A1** (328 mg, 0.73 mmol) was dissolved in dry DCM and cooled to -78 °C. DIBAL (2.92 ml, 1M in cyclohexane) was added dropwise and the reaction was left to stir at -78 °C for 1 hour. Quenched with MeOH at -78 °C and then left to stir at room temperature for 30 minutes. Filtered through a pad of celite and concentrated. Purified using column chromatography on silica gel (Heptane:EtOAc 60:40) to give **100** (303 mg, 99%). <sup>1</sup>H NMR (400MHz, CDCl<sub>3</sub>) δ 7.50 (d, *J* = 9.0 Hz, 2H), 7.02 (d, *J* = 2.2 Hz, 1H), 6.93 (d, *J* = 2.2 Hz, 1H), 6.83 (d, *J* = 9.0 Hz, 2H), 6.65 (d, *J* = 2.3 Hz, 2H), 6.59 (t, *J* = 2.3 Hz, 1H), 4.48 (s, 2H), 3.87 (s, 3H), 3.81 (s, 6H), 3.80 (s, 3H), OH proton not observed; <sup>13</sup>C NMR (100 MHz, CDCl<sub>3</sub>) δ 161.3 (2C), 159.3, 157.9, 154.7, 149.8, 136.7, 134.9, 127.4 (2C), 123.4, 121.2, 115.6, 113.9 (2C), 110.7, 108.2 (2C), 100.4, 94.9, 62.1, 55.8, 55.5 (2C), 55.3.

**5-(4-(Bromomethyl)-6-hydroxy-2-(4-hydroxyphenyl)benzofuran-3-yl)benzene-1,3-diol (101).** Compound **100** (100 mg, 0.238 mmol) was dissolved in dry DCM (4 ml) and BBr<sub>3</sub> (0.48 ml, 2.85 mmol) was added dropwise at -78 °C. Stirred at -78 °C and slowly allowed to reach room temperature over 17 hours. Cooled to 0 °C, quenched with NaHCO<sub>3</sub> (sat, aq)

and extracted with EtOAc. The organic layer was dried (Na<sub>2</sub>SO<sub>4</sub>), filtered and concentrated. Purified using column chromatography on silica gel (Heptane:EtOAc 50:50) to give **101** (79 mg, 0.185 mmol). <sup>1</sup>H NMR (400MHz, SO(CD<sub>3</sub>)<sub>2</sub>) δ 9.86-9.21 (m, 4H), 7.31 (d, *J* = 8.8 Hz, 2H), 6.93 (d, *J* = 2.2 Hz, 1H), 6.76 (d, *J* = 2.1 Hz, 1H), 6.72 (d, *J* = 8.7 Hz, 2H), 6.31 (t, *J* = 2.2 Hz, 1H), 6.29 (d, *J* = 2.3 Hz, 2H), 4.43 (s, 2H); <sup>13</sup>C NMR (100 MHz, SO(CD<sub>3</sub>)<sub>2</sub>) δ 159.2 (2C), 158.0, 155.7, 154.5, 149.7, 135.5, 131.3, 127.7 (2C), 121.6, 120.7, 115.9 (2C), 115.7, 114.9, 108.7 (2C), 103.0, 98.5, 60.2.

**5-(6-Hydroxy-4-(hydroxymethyl)-2-(4-hydroxyphenyl)benzofuran-3-yl)benzene-1,3-diol (102).** Compound **101** (41 mg, 0.096 mmol) was dissolved in dioxane (2 ml) and 20% NaNO<sub>3</sub> in water (2 ml) was added. Heated to 80 °C for 30 minutes, diluted with EtOAc and washed with water. The water layer was extracted with EtOAc and the organic layers were dried (Na<sub>2</sub>SO<sub>4</sub>), filtered and concentrated. Purified using column chromatography on silica gel (DCM:MeOH 91:9) to give **102** (24 mg, 69%). <sup>1</sup>H NMR (400MHz, SO(CD<sub>3</sub>)<sub>2</sub>) δ 9.66 (s, 1H), 9.47 (s, 1H), 9.41 (s, 2H), 7.28 (d, *J* = 8.7 Hz, 2H), 6.89 (d, *J* = 2.3 Hz, 1H), 6.78 (d, *J* = 2.3 Hz, 1H), 6.70 (d, *J* = 8.8 Hz, 2H), 6.29 (t, *J* = 2.2 Hz, 1H), 6.20 (d, *J* = 2.2 Hz, 2H), 4.98 (t, *J* = 5.5 Hz, 1H), 4.24 (d, *J* = 5.5 Hz, 2H); <sup>13</sup>C NMR (100 MHz, SO(CD<sub>3</sub>)<sub>2</sub>) δ 159.1 (2C), 157.6, 156.0, 154.1, 148.4, 137.3, 136.7, 127.3 (2C), 122.0, 118.8, 116.1, 115.8 (2C), 109.5, 108.5 (2C), 102.7, 95.7, 59.6.

**3-(3,5-Dimethoxyphenyl)-6-methoxybenzofuran-4-carbonitrile (A2).** Compound **110** (950 mg, 2.62 mmol) was dissolved in NMP (10 ml) and CuCN was added. Heated to 200 °C for 2 hours using microwave irradiation. Filtered through silica and concentrated. The precipitate was collected to give **A2** (528 mg, 65%). <sup>1</sup>H NMR (400MHz, SO(CD<sub>3</sub>)<sub>2</sub>) δ 8.29 (s, 1H), 7.74 (d, *J* = 2.3 Hz, 1H), 7.50 (d, *J* = 2.3 Hz, 1H), 6.75 (d, *J* = 2.3 Hz, 2H), 6.56 (t, *J* = 2.3 Hz, 1H), 3.90 (s, 3H), 3.81 (s, 6H). <sup>13</sup>C NMR (100 MHz, SO(CD<sub>3</sub>)<sub>2</sub>) δ 160.7 (2C), 157.8, 156.7, 145.4, 131.4, 121.9, 120.3, 118.3, 117.4, 107.8 (2C), 103.2, 103.2, 101.0, 56.8, 55.7 (2C).

**4-Bromo-3-(3,5-dimethoxyphenyl)-6-methoxy-2-(4-methoxyphenyl)benzofuran (A3).** Compound **110** (500 mg, 1.03 mmol), compound **115** (484 mg, 2.13 mmol), Pd(OAc)<sub>2</sub> (23 mg, 0.10 mmol), tricyclohexylphosphonium tetrafluoroborate (76 mg, 0.21 mmol), K<sub>2</sub>CO<sub>3</sub> (214 mg, 1.55 mmol) and pivalic acid (317 mg, 3.10 mmol) were mixed together in a Schlenk tube and nitrogen atmosphere was established. Meticulously freeze-thaw-degassed DMA (4 ml) was added and the reaction was stirred at 100 °C for 20 hours under nitrogen atmosphere. The mixture was diluted with EtOAc and washed with water followed by NaHCO<sub>3</sub> (sat, aq). The organic layer was dried (Na<sub>2</sub>SO<sub>4</sub>), filtered and concentrated.

Purified using column chromatography on silica gel (Heptane:EtOAc 93:7) to give **A3** (138 mg, 21%). <sup>1</sup>H NMR (400MHz, CDCl<sub>3</sub>) δ 7.37 (d, *J* = 8.9 Hz, 2H), 6.93 (q, *J* = 1.9 Hz, 2H), 6.70 (d, *J* = 9.0 Hz, 2H), 6.50-6.46 (m, 3H), 3.79-3.65 (m, 8H), 1.27-1.09 (m, 4H), 0.62-0.47 (m, 8H), 0.32-0.20 (m, 8H); <sup>13</sup>C NMR (100 MHz, CDCl<sub>3</sub>) δ 160.1 (2C), 158.9, 157.2, 154.6, 150.8, 134.5, 127.7 (2C), 123.0, 122.7, 116.6, 116.1, 114.5 (2C), 113.5, 110.2 (2C), 102.0, 96.3, 73.7, 73.0 (2C), 72.8, 10.3 (2C), 10.3, 10.2, 3.3 (2C), 3.2 (2C), 3.2 (4C).

**5-((2*SR*,3*SR*)-4-(methoxycarbonyl)-6-(pivaloyloxy)-2-(4-(pivaloyloxy)phenyl)-2,3-dihydrobenzofuran-3-yl)-1,3-phenylene bis(2,2-dimethylpropanoate) (A4).** Compound **121** (30 mg, 0.076 mmol), pivaloyl chloride (0.51 ml, 4.1 mmol) and pyridine (0.167 ml, 2.1 mmol) were dissolved in THF (3 ml) and heated to reflux for 19 hours. Diluted with EtOAc and washed with brine. The organic layer was dried (Na<sub>2</sub>SO<sub>4</sub>), filtered and concentrated. Purified using column chromatography on silica gel (Heptane:EtOAc 90:10) to give **A4** (29 mg, 52%). <sup>1</sup>H NMR (400MHz, CDCl<sub>3</sub>) δ 7.27-7.16 (m, 3H), 6.98 (d, *J* = 8.6 Hz, 2H), 6.89 (d, *J* = 2.3 Hz, 1H), 6.69 (t, *J* = 2.0 Hz, 1H), 6.59 (d, *J* = 2.0 Hz, 2H), 5.55 (d, *J* = 5.1 Hz, 1H), 4.79 (d, *J* = 5.1 Hz, 1H), 3.54 (s, 3H), 1.31 (s, 9H), 1.28 (s, 9H), 1.25 (s, 18H); <sup>13</sup>C NMR (100 MHz, CDCl<sub>3</sub>) δ 177.0, 176.8, 176.6 (2C), 165.2, 161.5, 152.1, 151.7 (2C), 151.1, 145.6, 138.2, 128.4, 127.0, 126.5 (2C), 121.9 (2C), 117.7 (2C), 116.4, 114.1, 108.2, 92.5, 57.4, 51.9, 39.2, 39.1 (3C), 27.1 (12C).

**5-((2*SR*,3*SR*)-4-formyl-6-(pivaloyloxy)-2-(4-(pivaloyloxy)phenyl)-2,3-dihydrobenzofuran-3-yl)-1,3-phenylene bis(2,2-dimethylpropanoate) (A5).** Compound **123** (15 mg, 0.041 mmol) pivaloyl chloride (0.12 ml 1.0 mmol) and pyridine (0.12 ml, 1.5 mmol) were dissolved in THF (1 ml) and heated to reflux for 25 hours. Diluted with EtOAc and washed with brine and NaHCO<sub>3</sub> (sat, aq). The organic layer was dried (Na<sub>2</sub>SO<sub>4</sub>), filtered and concentrated. Purified using column chromatography on silica gel (Heptane:EtOAc 90:10) to give **A5** (16 mg, 56%). <sup>1</sup>H NMR (400MHz, CDCl<sub>3</sub>) δ 9.68 (s, 1H), 7.23 (d, *J* = 8.7 Hz, 2H), 7.07 (d, *J* = 2.1 Hz, 1H), 6.98 (t, *J* = 8.6 Hz, 2H), 6.94 (d, *J* = 2.1 Hz, 1H), 6.74 (t, *J* = 2.0 Hz, 1H), 6.70 (d, *J* = 2.1 Hz, 2H), 5.67 (d, *J* = 5.3 Hz, 1H), 4.82 (d, *J* = 5.3 Hz, 1H), 1.32 (s, 9H), 1.28 (s, 9H), 1.26 (s, 18H); <sup>13</sup>C NMR (100 MHz, CDCl<sub>3</sub>) δ 189.5, 177.0, 176.7, 176.4 (2C), 161.7, 152.7, 151.8 (2C), 151.2, 144.6, 137.8, 133.0, 127.0, 126.4 (2C), 122.0 (2C), 118.0 (2C), 116.9, 114.5, 109.4, 93.3, 55.9, 39.2, 39.1 (2C), 39.1, 27.1 (12C).

**(2*RS*,3*SR*)-3-(3,5-bis(cyclopropylmethoxy)phenyl)-6-(cyclopropylmethoxy)-2-(4-(cyclopropylmethoxy)phenyl)-4-vinyl-2,3-dihydrobenzofuran (A6).** Compound **119** (65 mg, 0.11 mmol), methyltriphenylphosphonium bromide (60 mg, 0.17 mmol) and K<sub>2</sub>CO<sub>3</sub> (23

mg, 0.17 mmol) were dissolved in THF (7 ml) and heated to reflux for 48 hours. Diluted with EtOAc and washed with brine. The organic layer was dried ( $\text{Na}_2\text{SO}_4$ ), filtered and concentrated. Purified using column chromatography on silica gel (Heptane:EtOAc 85:15) to give **A6** (50 mg, 77%).  $^1\text{H}$  NMR (400MHz,  $\text{CDCl}_3$ )  $\delta$  6.98 (d,  $J = 8.7$  Hz, 2H), 6.70 (d,  $J = 2.0$  Hz, 1H), 6.66 (d,  $J = 8.8$  Hz, 2H), 6.52 (d,  $J = 2.1$  Hz, 1H), 6.44 (dd,  $J = 17.6$ , 10.9 Hz, 1H), 6.13 (d,  $J = 2.3$  Hz, 1H), 5.89 (d,  $J = 8.2$  Hz, 1H), 5.80 (d,  $J = 2.3$  Hz, 2H), 5.62 (dd,  $J = 17.6$ , 1.0 Hz, 1H), 5.13 (dd,  $J = 11.0$ , 1.0 Hz, 1H), 4.58 (d,  $J = 8.2$  Hz, 1H), 3.87 (d,  $J = 7.0$  Hz, 2H), 3.71 (d,  $J = 7.0$  Hz, 2H), 3.58-3.46 (m, 4H), 1.40-1.28 (m, 1H), 1.28-1.18 (m, 1H), 1.18-1.06 (m, 2H), 0.73-0.66 (m, 2H), 0.66-0.61 (m, 2H), 0.61-0.55 (m, 4H), 0.44-0.38 (m, 2H), 0.36-0.30 (m, 2H), 0.29-0.23 (m, 4H);  $^{13}\text{C}$  NMR (100 MHz,  $\text{CDCl}_3$ )  $\delta$  161.4, 160.3, 159.5 (2C), 158.4, 141.2, 135.3, 133.8, 129.1, 128.0 (2C), 120.6, 115.6, 113.8 (2C), 108.2 (2C), 104.1, 100.0, 96.5, 89.7, 73.1, 72.7 (2C), 72.7, 52.3, 10.4, 10.3, 10.2 (2C), 3.3 (2C), 3.2 (2C), 3.1 (4C).

# Acknowledgements

Jag har under min doktorandtid haft förmånen att arbeta tillsammans med många duktiga och trevliga människor:

Min handledare **Mikael Elofsson** för att du anställde mig som doktorand, lät mig gräva ner mig i synteskemi och uppmuntrade mig att bredda mig själv, för roliga diskussioner både inom kemi och andra områden samt för att du är en suverän chef.

Biträdande handledare **Anna Linusson** för dina bidrag och synpunkter på publikationer och avhandling.

Ni som varit inblandade i ARTD-projekten: **Sara, David** och **Rémi** här i Umeå och **Herwig, Tobias, Torun** och **Ann-Gerd** nere på KI för era respektive expertkunskaper. **Johan** för att du höll projekten på rätt spår i början.

Ni som varit inblandade i totalsyntesprojektet: **Mikael** och **Christopher** för många intressanta diskussioner om benzofuraner.

Övriga i grupp Elofsson: **Michael, Caroline, Naresh, Duy, Liena, Emil, Åsa, Olli, Charlotta, Pia** och **Sassa** för att ni gjort detta till fem intressanta och spännande år.

**Fredrik Almqvist** för att du en gång för länge sedan fick mig intresserad av organisk kemi.

**Christoffer Bengtsson** för att du fick mig att inse nöjet med namnreaktioner.

Examensarbetare: **Elin, Ton, Viktor** och **Artur** för era bidrag till avhandlingen.

**Weixing** och **Marcus** för er hjälp med HPLC instrumenten.

**Mattias** och **Pelle** för allt jobb ni lägger ner på att hålla igång NMR samt LC-MS instrumenten.

Övriga som jobbar eller jobbat på våningsplanet och som gör Umeå universitet till ett trevligt ställe att vara på.

Sist men inte minst tack till min familj: **Mamma** och **Pappa** för allt och för att ni visar intresse trots att jag inte riktigt kan förklara vad jag håller på med. **Cecilia** för att du alltid har tid för våra intressanta diskussioner, för att du korrekturläste min avhandling och för att du är världens bästa syster.



## References

- <sup>1</sup> Jang C. S., Fu F. Y., Wang C. Y., Huang K. C., Lu G., Chou T. C. *Ch'ang Shan, a Chinese Antimalarial Herb*. Science, 1946, 103(2663): 59.
- <sup>2</sup> Nagai N. *Ephedrin*. Pharmazeutische Zeitung. 1887, 32: 700.
- <sup>3</sup> Pelletier J., Magendie F. *Recherches chimiques et physiologiques sur l'ipecacuanha*. Annales de Chimie et Physique, 1817, 4: 172-185.
- <sup>4</sup> Niemann A. *Ueber eine neue organische Base in den Cocablättern*. Archiv der Pharmazie, 1860, 153(2): 129-155.
- <sup>5</sup> Geiger P. L., Hesse K. *Hyoscyamine*. Journal of the Philadelphia College of Pharmacy, 1834, 6(1): 318-319.
- <sup>6</sup> Hay J. E., Haynes L. J. *The Aloins. Part I. The Structure of Barbaloin*. Journal of the Chemical Society, 1956, 3141-3147.
- <sup>7</sup> Haden R. L. *Historical Aspects of Iron Therapy in Anemia*. The Journal of the American Medical Association, 1938, 111(12): 1059-1061.
- <sup>8</sup> Neumeyer J. L. *Historical Perspective of Medicinal Chemistry in Foye's Principles of Medicinal Chemistry 6<sup>th</sup> edition*. Lippincott Williams & Wilkins: Baltimore, 2008, 1-9.
- <sup>9</sup> Wöhler F. *Ueber künstliche Bildung des Harnstoffs*. Annalen der Physik, 1828, 87(2): 253-256.
- <sup>10</sup> Kolbe H. *Untersuchungen über die Elektrolyse organischer Verbindungen*. Justus Liebigs Annalen der Chemie, 1849, 69(3): 257-294.
- <sup>11</sup> Berthelot M. P. E. *Chimie organique fondée sur la synthèse*. Mallet-Bachelier, Paris, 1860.
- <sup>12</sup> Travis A. S. *Perkin's Mauve: Ancestor of the Organic Chemical Industry*. Technology and Culture, 1990, 31(1): 51-82.
- <sup>13</sup> Meth-Cohn O., Smith M. *What did W. H. Perkin actually make when he oxidised aniline to obtain mauveine?* Perkin Transactions 1, 1994, 1: 5-7.

<sup>14</sup> Baeyer A., Drewsen V. *Darstellung von Indigblau aus Orthonitrobenzaldehyd*. Berichte der deutschen chemischen Gesellschaft, 1882, 15(2): 2856-2864.

<sup>15</sup> Cahn A., Hepp P. *Das Antifebrin, ein neues Fiebermittel*. Centralblatt für Klinische Medizin, 1886, 7: 561-564.

<sup>16</sup> Sneader W. *The discovery of aspirin: a reappraisal*. British Medical Journal, 2000, 321: 1591-1594.

<sup>17</sup> Daemrich A., Bowden M. E., *A rising drug industry*. Chemical & Engineering News, 2005, 83(25): 28-42.

<sup>18</sup> Chast F. *A Brief History of Drugs: From Plant Extracts to DNA Technology in The Practice of Medicinal Chemistry*. Academic Press, London, 2003, 3-28.

<sup>19</sup> Bachmann W.E., Wayne C., Wilds A. L. *The total synthesis of the sex hormone equilenin*. Journal of the American Chemical Society, 1939, 61(4): 974-975.

<sup>20</sup> Woodward R. B., Cava M. P., Ollis W. D., Hunger A., Daeniker H. U., Schenker K. *The total synthesis of strychnine*. Journal of the American Chemical Society, 1954, 76(18): 4749-4751.

<sup>21</sup> Nicolaou K. C., Rutjes F. P. J. T., Theodorakis E. A., Tiebes J., Sato M., Untersteller E. *Total Synthesis of Brevetoxin B. 2. Completion*. Journal of the American Chemical Society, 1995, 117(3): 1173-1174.

<sup>22</sup> Nicolaou K. C., *The Total Synthesis of Brevetoxin B: A Twelve-Year Odyssey in Organic Synthesis*. Angewandte Chemie International Edition, 1996, 35(6): 588-607.

<sup>23</sup> Nicolaou K. C., Cole K. P., Frederick M. O., Aversa R. J., Denton R. M. *Chemical Synthesis of the GHIJK Ring System and Further Experimental Support for the Originally Assigned Structure of Maitotoxin*. Angewandte Chemie International Edition, 2007, 46(46): 8875-8879.

<sup>24</sup> Nicolaou K. C., Frederick M. O., Burtoloso A. C. B., Denton R. M., Rivas F., Cole K. P., Aversa R. J., Gibe R., Umezawa T., Suzuki T. *Chemical Synthesis*

of the *GHIJKLMNO* Ring System of Maitotoxin. *Journal of the American Chemical Society*, 2008, 130(23): 7466-7476.

<sup>25</sup> Nicolaou K. C., Aversa R. J., Jin J., Rivas F. *Synthesis of the ABCDEFG Ring System of Maitotoxin*. *Journal of the American Chemical Society*, 2010, 132(19): 6855-6861.

<sup>26</sup> Nicolaou K. C., Heretsch P., Nakamura T., Rudo A., Murata M., Konoki K. *Synthesis and Biological Evaluation of QRSTUVWXYZA' Domains of Maitotoxin*. *Journal of the American Chemical Society*, 2014, 136(46): 16444-16451.

<sup>27</sup> Williams K. J. *The introduction of 'chemotherapy' using arsphenamine – the first magic bullet*. *Journal of the Royal Society of Medicine*, 2009, 102(8): 343-348.

<sup>28</sup> Fleming A. *On the antibacterial action of cultures of a penicillum, with special reference to their use in the isolation of B. influenzae*. *British Journal of Experimental Pathology*, 1929, 10: 226-236.

<sup>29</sup> Wolf G. *The Discovery of Citamin D: The Contribution of Adolf Windaus*. *Journal of Nutrition*, 2004, 134: 1299-1302.

<sup>30</sup> Reichstein T., Grüssner A. *Eine ergiebige Synthese der L-Ascorbinsäure (C-Vitamin)*. *Helvetica Chimica Acta*, 1934, 17: 311-328.

<sup>31</sup> Domagk G. *Ein Beitrag zur Chemotherapie der bakteriellen Infektionen* *Deutsche Medizinische Wochenschrift*, 1935, 61: 250.

<sup>32</sup> Harington C. R., Barger G. *Chemistry of Thyroxine: Constitution and Synthesis of Thyroxine*. *The Biochemical Journal*, 1927, 21(1): 169-183

<sup>33</sup> Kline N. S. *Clinical experience with iproniazid (Marsilid)*. *Journal of Clinical and Experimental Psychopathology*, 1958, 19(2): 72-78.

<sup>34</sup> Nelson W. L., *Antihistamines and Related Antiallergic and Antiulcer Agents in Foye's Principles of Medicinal Chemistry 6<sup>th</sup> edition*. Lippincott Williams & Wilkins: Baltimore, 2008, 1004-1027.

- <sup>35</sup> Fourneau E., Bovet D. *Recherches sur l'action sympatholytique d'un nouveau derive du dioxane*. Archives Internationales de Pharmacodynamie et de Thérapie, 1933, 46: 178-191.
- <sup>36</sup> Lloyd N. C., Morgan H. W., Nicholson B. K., Ronimus R. S. *The Composition of Ehrlich's Salvarsan: Resolution of a Century-Old Debate*. Angewandte Chemie International Edition, 2005, 44(6): 941-944.
- <sup>37</sup> DiMasi J. A., Hansen R. W., Grabowski H. G. *The price of innovation: new estimates of drug development costs*. Journal of Health Economics, 2003, 22(2): 151-185.
- <sup>38</sup> Hansch C., Maloney P. P., Fujita T., Muir R. M. *Correlation of Biological Activity of Phenoxyacetic Acids with Hammett Substituent Constants and Partition Coefficients*. Nature, 1962. 194: 178-180.
- <sup>39</sup> Hansch C., Fujita T.  *$\rho$ - $\sigma$ - $\pi$  Analysis. A Method for the Correlation of Biological Activity and Chemical Structure*. Journal of the American Chemical Society, 1964. 86(8): 1616-1626.
- <sup>40</sup> Kendrew J. C., Bodo G., Dintzis H. M., Parrish R. G., Wyckoff H., Phillips D. C. *A three-dimensional model of the myoglobin molecule obtained by x-ray analysis*. Nature, 1958, 181: 662-666.
- <sup>41</sup> Journal of Computational Chemistry, 1980, 1(1): 3-109.
- <sup>42</sup> Kier L. B. *Molecular Orbital Calculation of Preferred Conformations of Acetylcholine, Muscarine, and Muscarone*. Molecular Pharmacology, 1967, 3(5): 487-494.
- <sup>43</sup> Kier L. B. *Molecular orbital theory in drug research*. Academic Press Inc. New York, 1971.
- <sup>44</sup> Kuntz I. D., Blaney J. M., Oatley S. J., Langridge R., Ferrin T. E. *A geometric approach to macromolecule-ligand interactions*. Journal of Molecular Biology, 1982, 161(2): 269-288.
- <sup>45</sup> McCammon J. A., Gelin B. R., Karplus M. *Dynamics of folded proteins*. Nature, 1977, 267: 585-590.

- <sup>46</sup> Horvath D. *A Virtual Screening Approach Applied to the Search for Trypanothione Reductase Inhibitors*. *Journal of Medicinal Chemistry*, 1997, 40: 2412-2423.
- <sup>47</sup> Lowe III J. A., Lombardino J. G. *The Role of the Medicinal Chemist in Drug Discovery Then and Now*. *Nature Reviews Drug Discovery*, 2004, 3: 853-862.
- <sup>48</sup> Pereira D. A., Williams J. A. *Origin and evolution of high throughput screening*. *British Journal of Pharmacology*, 2007, 152: 53-61.
- <sup>49</sup> Yokoyama A., Murata M., Oshima Y., Iwashita T., Yasumoto T. *Some Chemical Properties of Maitotixin, a Putative Calcium Channel Agonist Isolated from a Marine Dinoflagellate*. *Journal of Biochemistry*, 1988, 104(2): 184-187.
- <sup>50</sup> Murata M., Naoki H., Iwashita T., Matsunaga S., Sasaki M., Yokoyama A., Yasumoto T. *Structure of maitotoxin*. *Journal of the American Chemical Society*, 1993, 115(5): 2060-2062.
- <sup>51</sup> Gallimore A. R., Spencer J. B. *Stereochemical Uniformity of Marine Polyether Ladder – Implications for the Biosynthesis and Structure of Maitotoxin*. *Angewandte Chemie International Edition*, 2006, 45(27): 4406-4413.
- <sup>52</sup> Watson H. C. *The Stereochemistry of the Protein Myoglobin*. *Progress in stereochemistry*, 1969, 4: 299-333.
- <sup>53</sup> Merrifield R. B. *Solid Phase Peptide Synthesis. I. The Synthesis of a Tetrapeptide*. *Journal of the American Chemical Society*, 1963, 85(14): 2149-2154.
- <sup>54</sup> Geysen H. M., Meloan R. H., Barteling S. J. *Use of peptide synthesis to probe viral antigens for epitopes to a resolution of a single amino acid*. *Proceedings of the National Academy of Sciences of the United States of America*, 1984, 81(13): 3998-4002.
- <sup>55</sup> Lidström P., Tierney J., Wathey B., Westman J. *Microwave assisted organic synthesis – a review*. *Tetrahedron*, 2001, 57: 9225-9283.

- <sup>56</sup> Jas G., Kirsching A. *Continuous Flow Techniques in Organic Synthesis*. Chemistry a European Journal, 2003, 9(23): 5708-5723.
- <sup>57</sup> Bürkle A. *Poly(ADP-ribose). The most elaborate metabolite of NAD<sup>+</sup>*. FEBS Journal, 2005, 272: 4576-4589.
- <sup>58</sup> Schreiber V., Dantzer F., Ame J. C., de Murcia G. *Poly(ADP-ribose): novel functions for an old molecule*. Nature Reviews Molecular Cell Biology, 2006, 7: 517-528.
- <sup>59</sup> Hassa P. O., Hottiger M. O. *The diverse biological roles of mammalian PARPs, a small but powerful family of poly-ADP-ribose polymerases*. Frontiers in Bioscience, 2008, 13: 3046-3082.
- <sup>60</sup> Gibsin B. A., Kraus W. L. *New insights into the molecular and cellular functions of poly(ADP-ribose) and PARPs*. Nature Reviews Molecular Cell Biology, 2012, 13: 411-424.
- <sup>61</sup> Hottiger M. O., Hassa P. O., Lüscher B., Schüler H., Koch-Nolte F. *Toward a unified nomenclature for mammalian ADP-ribosyltransferases*. Trends in Biochemical Sciences, 2010, 35: 208-219.
- <sup>62</sup> Karlberg T., Langelier M. F., Pascal J. M., Schüler H. *Structural biology of the writers, readers, and erasers in mono- and poly(ADP-ribose) mediated signaling*. Molecular Aspects of Medicine, 2013, 34: 1088-1108.
- <sup>63</sup> Kleine H., Poreba E., Lesniewicz K., Hassa P. O., Hottiger M. O., Litchfield D. W., Shilton B. H., Lüscher B. *Substrate-assisted catalysis by PARP10 limits its activity to mono-ADP ribosylation*. Molecular Cell, 2008, 32: 57-69.
- <sup>64</sup> Vyas S., Matic I., Uchima L., Rood J., Zaja R., Hay R. T., Ahel I., Chang P. *Family-wide analysis of poly(ADP-ribose) polymerase activity*. Nature Communications, 2014, 5: 4426.
- <sup>65</sup> Kim M. Y., Zhang T., Kraus W. L. *Poly(ADP-ribosylation) by PARP-1: 'PAR-lying' NAD<sup>+</sup> into a nuclear signal*. Genes & Development, 2005, 19: 1951-1967.

<sup>66</sup> Barkauskaite E., Jankevicius G., Ladurner A. G., Ahel I., Timinszky G. *The recognition and removal of cellular poly(ADP-ribose) signals*. FEBS Journal, 2013, 280: 3491-3507.

<sup>67</sup> Moroni F. *Poly(ADP-ribose)polymerase 1 (PARP-1) and postischemic brain damage*. Current Opinion in Pharmacology, 2008, 8: 96-103.

<sup>68</sup> Basu B., Yap T. A., Molife L. R., de Bono J. S. *Targeting the DNA damage response in oncology: Past, present, and future perspectives*. Current Opinion in Oncology, 2012, 24: 316-324.

<sup>69</sup> Lord C. J., Ashworth A. *The DNA damage response and cancer therapy*. Nature, 2012, 481: 287-294.

<sup>70</sup> Ekblad T., Camaioni E., Schüler H., Macchiarulo A. *PARP inhibitors: poly-pharmacology versus selective inhibition*. FEBS Journal, 2013, 280: 3562-3575

<sup>71</sup> Papeo G., Casale E., Montagnoli A., Cirila A. *PARP inhibitors in cancer therapy: an update*. Expert Opinion on Therapeutic Patents, 2013, 23: 503-514.

<sup>72</sup> Riffell J. L., Lord C. J., Ashworth A. *Tankyrase-targeted therapeutics: expanding opportunities in the PARP family*. Nature Reviews Drug Discovery, 2012, 11: 923-936.

<sup>73</sup> Curtin N. J., Szabo C. *Therapeutic applications of PARP inhibitors: anticancer therapy and beyond*. Molecular Aspects of Medicine, 2013, 34: 1217-1256.

<sup>74</sup> U.S. Food and Drug Administration. Approved drugs. <http://www.fda.gov/Drugs/InformationOnDrugs/ApprovedDrugs/ucm427598.htm> (accessed Apr 29, 2015).

<sup>75</sup> Underhill C., Toulmonde M., Bonnefoi H. *A review of PARP inhibitors: from bench to bedside*. Annals of Oncology, 2011, 22: 268-279.

<sup>76</sup> Lehtio L, Jemth A. S., Collins R., Loseva O., Johansson A., Markova N., Hammarstrom M., Flores A., Holmberg-Schiavone L., Weigelt J., Helleday T., Schüler H., Karlberg T. *Structural basis for inhibitor specificity in*

*human poly(ADP-ribose)polymerase-3*. *Journal of Medicinal Chemistry*, 2009, 52:3108-3111.

<sup>77</sup> Rouleau M., McDonald D., Gagné P., Oullet M. E., Droit A., Hunter J. M., Dutertre S., Prigent C., Hendzel M. J., Poirier G. G. *PARP-3 associates with polycomb group bodies and with components of the DNA damage repair machinery*. *Journal of Cellular Biochemistry*, 2007, 100:385-401.

<sup>78</sup> Altmeyer M., Messner S., Hassa P. O., Fey M., Hottiger M. O. *Molecular mechanism of poly(ADP-ribosyl)ation by PARP1 and identification of lysine residues as ADP-ribose acceptor sites*. *Nucleic Acids Research*, 2009, 37: 3723-3738.

<sup>79</sup> Boehler C., Gauthier L. R., Mortusewicz O., Biard D. S., Saliou J. M., Bresson A., Sanglier-Cianferani S., Smith S., Schreiber V., Boussin F., Dantzer F. *Poly(ADP-ribose) polymerase 3 (PARP3), a newcomer in cellular response to DNA damage and mitotic progression*. *Proceedings of the National Academy of Sciences*, 2011, 108: 2783-2788.

<sup>80</sup> Rulten S. L., Fisher A. E., Robert I., Zuma M. C., Rouleau M., Ju L., Poirier G., Reina-San-Martin B., Caldecott K. W. *PARP-3 and APLF function together to accelerate nonhomologous end-joining*. *Molecular Cell*, 2011, 41: 33-45.

<sup>81</sup> Fenton A. L., Shirodkar P., Macrae C. J., Meng L., Koch C. A. *The PARP3- and AT-dependent phosphorylation of APLF facilitates DNA double-strand break repair*. *Nucleic Acids Research*, 2013, 41: 4080-4092.

<sup>82</sup> Aguiar R. C. T., Takeyama K., He C. Y., Kreinbrink K., Shipp M. A. *B-Aggressive lymphoma family proteins have unique domains that modulate transcription and exhibit poly(ADP-ribose) polymerase activity*. *Journal of Biological Chemistry*, 2005, 280: 33756-33765.

<sup>83</sup> Goenka S., Cho S. H., Boothby M. *Collaborator of stat6 (CoaSt6)-associated poly(ADP-ribose) polymerase activity modulates stat6-dependent gene transcription*. *Journal of Biological Chemistry*, 2007, 282: 18732-18739.

<sup>84</sup> Mehrotra P., Riley J. P., Patel R., Li F., Voss L., Goenka S. *PARP-14 functions as a transcriptional switch for stat6-dependent gene activation*. *Journal of Biological Chemistry*, 2011, 286: 1767-1776.

- <sup>85</sup> Iqbal M. B., Johns M., Cao J., Liu Y., Yu S. C., Hyde G. D., Laffan M. A., Marchese F. P., Cho S. H., Clark A. R., Gavins F. N., Woollard K. J., Blackshear P. J., Mackman N., Dean J. L., Boothby M., Haskard D. O. *PARP-14 combines with tristetraprolin in the selective post-transcriptional control of macrophage tissue factor expression*. *Blood*, 2014, 124: 3646-3655.
- <sup>86</sup> Cho S. H., Ahn A. K., Bhargava P., Lee C. H., Eischen C. M., McGuinness O., Boothby M. *Glycolytic rate and lymphomagenesis depend on PARP14, an ADP ribosyltransferase of the B aggressive lymphoma (BAL) family*. *Proceedings of the National Academy of Sciences*, 2011, 108: 15972-15977.
- <sup>87</sup> Verheugd P., Forst A. H., Milke L., Herzog N., Feijs K. L., Kremmer E., Kleine H., Lüscher B. *Regulation of NF- $\kappa$ B signalling by the mono-ADP-ribosyltransferase ARTD10*. *Nature Communications*, 2013, 4: 1683.
- <sup>88</sup> Wahlberg I., Karlberg T., Kouznetsova E., Markova N., Macchiarulo N., Thorsell A-G., Pol E., Frostell Å., Ekblad T., Öncü D., Kull B., Robertson G., Pellicciari R., Schüler H., Weigelt J. *Family wide chemical profiling and structural analysis of PARP and Tankyrase inhibitors*. *Nature Biotechnology*, 2012, 30: 283-288.
- <sup>89</sup> Steffen J. D., Brody J. R., Armen R. S., Pascal J. M. *Structural implications for selective targeting of PARPs*. *Frontiers in Oncology*, 2013, 3, 301.
- <sup>90</sup> Frye S. V. *The art of the chemical probe*. *Nature Chemical Biology*. 2010, 6(3): 159-161.
- <sup>91</sup> Newman D. J., Cragg G. M. *Natural Products As Sources of New Drugs over the 30 Years from 1981-2010*. *Journal of Natural Products*, 2012, 75: 311-335.
- <sup>92</sup> Newman D. J. *Natural Products as Leads to Potential Drugs: An Old Process or the New Hope for Drug Discovery?*. *Journal of Medicinal Chemistry*, 2008, 51: 2589-2599.
- <sup>93</sup> Quideau S., Deffieux D., Douat-Casassus C., Pouységu L. *Plant Polyphenols: Chemical Properties, Biological Activities, and Synthesis*. *Angewandte Chemie International Edition*, 2011, 50: 586-621.

- <sup>94</sup> Haslam E., Cai Y. *Plant polyphenols (vegetable tannins): gallic acid metabolism*. Natural Product Report, 1994, 11: 41-66.
- <sup>95</sup> Coggon P., King T. J., Wallwork S. C. *The Structure of Hopeaphenol*. Chemical Communications (London), 1966, 13: 439-440.
- <sup>96</sup> Zetterström C. E., Hasselgren J., Salin O., Davis R. A., Quinn R. J., Sundin C., Elofsson M. *The resveratrol tetramer (-)-hopeaphenol inhibits type III secretion in the gram-negative pathogens Yersinia pseudotuberculosis and Pseudomonas aeruginosa*. PLoS ONE, 2013, 8(12): e81969.
- <sup>97</sup> Davis R. A., Beattie K. D., Xu M., Yang X., Yin S., Holla H., Healy P. C., Sykes M., Shelper T., Avery V. M., Elofsson M., Sundin C., Quinn R. J. *Solving the Supply of Resveratrol Tetramers from Papua New Guinean Rainforest Anisoptera Species That Inhibit Bacterial Type III Secretion Systems*. Journal of Natural Products, 2014, 77(12): 2633-2640.
- <sup>98</sup> Charro N., Mota L. J. *Approaches targeting the type III secretion system to treat or prevent bacterial infections*. Expert Opinions in Drug Discovery, 2015, 10(4): 373-387.
- <sup>99</sup> Rosqvist R., Magnusson K. E., Wolf-Watz H. *Target cell contact triggers expression and polarized transfer of Yersinia YopE cytotoxin into mammalian cells*. The EMBO Journal, 1994, 13: 964-972.
- <sup>100</sup> Hueck C. *Type III protein secretion systems in bacterial pathogens of animals and plants*. Microbiology and Molecular Biology Reviews, 1998, 62(2): 379-433.
- <sup>101</sup> Cornelis G. R. *The Yersinia Ysc-Yop "type III" weaponry*. Nature Review Molecular Cell Biology, 2002, 3: 742-752.
- <sup>102</sup> Cornelis G. R., Wolf-Watz H. *The Yersinia Yop virulon: a bacterial system for subverting eukaryotic cells*. Molecular Microbiology, 1997, 23: 861-867.
- <sup>103</sup> Forsberg A., Wolf-Watz H. *The virulence protein Yop5 of Yersinia pseudotuberculosis is regulated at transcriptional level by plasmid-plB1 – encoded transacting elements controlled by temperature and calcium*. Molecular Microbiology, 1988, 2: 121-133.

- <sup>104</sup> Andersson K., Carballeira N., Magnusson K. E., Persson C., Stendahl O., Wolf-Watz H., Fällman M. *YopH of Yersinia pseudotuberculosis interrupts early phosphotyrosine signalling associated with phagocytosis*. *Molecular Microbiology*, 1996, 20: 1057-1069.
- <sup>105</sup> Bölin I., Wolf-Watz H. *The plasmid-encoded Yop2b protein of Yersinia pseudotuberculosis is a virulence determinant regulated by calcium and temperature at the level of transcription*. *Molecular Microbiology*, 1988, 2: 237-245.
- <sup>106</sup> Trosky J. E., Liverman A. D. B., Orth K. *Yersinia outer proteins: Yops*. *Cellular Microbiology*, 2008, 10: 557-565.
- <sup>107</sup> Viboud G. J., Bliska J. B. *Yersinia outer proteins: role in modulation of host cell signaling responses and pathogenesis*. *Annual Review of Microbiology*, 2005, 59: 69-89.
- <sup>108</sup> Galán J. E., Wolf-Watz H. *Protein delivery into eukaryotic cells by type III secretion machines*. *Nature*, 2006, 444: 567-573.
- <sup>109</sup> Wang G-W., Wang H-L., Capretto D. A., Han Q., Hu R-B., Yang S-D. *Tf<sub>2</sub>O-catalyzed Friedel-Crafts alkylation to synthesize dibenzof[a,d]cycloheptene cores and application in the total synthesis of Diptoindonesin D, Pauciflorial F and (±)-Ampelopsin B*. *Tetrahedron*, 2012, 68(26): 5216-5222.
- <sup>110</sup> Li W., Li H., Li Y., Hou Z. *Total synthesis of (±)-Quadrangularin A*. *Angewandte Chemie International Edition*, 2006, 45: 7609-7611.
- <sup>111</sup> Takaya Y., Yan K-X., Terashima K., Ito J., Niwa M. *Chemical determination of the absolute structures of resveratrol dimers, ampelopsins A, B, D and F*. *Tetrahedron*, 2002, 58(36): 7259-7265.
- <sup>112</sup> Staudinger H., Meyer J. *Über neue organische Phosphorverbindungen III. Phosphinmethylderivate und Phosphinimine*. *Helvetica Chimica Acta*, 1919, 2: 635-646.
- <sup>113</sup> Ferraris D. V. *Evolution of Poly(ADP-ribose) Polymerase-1 (PARP-1) Inhibitors. From Concept to Clinic*. *Journal of Medicinal Chemistry*, 2010, 53(12): 4561-4584.

- <sup>114</sup> Appel R. *Tertiary phosphane/tetrachloromethane, a versatile reagent for chlorination, dehydration, and P-N linkage*. *Angewandte Chemie International Edition*, 1975, 14: 801-811.
- <sup>115</sup> Bavetsias V. *A facile route to quinazolin-4(3H)-ones functionalized at the 2-position*. *Synthetic Communications*, 1998, 28: 4547-4559.
- <sup>116</sup> Xu W., Fu H. *Amino Acids as the Nitrogen-Containing Motifs in Copper-Catalyzed Domino Synthesis of N-Heterocycles*. *Journal of Organic Chemistry*, 2011, 76, 3846-2852.
- <sup>117</sup> Kaiser N-F K., Hallberg A., Larhed M. *In Situ Generation of Carbon Monoxide from Solid Molybdenum Hexacarbonyl. A Convenient and Fast Route to Palladium-Catalyzed Carbonylation Reactions*. *Journal of Combinatorial Chemistry*, 2002, 4(2): 109-111.
- <sup>118</sup> Georgsson J., Hallberg A., Larhed M. *Rapid Palladium-Catalyzed Synthesis of Esters from Aryl Halides Utilizing Mo(CO)<sub>6</sub> as a Solid Carbon Monoxide Source*. *Journal of Combinatorial Chemistry*, 2003, 5(4): 350-352.
- <sup>119</sup> Eldridge M. D., Murray C. W., Auton R. E., Paolini G. V., Mee R. P. *Empirical scoring functions 0.1. The development of a fast empirical scoring function to estimate the binding affinity of ligands in receptor complexes*. *Journal of Computer-Aided Molecular Design*, 1997, 11: 425-445.
- <sup>120</sup> Verkhivker G. M., Bouzida D., Gehlhaar D. K., Rejto P. A., Arthurs S., Colson A. B., Freer S. T., Larson V., Luty B. A., Marrone T., Rose P. W. *Deciphering common failures in molecular docking of ligand-protein complexes*. *Journal of Computer-Aided Molecular Design*, 2000, 14: 731-751.
- <sup>121</sup> Stahl M., Rarey M. *Detailed analysis of scoring functions for virtual screening*. *Journal of Medicinal Chemistry*, 2001, 44: 1035-1042.
- <sup>122</sup> Grant J. A., Pickup B. R., Nicholls A. *A smooth permittivity function for Poisson-Boltzmann solvation methods*. *Journal of Computational Chemistry*, 2001, 22: 608-640.
- <sup>123</sup> Oprea T. I., Allu T. K., Fara D. C., Rad R. F., Ostopovici L., Bologa C. G. *Lead-like, drug-like or "pub-like": how different are they?* *Journal of Computer Aided-Molecular Design*, 2007, 21: 113-119.

- <sup>124</sup> Holdgate G. A., Ward H. J. *Measurements of binding thermodynamics in drug discovery*. Drug Discovery Today, 2005, 10(22): 1542-1550.
- <sup>125</sup> Workman P., Collins I. *Probing the probes: fitness factors for small molecule tools*. Chemistry & Biology, 2010, 17(6): 561-577.
- <sup>126</sup> Villemin D. *Synthese de macrolides par metathese*. Tetrahedron Letters, 1980, 21(18): 1715-1718.
- <sup>127</sup> Fu G. C., Grubbs R. H. *The application of catalytic ring-closing olefin metathesis to the synthesis of unsaturated oxygen heterocycles*. Journal of the American Chemical Society, 1992, 114(13): 5426-5427.
- <sup>128</sup> Fu G. C., Grubbs R. H. *The synthesis of nitrogen heterocycles via catalytic ring-closing metathesis of dienes*. Journal of the American Chemical Society, 1992, 114(18): 7324-7325.
- <sup>129</sup> Fu G. C., Nhuyen S. T., Grubbs R. H. *Catalytic ring-closing metathesis of functionalized dienes by a ruthenium carbene complex*. Journal of the American Chemical Society, 1993, 115(21): 9856-9857.
- <sup>130</sup> Scholl M., Ding S., Lee C. W., Grubbs R. H. *Synthesis and Activity of a New Generation of Ruthenium-Based Olefin Metathesis Catalysts Coordinated with 1,3-Dimesityl-4,5-dihydroimidazol-2-ylidene Ligands*. Organic Letters, 1999, 1(6): 953-956.
- <sup>131</sup> Nahm S., Weinreb S. M. *N-methoxy-n-methylamides as effective acylating agents*. Tetrahedron Letters, 1981, 22(39): 3815-3818.
- <sup>132</sup> Eglén R. M., Reisine T., Roby P., Rouleau N., Illy C., Bossé R., Bielefeld M. *The Use of AlphaScreen Technology in HTS: Current Status*. Current Chemical Genomics, 2008, 1: 2-10.
- <sup>133</sup> Huisgen R. *1,3-Dipolare Cycloadditionen Rückschau und Ausblick*. Angewandte Chemie, 1963, 75(13): 604-637.
- <sup>134</sup> Huisgen R. *1,3-Dipolar Cycloadditions. Past and Future*. Angewandte Chemie International Edition, 1963, 2(10): 565-598.

- <sup>135</sup> Huisgen R. *Kinetics and Mechanism of 1,3-Dipolar Cycloadditions*. *Angewandte Chemie International Edition*, 1963, 2(11): 633-645.
- <sup>136</sup> Rosenmund K. W., Struck E. *Das am Ringkohlenstoff gebundene Halogen und sein Ersatz durch andere Substituenten. I. Mitteilung: Ersatz des Halogens durch die Carboxylgruppe*. *Berichte der deutschen chemischen Gesellschaft*, 1919, 52(8): 1749-1756.
- <sup>137</sup> von Braun J., Manz G. *Fluoranthren und seine Derivate*. *Justus Liebigs Annalen der Chemie*, 1931, 488(1): 111-126.
- <sup>138</sup> Sonogashira K., Tohda Y., Hagihara N. *A convenient synthesis of acetylenes: catalytic substitutions of acetylenic hydrogen with bromoalkenes, iodoarenes and bromopyridines*. *Tetrahedron Letters*, 1975, 16(50): 4467-4470.
- <sup>139</sup> Snyder S. A., Thomas S. B., Mayer A. C., Breazzano S. P. *Total Syntheses of Hopeanol and Hopeahainol A Empowered by a Chiral Brønsted Acid Induced Pinacol Rearrangement*. *Angewandte Chemie International Edition*, 2012, 51(17): 4080-4084.
- <sup>140</sup> Choi Y. L., Kim B. T., Heo J-N. *Total Synthesis of Laetevireno A*. *Journal of Organic Chemistry*, 2012, 77(19): 8762-8767.
- <sup>141</sup> Kurosawa W., Kobayashi H., Kan T., Fukuyama T. *Total synthesis of (-)-ephedradine A: an efficient construction of optically active dihydrobenzofuran-ring via C-H insertion reaction*. *Tetrahedron*, 2004, 60(43): 9615-9628.
- <sup>142</sup> Snyder S. A., Gollner A., Chiriac M. I. *Regioselective reactions for programmable resveratrol oligomer synthesis*. *Nature*, 2011, 474(7352): 461-466.
- <sup>143</sup> Chen D. Y-K., Kang Q., Wu T. R. *Modular Synthesis of Polyphenolic Benzofurans, and Application in the Total Synthesis of Malibatol A and Shoreaphenol*. *Molecules*, 2010, 15(9): 5909-5927.
- <sup>144</sup> Kraus G. A., Gupta V. *A new synthetic strategy for the synthesis of bioactive stilbene dimers. A direct synthesis of amurensin H*. *Tetrahedron Letters*, 2009, 50(51): 7180-7183.

- <sup>145</sup> Chiummiento L., Funicello M., Lopardo M. T., Lupattelli P., Choppin S., Colobert F. *Concise Total Synthesis of Permethylated Anigopreissin A, a New Benzofuryl Resveratrol Dimer*. *European Journal of Organic Chemistry*, 2012, 1: 188-192.
- <sup>146</sup> Kraus G. A., Kim I. *Synthetic Approach to Malibatol A*. *Organic Letters*, 2002, 5(8): 1191-1192.
- <sup>147</sup> Kim I., Lee S-H., Lee S. *BCl<sub>3</sub>-promoted synthesis of benzofurans*. *Tetrahedron Letters*, 2008, 49(46): 6579-6584.
- <sup>148</sup> Soldi C., Lamb K. N., Squitieri R. A., González-López M., Di Maso M. J., Shaw J. T. *Enantioselective Intramolecular C-H Insertion Reactions of Donor-Donor Metal Carbenoids*. *Journal of the American Chemical Society*, 2014, 136(43): 15142-15145.
- <sup>149</sup> Markina N. A., Chen Y., Larock R. C. *Efficient microwave-assisted one-pot three-component synthesis of 2,3-disubstituted benzofurans under Sonogashira conditions*. *Tetrahedron*, 2013, 69(13): 2701-2713.
- <sup>150</sup> Zhou R., Wang W., Jiang Z-J., Wang K., Zheng X-L., Fu H-Y., Chen H., Li R-X. *One-pot synthesis of 2-substituted benzo[b]furans via Pd-tetraphosphine catalyzed coupling of 2-halophenols with alkynes*. *Chemical Communications*, 2014, 50(45): 6023-6026.
- <sup>151</sup> Lee J. H., Kim M., Kim I. *Palladium-Catalyzed  $\alpha$ -Arylation of Aryloxyketones for the Synthesis of 2,3-Disubstituted Benzofurans*. *Journal of Organic Chemistry*, 2014, 79(13): 6153-6163.
- <sup>152</sup> Kim I., Choi J. *A versatile approach to oligostilbenoid natural products – synthesis of permethylated analogues of viniferifuran, malibatol A, and shoreaphenol*. *Organic & Biomolecular Chemistry*, 2009, 7, 2788-2795.
- <sup>153</sup> Achermann L. *Carboxylate-Assisted Transition-Metal-Catalyzed C-H Bond Functionalizations: Mechanism and Scope*. *Chemical Reviews*, 2010, 111(3), 1315-1345.
- <sup>154</sup> Liégault B., Lapointe D., Caron L., Vlassova A., Fagnou K. *Establishment of Broadly Applicable Reaction Conditions for the Palladium-Catalyzed*

*Direct Arylation of Heteroatom-Containing Aromatic Compounds.* Journal of Organic Chemistry, 2009, 74(5): 1826-1834.

<sup>155</sup> Dess D. B., Martin J. C. *Readily accessible 12-I-5 oxidant for the conversion of primary and secondary alcohols to aldehydes and ketones.* Journal of Organic Chemistry, 1983, 48(22): 4155-4156.

<sup>156</sup> Horner L., Hoffmann H. M. R., Wippel H. G. *Phosphororganische Verbindungen, XII. Phosphinoxyde als Olefinierungsreagenzien.* Chemische Berichte, 1958, 91(1): 61-63.

<sup>157</sup> Horner L., Hoffmann H., Wippel H. G., Klahre G. *Phosphororganische Verbindungen, XX. Phosphinoxyde als Olefinierungsreagenzien.* Chemische Berichte, 1959, 92(10): 2499-2505.

<sup>158</sup> Wadsworth W. S., Emmons W. D. *The Utility of Phosphonate Carbanions in Olefin Synthesis.* Journal of the American Chemical Society, 1961, 83(7): 1733-1738.

<sup>159</sup> Kim K., Kim I. *Total Synthesis of Diptoindonesin G via a Highly Efficient Domino Cyclodehydration/Intramolecular Friedel-Crafts Acylation/Regioselective Demethylation Sequence.* Organic Letters, 2010, 12(22): 5314-5317.

<sup>160</sup> Nagata W., Okada K., Itazaki H., Uyeo S. *Synthetic Studies on Isoquinoline Alkaloids. II. Selective Conversion of 3,9,10-Substituted Tetrahydroprotoberberines into 3,9,10-Substituted 14-Deoxoprotopines. Total Synthesis of 3,9,10-Substituted 5,6,7,8,13,14-Hexahydrodibenz(c,g)azecines.* Chemical and Pharmaceutical Bulletin, 1975, 23: 2878-2890.

<sup>161</sup> Barnard C. F. J. *Carbonylation of Aryl Halides: Extending the Scope of the Reaction.* Organic Process Research & Development, 2008, 12(4): 566-574.

<sup>162</sup> Schöllkopf U., Wittig G. *Über Triphenyl-phosphin-methylene als olefinbildende Reagenzien (I).* Chemische Berichte, 1954, 87(9): 1318-1330.

<sup>163</sup> Haag W., Wittig G. *Über Triphenyl-phosphinmethylene als olefinbildende Reagenzien (II).* Chemische Berichte, 1955, 88(11): 1654-1666.

<sup>164</sup> Heck R. F., Nolley J. P. *Palladium-catalyzed vinylic hydrogen substitution reactions with aryl, benzyl, and styryl halides*. Journal of Organic Chemistry, 1972, 37(14): 2320-2322.

<sup>165</sup> Mizoroki T., Mori K., Ozaki A. *Arylation of Olefin with Aryl Iodide Catalyzed by Palladium*. Bulletin of the Chemical Society of Japan, 1971, 44(2): 581.